

DEVELOPMENT OF A LOAD-BASED METHOD OF
TEST FOR LIGHT COMMERCIAL UNITARY HVAC

By

PEDRO PABLO PEREZ PAEZ

Bachelor of Science in Mechanical Engineering

Universidad del Zulia

Maracaibo, Venezuela

2009

Submitted to the Faculty of the
Graduate College of the
Oklahoma State University
in partial fulfillment of
the requirements for
the Degree of
MASTER OF SCIENCE
December, 2015

DEVELOPMENT OF A LOAD-BASED METHOD OF
TEST FOR LIGHT COMMERCIAL UNITARY HVAC

Thesis Approved:

Dr. Lorenzo Cremaschi

Thesis Adviser

Dr. Daniel Fisher

Dr. Christian Bach

ACKNOWLEDGEMENTS

I would like to thank Dr. Lorenzo Cremaschi for the opportunity to work in the Oklahoma State University HVAC research group, where I had the chance to gain experimental experience in a great facility such as the Psychrometric Chamber Laboratory. I also thank him for the knowledge imparted, and his good advice and support throughout my thesis project. I am thankful for all the high quality people and friends I worked with at OSU, such as: Andrea Bigi, Pratik Deokar, Jeremy Smith, Xiaoxiao Wu, Sarath Mulugurthi, Thiam Wong and Carlo Andres.

I am incredibly grateful to my mother Janny Paez, my sister Paola Perez, my grandparents Pedro Paez and Aira Paez and my uncle Ronald Paez for their love, support and for always encouraging me to chase my dreams.

Finally, I would like to thank Zaida Briceno for her love, support and for always being there for me.

Name: PEDRO PABLO PEREZ PAEZ

Date of Degree: DECEMBER, 2015

Title of Study: DEVELOPMENT OF A LOAD-BASED METHOD OF TEST FOR
LIGHT COMMERCIAL UNITARY HVAC.

Major Field: MECHANICAL AND AEROSPACE ENGINEERING

Abstract:

Packaged unitary HVAC equipment and systems are factory-made assemblies that often provide heating and cooling to buildings all year round. In the commercial sector only, roughly 60% of the commercial building floor space of the U.S. use packaged rooftop air conditioning units. RTUs have an associated annual primary energy consumption of over 2.6 quads. This is about 2% of total U.S. primary energy consumption. In order to reduce that number, equipment efficiency requirements are periodically increased by the US DOE. Efficiency of rooftop units are typically measured by a series figures of merit (EER, SEER and HSPF) that are obtained through laboratory testing.

Increasing efficiency requirements leads to energy savings, but there are space, material cost and theoretical limitations to how much efficiency can continue to be improved. There is a series of technological innovations that reduce energy consumption that are not captured by the currently used figures of merit and methods of test. Simulation and field testing can provide good information but computational models are difficult to calibrate and field samples are typically small. Therefore, there is a need to develop a standardized laboratory protocol that can capture the energy savings that occur outside of the realm of steady-state efficiency.

An experimental procedure for load-based testing that includes minor modifications to typical environmental chamber arrangements was developed. The method uses outside air temperature and humidity and constant indoor loading as boundaries for testing rooftop units. In order to simulate the conditions that rooftop units typically encounter on a building, temperature and load profiles for two different climate zones were imposed in the chamber and external static pressure of the ducting system was set to values typically measured on the field. A series of pre-calibration tests, guidelines for chamber operation and recommendations for data analysis are all included as part of the method.

A total of 84 tests were performed in the Oklahoma State University Psychrometric Chamber laboratory to develop and validate the new method of test. A 15-ton (53 kW) nominal packaged rooftop unit equipped with an outside air economizer, supply air fan speed control and short-cycling digital scroll compressors was tested. The effect of these technologies and various unit control approaches were studied and presented in this work.

TABLE OF CONTENTS

Chapter		Page
I.	INTRODUCTION	1
II.	LITERATURE REVIEW	7
2.1	A brief historical remark	7
2.2	Current methods of testing of air conditioning systems.....	8
2.3	Figures of merit used in current methods of testing.....	11
2.4	Issues related to current figures of merit and methods of testing.....	13
2.5	Field testing.....	15
2.6	The need for an additional testing protocol for RTUs	18
III.	OBJECTIVES	21
3.1	Specific Objectives of my thesis.....	21
3.2	Thesis organization and brief highlights of each chapter.....	25
IV.	EXPERIMENTAL SETUP.....	26
4.1	Psychrometric Chamber Facility.....	26
4.2	Experimental test bed: 15-ton Rooftop Unit	41
V.	TEST CONDITIONS AND EXPERIMENTAL METHODOLOGY	48
5.1	Indoor Room Load Setting Principle	49
5.2	Test Conditions	51
5.3	Example of a load-based cooling test	54
5.4	Initial Definition of the Test Conditions	55
5.5	Experimental Methodology.....	69
VI.	DATA REDUCTION	102
6.1	Variables to be recorded and calculated.....	104
6.2	Moist air properties estimation	105
6.3	Main equations used during the data reduction.....	105
6.4	Verification of capacity measurements taken with the OSU psychrometric facility	112
VII.	RESULTS AND DISCUSSION	116
7.1	Summary of actual tested conditions used in the present study	118

Chapter	Page
7.2 Discussion of Results	127
VIII. CONCLUSIONS AND RECOMMENDATIONS FOR FUTURE WORK	171
8.1 Conclusions	171
8.2 Recommendations for Future Research on This Topic Area	173
NOMENCLATURE	175
ACRONYMS	178
REFERENCES	179

LIST OF TABLES

Table	Page
Table 1: Summary of OSU psychrometric chamber main instrumentation	31
Table 2: RTDs calibration ranges	33
Table 3: Specifications of the Roof Top Unit (RTU) used in the present work	41
Table 4: Details of the experimental test conditions of the tests of the present work.....	52
Table 5: Definition of test conditions and summary of the tests for each series.....	57
Table 6: Estimation of fan power for one bay based on VFD current and voltage values	74
Table 7: Test Tolerances for Load-based Tests	89
Table 8: Variables to be recorded and calculated	104
Table 9: Comparison of measured capacity with Corti and Marelli (2013) data.....	114
Table 10: Test conditions for heat balance	115
Table 11: Estimated heat balance results	115
Table 12: Summary of experimental results of the present work	125
Table 13: Sensitivity analysis towards uncertainty propagation.....	135
Table 14: Uncertainty	137

LIST OF FIGURES

Figure	Page
Figure 1: Schematic floor layout of the RTU under testing when it was installed inside the OSU psychrometric chamber facility; locations of the main measuring sensing points, and definition of the conditioning bays of the chamber	29
Figure 2: Schematic representation of the conditioning bays (bay 1 and 3, bay 4 and 6) and code tester bays (bay 2 and bay 5) for outdoor and indoor rooms.	30
Figure 3: Outdoor sampling probe	32
Figure 4: Example of an OSU in-house custom-made dry and wet bulb probe located in the outdoor room of the psychrometric facility	34
Figure 5: Indoor room code tester showing the airflow nozzles, RTDs, pitot tubes, and the corresponding LabVIEW data acquisition graphic user interface for the selection of the nozzle configuration	36
Figure 6: Installation of the pressure taps across the economizer in order to estimate the airflow rate entering the economizer	38
Figure 7: Example of the in-house custom-made Real Time LabVIEW graphic user interface used to monitor and control the psychrometric conditions of the outdoor and indoor rooms during the tests	40
Figure 8: Photos of the 15-ton nominal capacity air-to-air RTU used in the present work and installed inside OSU psychrometric chamber	42
Figure 9: Photo and graphic user interface of the RTU custom-made controller	43
Figure 10: Side view schematic the RTU with economizer when it was installed in the OSU outdoor room chamber for the tests of the present study (RA: return air, SA: supply air, OA: outside air, MA: mixed air)	46
Figure 11: Photo of the economizer controller (standard commercially available JADE model controller) used in the RTU for the tests of the present work	47
Figure 12: Indoor room energy balance during a typical load-based test	50
Figure 13: Example of complete load-based cooling test from startup of the RTU (both outdoor and indoor rooms were temperature controlled during the initial steady state part of the test, then the indoor room was switched to load controlled mode at the beginning of the transition period; the actual recording period started at the end of the transition period, referred as to “load-based test recording” section)	55
Figure 14: Total cooling Load ($Q_{total, cooling}$) versus outside dry bulb temperature ($T_{db,out}$) for the location of SALEM, OR (ZONE 4C) (results from PNNL simulations of a small office building of approximately 5500 ft ² (511 m ²)).	59
Figure 15: Heating load ($Q_{total, heating}$) versus outside dry bulb temperature ($T_{db,out}$) for the location of SALEM, OR (ZONE 4C) (results from PNNL simulations of a small office building of approximately 5500 ft ² (511 m ²))	64
Figure 16: Outdoor Temperature ($T_{db,out}$) vs. Time (h) for three heating season days in Salem, OR (ZONE 4C).....	65

Figure	Page
Figure 17: Total heating load ($Q_{total,heating}$) vs Time (h) for three heating season days in Salem, OR (Zone 4C)	66
Figure 18 Heating load ($Q_{total,heating}$) versus outside dry bulb temperature ($T_{db,out}$) for three heating season days in the location of SALEM, OR (ZONE 4C) (results from PNNL simulations of a small office building of approximately 5500 ft ² (511 m ²)).....	66
Figure 19: Total cooling load ($Q_{total,cooling}$) versus outside outdoor temperature ($T_{db,out}$) for the location of MEMPHIS, TN (ZONE 3A) (results from PNNL simulations of a small office building of approximately 5500 ft ² (511 m ²)).....	68
Figure 20: Economizer and fan characteristic curves for the RTU tested in the present work.....	72
Figure 21: Results of the sensible heat transfer rate rejected by the chamber conditioning equipment air circulating fans at various outdoor dry bulb temperatures and for the case of economizer fully open (blue diamond points) and for the cases of economizer in MOA position with full speed (red square points) and low speed fan (green triangle points).	81
Figure 22: Example of the thermostatic settings used in the present work for the cooling mode load-based tests with minimum outside air and with full fan speed tests	93
Figure 23: Example of the thermostatic settings used in the present work for the cooling mode load-based tests with fan speed control technology integrated in the RTU.	95
Figure 24: Example of the thermostatic settings used in the present work for the cooling mode load-based tests with economizer technology integrated in the RTU.....	98
Figure 25: Example of the thermostatic settings used in the present work for the heating mode load-based tests	101
Figure 26: Sensible Load vs. Outdoor Dry Bulb Temperature in Cooling Mode	127
Figure 27: Total Load vs. Outdoor Dry Bulb Temperature in Cooling Mode	129
Figure 28: COP Sensible vs Outdoor Dry Bulb Temperature in Cooling Mode	132
Figure 29: COP vs. Outdoor Dry Bulb Temperature in Cooling Mode.....	133
Figure 30: Sensible Load and Sensible COP uncertainties in Cooling Mode.....	136
Figure 31: Total load and COP uncertainties in Cooling Mode.....	137
Figure 32: Total Load and COP for Series B repetition tests (easy tests to set up and execute in cooling mode)	138
Figure 33: Total Load and COP for Series C repetition tests (moderate tests to set up and execute in cooling mode)	139
Figure 34: Total Load and COP for Series D repetition tests (difficult tests to set up and execute in cooling mode)	139
Figure 35: Total Load and COP for Series G: Tests for studying short-cycling effect (RTU in cooling mode operation)	140
Figure 36: Total Load and COP for Series D repetition tests (RTU running in cooling mode) ..	141
Figure 37: Normalized COP vs Time - Series B: 72°F (22.2°C) Full Fan Speed Test.....	142
Figure 38: Normalized COP vs Time - Series B: 72°F (22.2°C) Full Fan Speed Test – After two cycles	144
Figure 39: Normalized COP vs Time - Series C: 72°F (22.2°C) Fan Speed Control Test	146
Figure 40: Normalized COP vs Time - Series C: 72°F (22.2°C) Fan Speed Control Test - After two cycles	147
Figure 41: Normalized COP vs Time - Series D: 72°F (22.2°C) Economizer with Fan Speed Control (4C) Test	148
Figure 42: Normalized COP vs Time - Series C: 72°F (22.2°C) Economizer with Fan Speed Control Test - After two cycles.....	149
Figure 43: Normalized COP vs Time for a test in which cycling did not occur- Series E: 65°F (18.3°C) Economizer with Fan Speed Control (3A) Test.....	151
Figure 44: Normalized COP vs Time for digital scroll full modulation tests.....	153

Figure	Page
Figure 45: COP vs Outdoor Dry Bulb temperature for Series B, C and D (RTU run in Cooling Mode).....	155
Figure 46: COP vs Outdoor Dry Bulb temperature for Series D and E (RTU run in Cooling Mode)	157
Figure 47: COP vs Outdoor Dry Bulb temperature for Series B: full fan speed tests with ON-OFF (M1) and digital scroll modulating compressors (M2)	158
Figure 48 COP _{no fan power} vs Outdoor Dry Bulb temperature for Series B: full fan speed tests with ON-OFF (M1) and digital scroll modulating compressors (M2).....	160
Figure 49: Comparison of total load with and without ventilation contribution for series B, C and D (The apostrophe notation (symbol ') in the legend indicates that the loads were calculated without considering the sensible and latent load contributions from the ventilation air, and as summarized by the equations (38) and (39)).	163
Figure 50: Comparison of COP with and without ventilation for series B, C and D (The apostrophe notation (symbol ') in the legend indicates that the COPs were calculated without considering the sensible and latent load contributions from the ventilation air, and as summarized by the equations (38) to (40)).	164
Figure 51: Sensible Heating Load vs. Outdoor Dry Bulb Temperature.....	166
Figure 52: COP Sensible vs Outdoor Dry Bulb Temperature.....	167
Figure 53: Psychrometric process of the 55F load-based heating test.....	170
Figure 54: Representation of the air side psychrometric states of RTU for the 55°F load-based test with the RTU in heating mode.....	170

CHAPTER I

I. INTRODUCTION

Packaged unitary HVAC equipment and systems are factory-made assemblies that often provide heating and cooling to buildings all year round. They consist of an evaporator or cooling coil, a combination of compressor and condenser, constant or variable speed fans and motors, and a set of accessories and controls that are configured to cost-effectively run the system either for a single zone or for multiple zones at full or at part loads conditions.

In 2014, approximately 40 quads (quadrillions of BTU) of energy were consumed by residential and commercial buildings in the U.S., which constitutes 41% of the total energy consumption of the country. Approximately 40% of the energy required by the buildings was for heating, ventilating and space air conditioning (EIA 2015a). In the commercial sector, roughly 60% of the commercial building floor space of the U.S. use packaged rooftop air conditioning units (RTUs) with an associated annual primary energy consumption of over 2.6 quads (Wang, Katipamula et al. 2015). This accounts for about 2% of total U.S. primary energy consumption (EIA 2015b). In recent years, given the critical importance of energy savings during actual field operation, an integrated energy efficiency ratio (IEER) is used as a single number figure of merit expressing cooling part-load COP efficiency for unitary air-conditioning and heat pump equipment on the basis of weighted operation at various load capacities for the equipment.

Yet, advanced RTUs include a series of accessories and controls that often improve the non-steady-state efficiency but their potential energy savings are not properly quantified by conventional steady state energy performance methods of testing.

When packaged RTU are integrated in actual buildings, some estimates of the yearly energy performance can be simulated in computer models. However, current models for unitary systems are not well calibrated to actual system operation. This is mainly due to inaccurate representation of the system behavior at various ambient conditions when it cycled through various states to balance the building indoor thermal loads. The lack of a systematic and comprehensive method of testing for the RTU that includes advanced controls and additional technologies, such as economizer and variable speed fans for example makes it difficult to develop accurate models for the RTU during actual in-building operation. Field testing provides some data but conducting field tests of large samples is time-consuming and expensive. Field testing also involves significant delays while waiting for full seasonal weather impacts. Thus, there is a need for developing a standard test procedure in laboratory that can provides a figure of merit of packaged air-source RTUs similar to the miles per gallon figure of merit used in the automotive industry. To address this need, the American Society for Heating, Refrigerating, and Air Conditioning Engineers (ASHRAE) proposed a research project that focused on developing new lab-based performance testing procedures to allow a range of control and other technologies to be tested and system performance determined for multiple climates using regression based hourly projections. The ASHRAE project, referred as to ASHRAE Project RP-1608 and entitled “Development of a Load-Based Method of Test for Light Commercial Unitary HVAC” started approximately 2 years ago and this thesis describes the work conducted for this project and highlight the main findings of the study.

Brief description of packaged rooftop units (RTUs)

Most of us are familiar with the air conditioning system of our home, which typically consists of an outdoor “box” and an indoor assembly. The outdoor box includes a compressor, a condenser, and a condenser fan, which is visible on the top of the box. The indoor assembly includes the expansion valve, the evaporator, and the indoor blower and these components are installed in one location of the air ducts inside the home. These type of systems are referred as to split systems because the components of the air conditioning system are “split” between outdoor box and indoor assembly. On the contrary, packaged RTUs are air conditioning systems in which all the components are assembled together in one “box” located on the outdoor of the building. In other words, compressors, condensers, evaporators, expansion valves, and controls and auxiliaries are all positioned inside the outdoor box, which is usually made of metal panels and is typically located on the roofs of commercial buildings building. Packaged RTUs are used for space cooling but they can also provide heating to the space. In such case, the outdoor “box” includes all the components of a heat pump system. A set of accessories and controls are configured to cost-effectively run the system either for a single zone or for multiple zones at full or at part loads conditions. Besides heating and cooling, the units can provide humidity control, filtration, air circulation and ventilation to achieve comfort and/or obtain a controlled environment for products or manufacturing processes. There are three general categories for unitary HVAC equipment: residential, light commercial and commercial. Residential unitary equipment operates with single-phase electric power supply and with a cooling capacity of 65,000 Btu/h (5.42 TONS) or less and is designed specifically for residential application. Light commercial equipment generally uses a three-phase electrical power supply and has a cooling capacity of up to 135,000 Btu/h (11.25 TONS), and it is used in small businesses and commercial properties. Commercial unitary equipment has cooling capacity higher than 135,000 Btu/h and is designed for large commercial buildings. (ASHRAE 2012). According to ASHRAE Handbook (2012 HVAC Systems and Equipment ASHRAE Handbook), size, shape, and

use of the building, availability and cost of energy, building aesthetics (equipment located outdoors), and space available for equipment must be considered to determine the type of unitary equipment best suited to a given application. In general, roof-mounted single-package unitary equipment is limited to five or six stories because duct space and available blower power become excessive in taller buildings.

Motivations of this study

Studying the performance of HVAC rooftop units means assessing their capability to provide indoor comfort conditions to the occupied space, evaluating their energy consumption required to run and meet the building load demands, and accounting for their energy conversion efficiency of the overall system, i.e., investigating and designing the best possible ways to minimize energy losses of the air conditioning system for given cost and space constraints. There are three approaches to study the performance of HVAC RTUs: simulation, field testing, and laboratory testing. The American Society of Heating, Refrigerating and Air Conditioning Engineers (ASHRAE) and the Air Conditioning, Heating and Refrigeration Institute (AHRI) are the two major organizations that provide standards and guidance for laboratory testing of RTUs in the U.S. In a regulatory level, the U.S. Department of Energy (DOE) dictates the requirements for testing and rating HVAC equipment and the procedure to do so is documented in Appendix M to Subpart 430 of Section 10 of the Code of Federal Regulations, Uniform Test Method of Measuring the Energy Consumption of Central Air Conditioners. These testing procedures summarize their results in a series of steady state metrics or figures of merit, such as the energy efficiency ratio (EER), the seasonal energy efficiency ratio (SEER), the heat seasonal performance factor (HSPF) and the integrated energy efficiency ratio (IEER). In recent years, given the critical importance of energy savings during actual field operation, the integrated energy efficiency ratio (IEER) is used as a single number figure of merit expressing cooling part-load coefficient of performance (COP) efficiency for unitary air-conditioning and heat pump equipment based on weighted operation at

various load capacities for the equipment. IEER represents an improvement from the previously developed steady state full load figures of merit but it still lacks the ability to capture non-steady state efficiency gains that currently available technologies can provide, such as:

- Economizer function, including dynamic cycling and air stream interaction.
- New technologies that mitigate refrigeration system cycling degradation.
- New technologies that dynamically change airflow at a particular part-load condition; for example, reducing air speed or cycling the fan when cooling or heating is not operating.
- Evaporative, heat recovery, and other technologies involving a change in outdoor conditions seen by the system and interaction of indoor and outdoor air.
- Systems that vary compressor speed or refrigerant flow to match changes in load.
- Systems that have the capability to produce discrete results based on various outdoor and indoor load conditions that can then be applied to climate and building load profiles to arrive at regional performance results.

Field-testing gives a good insight on system performance but it involves significant delays while waiting for full seasonal weather impacts and does not provide consistent conditions that could be fairly comparable to other samples or studies. Sampling size is also an issue on field-testing since the amount of data is usually small because taking field measurements is time-consuming and expensive; therefore, there is a lack of consistent data for comparison.(ASHRAE 2013).

Computer simulation can also provide good information but current models are not well calibrated. This is mainly due to inaccurate representation of the system behavior at different ambient conditions when it cycles through several states to balance the building indoor thermal loads. Several small details in the configuration of the system that can affect its efficiency are difficult to account for during system simulation.

There are many technological innovations that can enhance non-steady state system performance, but traditionally, those technologies are tested through separate procedures. Therefore, there is a lack of a systematic and comprehensive method of testing for roof top units that includes advanced controls and additional energy saving technologies. Develop accurate models for unitary equipment during actual in-building operation requires experimental data that includes such technologies. Consequently, there is a need for developing a standard test procedure in laboratory that can provide comprehensive figures of merit of packaged air-source RTUs similar to the miles per gallon figure of merit used in the automotive industry. Such standard test procedure must assess unit efficiency during non-steady state operation when modern technologies such as economizers and variable fan speeds are integrated in the RTU system. Figures of merit that result when testing rooftop units with this method allows evaluating potential energy savings or highlighting the shortcomings of each technology in a more standardized manner. Additionally, the data obtained when applying this method will allow for better calibration of computer models to predict actual unitary system energy consumption, as pointed out in several studies in the literature (Hart, Morehouse et al. 2008, ASHRAE 2013).

CHAPTER II

II. LITERATURE REVIEW

2.1 A brief historical remark

A little over a hundred years have gone by since the era on which modern air conditioning systems are considered to be invented. Much of the theory and first application attempts took place during the latter part of the nineteenth century, but it was in the first decade of the twentieth century when Willis Carrier while working for Buffalo Forge Co. worked on the solution of a humidity control problem at a printing plant, which would be the first of his many developments towards the modern air conditioner (Nagengast 1999). Also during this time, he came up with the first version of the psychrometric chart, a tool extensively used for many years by Heating, Ventilating and Air Conditioning (HVAC) engineers to determine moist air properties. Although obtaining these properties nowadays can be done with readily available software, the chart remains a great tool for teaching purposes, as well as for quickly visualizing and diagnosing psychrometric processes (Gatley 2004). These contributions along with the work of many others became the foundation that allows air conditioning systems to bring comfort to homes, offices and commercial facilities indoor environments around the world.

Thermal comfort of the human body depends primarily on three factors: air temperature, relative humidity and air motion (Cengel and Ghajar 2014). Nevertheless, HVAC systems not only provide human comfort but they also make possible the production and storage of many goods in a better, faster and more economical way by controlling the temperature, humidity and air quality of indoor environments. The development and industrialization of the United States, especially of the Southern States and many other world countries would not have been possible without the appropriate environment control. In these days and age it is difficult to imagine a residential, commercial, industrial or institutional building in the industrialized countries of the world without systems that condition their indoor environment all year long (McQuiston, Parker et al. 2005). For this reason, it is of great importance to study HVAC systems performance and energy consumption to provide a ground basis for improvement in the years to come.

2.2 Current methods of testing of air conditioning systems

Today, standards ANSI/ASHRAE 116-2010 (ASHRAE 2010) and ANSI/ASHRAE 37-2009 (ASHRAE 2009a) describe several methods to measure heating and cooling capacities and calculate the system performance using environmental testing rooms. These methods are summarized as follows:

- a) Indoor air enthalpy method: This method requires dry bulb and wet bulb temperatures of the indoor room, supply mass flow rate of the air and unit energy consumption to be measured. Out of the four methods contemplated in the standards, this is the only one that is direct, since it measures variables in the room that is being conditioned.
- b) Outdoor air enthalpy method: Method that measures dry bulb and wet bulb temperatures of the outdoor room, the mass flow rate of the air passing through the condenser and the energy consumption of the unit being tested. This allows calculating the heat transfer between the unit condenser and the outdoor room, and then the capacity of the unit is determined through an

energy balance. A disadvantage of this method is that in order to apply it to determine unit capacity and performance, it must be determined if the flow measurement apparatus in the outdoor side, affects unit performance.

- c) Compressor calibration method: Pressures and temperatures of the refrigerant entering and leaving the compressor need to be measured, superheat of the refrigerant leaving the evaporator needs to be determined and it is required to be higher than 5°F. A calorimeter is required to determine compressor flow rate.
- d) Refrigerant enthalpy method: Pressure and temperature of the refrigerant entering and leaving the indoor coil of the unit need to be measured, as well as, mass flow rate of the refrigerant. For cooling tests the refrigerant leaving the flow meter needs to be 3°F sub-cooled, for heating tests the liquid leaving the flow meter needs to be 3°F sub-cooled and vapor entering needs to be 5°F superheated.

Standards indicate that all four methods can be applied for single package air-to-air heat pumps, which is the system of the study in this thesis. However, this is not true for other types of equipment. Methods a and b are considered primary methods, while methods c and d can be used to confirm or validate the findings from methods a and b through system energy balance calculations. Methods c and d are considered not valid for assessing the performance of RTUs during cycling operation. Method c is also not valid if the compressor of the unit is uninsulated and/or ventilated by indoor air. ASHRAE Standard 23 Methods of Testing for Rating Positive-Displacement Compressors and Condensing Units must be consulted to understand all the details of the test and make sure that everything is properly accounted for when assessing the performance of the RTU with method c. Standards 116 and 37 indicate also that method d can be used by manufacturers but cannot be used for certification purpose. Major limitations of methods c and d is that they require modifications of the unit being tested, because additional instrumentation on the refrigerant side of the vapor compression system is needed in addition to what manufacturers usually include in their units.

These modifications causes these methods to be referred as to “intrusive” methods; installing additional instrumentation and modifying the refrigerant pipelines can potentially affects the actual performance of the unit. As such the figures of merit measured with intrusive methods of test are not necessarily representative of unit performance in field operation and often do not agree with the figures of merit provided by the manufacturer. For these reasons, the indoor air enthalpy method is the preferred choice adopted by testing laboratories. It uses direct measurements of the unit cooling capacity, unit power, and unit airflow rate and air temperatures and all the instrumentation are external to the unit, which makes this method not intrusive. The indoor air enthalpy method was also the one used in the present thesis, but few modifications were made in order to conform to the requirements dictated by testing the unit when it was subjected to a set thermal load, rather than a pair of constant indoor and outdoor temperatures. Exposing the unit to a set thermal load and measuring the unit performance while it reacts to such thermal load in order to continue to provide indoor comfort conditions is referred as to load-based method of test throughout this thesis. On the contrary, exposing the unit to a pair of indoor and outdoor temperatures and measuring the unit performance at such temperatures is referred as to temperature-based method of test in this thesis. ASHRAE standards 116 and 37 describes temperature-based method of tests. In addition to standards ANSI/ASHRAE 116-2010 and ANSI/ASHRAE 37-2009 (ASHRAE 2009a, ASHRAE 2010), AHRI Standard 210/240 and AHRI 340/360 (ANSI/AHRI 2007, ANSI/AHRI 2008) also provide guidelines for temperature-based tests requirements, such as data to be recorded and tolerance needed to publish equipment ratings in manufacturer literature and nameplates.

2.3 Figures of merit used in current methods of testing

Current testing standards summarize their results in a series of steady state metrics or figures of merit, such as the energy efficiency ratio (EER), the seasonal energy efficiency ratio (SEER), the heat seasonal performance factor (HSPF) and the integrated energy efficiency ratio (IEER).

Two of the most important and currently used figures of merit are the SEER and the HSPF. The seasonal energy efficiency ratio (SEER) is the ratio of total seasonal cooling output measured in Btu to total seasonal watt-hours of input energy. This value is obtained through environmental chamber laboratory testing at various indoor and outdoor temperature and humidity conditions, and a performance test under cyclic operation. In general at least four cooling tests are required to rate packaged unitary equipment. According to ASHRAE 116-2010 standard, these tests are two steady state tests at different outdoor conditions (A and B), a steady state dry coil test (C) and a cycling dry coil tests (D). The dry coil condition is achieved by maintaining outdoor room dew point temperature low enough so no condensation is formed in the evaporator coil. The procedure for calculating SEER is based in tests A, B, C and D for single-speed, two speed and two-compressor systems. When variable speed systems are tested, some additional tests, such as the intermediate speed test I are required. The SEER depends on outlining system capacity and power profiles over different temperature bins based on tests results. System performance at individual bins and bin hours are weighed to obtain the final number. Bin methods are very commonly used to estimate building energy consumption (Knebel 1983) and in this case, bin weather data is used to determine the periods of time a tested unit would operate under certain weather conditions. These bin periods of time are then used to do the weigh average for SEER calculation A degradation factor is also included in the ASHRAE 116-2010 SEER formulas to account for cycling losses during part-load operation (ASHRAE 2010, ASHRAE 2012).

In a similar way, the heating seasonal performance factor (HSPF) measures seasonal heating mode efficiencies of heat pumps as the ratio of total heating output to total seasonal input energy. Like the SEER, the HSPF is also determined in an environmental chamber laboratory from test results at different indoor and outdoor temperature and humidity conditions, including cycling performance and defrosting tests. The results of these tests are an input to algorithm used to calculate the HSPF. Nonetheless, the HSPF depends on climatic conditions and building heating load relative to the equipment capacity besides the measured equipment performance. Like with SEER, the type of heat pump system being tested is an important factor on the calculation of the HSPF. The control logic for turning on and off the compressors, and whether the unit has a single-speed or a variable-speed compressor among other factors influence the way the HSPF is calculated. Another very important factor is the climatic region on which the heat pump equipment will operate, as well as the building required heating load relative to the capacity of the unit at different outdoor temperatures. There United States Department of Energy defines six US climate regions used for HSPF rating purposes. Such a number of regions and different ranges of load for design can lead up to 30 different HSPF ratings for a single unit. However, for the purpose of comparison and performance ratings, the US DOE established region 4 (moderate northern climate) and minimum design load as the typical climatic region and building design load as parameters for comparison. Like with the SEER, the HSPF uses the temperature bin analysis as the basic approach for calculation. Moreover, the HSPF also accounts for cycling losses and a penalty for outdoor coil frosting (ASHRAE 2010, ASHRAE 2012).

The integrated energy efficiency ratio (IEER) has gained importance in the last years as a single number figure of merit expressing cooling part-load efficiency. The IEER figure of merit was included in AHRI 340/360-2007 and AHRI 210/240-2008 and it became effective in 2010 as a part of the rating program. The IEER is based on weighted averages of the EER, which is the ratio of the cooling capacity in Btu/h to the power input values in watts at any given set of rating conditions. IEER and EER are both expressed in Btu/W·h. The IEER considers the assumption that units work

under 100% load conditions a 2% of the time, 75% part load during 61.7% of the time, 50% part load 23.8% of the time and 25% part load during 12.5% of the time. This expressed in the IEER equation as follows:

$$IEER = 0.020EER_{100\%} + 0.617EER_{75\%} + 0.238EER_{50\%} + 0.125EER_{25\%} \quad (1)$$

AHRI standards provide instructions on how to reduce outdoor air temperature when part load conditions are tested. Additionally, it allows performing linear interpolation if the unit cannot be unloaded to the specified percentage part load conditions. From equation (1), it is observed how IEER moves away from SEER and HSPF, by introducing part load testing instead of using the bin temperature based algorithm to encounter seasonal performance figures of merit. The IEER provides great improvements with respect to the previously developed figures of merit since units typically operate a significant amount of time under part load conditions. (ANSI/AHRI 2007, ANSI/AHRI 2008).

2.4 Issues related to current figures of merit and methods of testing

Every few years, SEER requirements for manufacturers are increased in the hopes of increasing energy savings. Kavanaugh (2002), expressed concerns that basing predictions on energy savings based on a single figure of merit could be inaccurate. Comparing AHRI 210/240 tests for two units made by the same manufacturer, he observed that a unit with 18-SEER had only a 6% higher EER at 95°F (35°F) than a 10-SEER rated unit. Furthermore, he indicated that some factors inflated SEER such as the bin temperatures used for calculation being lower than the actual indoor temperature during 66% of the time. Kavanaugh also mentions that the external static pressures required in the AHRI standard are typically much lower than field-measured data as indicated by Proctor and Parker (2000). Another issue, raised by Kavanaugh was the fact that SEER does not have any consideration for dehumidification and how units could be potentially designed with evaporators that are oversized with respect to the compressors used, which reduces power

consumption but can hinder dehumidification capability of the unit due to higher evaporating temperatures. Even if SEER, is related to cooling seasonal performance only, it was found that the higher SEER product line had in average a 2% HSPF lower than the lower SEER product line, therefore indicating that there is no correlation between a high SEER and a high HSPF. Kavanaugh concludes his paper by recommending a new method of testing that does not allow efficiency to be attained by hindering dehumidification capacity, has indoor return temperatures within human comfort zone and uses external static pressure difference values closer to field data.

Fairey et al (2004) also studied some of the issues of HSPF and SEER. They mentioned that even though these figures of merit provide a means for comparison between equipment, they are usually misunderstood, especially when extrapolating the results across different climate regions. Even though HSPF is region specific, US DOE nameplate requirements are based on the Climate Region 4. This paper mentions how manufacturers typically only report values for this region although AHRI standards provide procedures for calculating HSPF for the remaining five climatic regions. Additionally, consumers typically do not have access to the tested data points to calculate HSPF for different regions themselves. Consequently, HSPF for region 4 is commonly used to estimate energy performance across regions. Another concern raised in this paper, is the broadness of some of the defined climate regions. It is indicated that some cities within a same climate region can have climate conditions that widely diverge from each other. This means, an energy performance estimate for a particular region could be lacking in accuracy for a city within that same region. The authors also mention how the bin data used to calculate HSPF implicitly assume an indoor return temperature of 65°F (18.3°C) instead of a “more commonly preferred” 68°F (20.0°C) that they decided to use in their study. A 68°F (20.0°C) indoor setting increases building load, while decreasing the HSPF. Regarding SEER, the authors highlight the fact that there is no different climate region considerations for its calculation. They also mention how the EER at 95°F (35°C) is of less importance in the SEER calculation when compared to the EER at 82°F (27.8°C) which is

concerning because peak loads are typically found at higher outdoor temperatures. Like Kavanaugh (2002), this study also mentions how the static pressure differences are very low in the standards and how the more realistic values translate into lower airflow rate through the coil which increases the energy required in dry climates and decreases performance in all regions. Similar to the heating case, the indoor return temperature was decreased from 80°F (26.7°C) to 78°F (25.6°C) for their study. This causes the capacity to increase and the SEER to decrease. With these considerations, the study simulated unit performance across 15 locations in the United States to understand the variation of SEER and HSPF with climate conditions. It was found that the SEER could vary as much as 22% from the reported nameplate values. The hottest climates showed the larger decrease in performance with respect to the nameplate SEER. HSPF was found to vary even more than SEER did, with values ranging from 50% less to 40% more than the reported HSPF depending on the severity of the winter conditions studied.

2.5 Field testing

Field data is of great importance in understanding unitary HVAC performance. In this section, studies that gathered field data for rooftop units will be reviewed. Jacobs et al (2003), studied 215 roof top units in 75 newly constructed buildings in California. The goal of the project was to investigate inefficient design and installation of small commercial HVAC systems, which are well known for consuming more energy than necessary to conditioning indoor environments. In the study, the most commonly found packaged unit size was 5 TONS, while units between 1 and 10 TONS are the most commonly sold (90% of total sales) for new buildings in California. Some challenges were pointed out such as non-working economizers, improper refrigerant charge, fans that did not provide adequate ventilation air, simultaneous heating and cooling and thermostats not properly set up. One of the technologies tested in this thesis, the outside air economizer, constituted a large fraction of the issues highlighted in Jacobs et al. study. For example, 123 of the 215 units considered in their study had economizers and out of which 64% of the economizers had some type

of malfunctioning, including some of them not functioning at all (24%). Supply airflow rate was measured for 79 of the units. It was found that 39% had airflow less than 300 cfm/ton, with an average airflow rate of 325 cfm/ton. This is much less than the 400 cfm/ton on which AHRI standards are based on. This lower airflow was a consequence of the average external static pressure drop, which was reported to be close to 0.5 inches of water. This value of static pressure is quite higher than that prescribed by the AHRI laboratory testing conditions. The study highlighted a series of recommendations to the issues observed in the field, such as, improving economizer design and strongly advising to install economizers on factory rather than on site. Additionally, they recommended adding a performance based test among the AHRI standards on which economizers could be included in the RTU being tested in the lab. According to Jacobs et al. this test, together with a series of specifications on efficiency, controls and reliability are expected to incentive manufactures to develop high performance small package HVAC units.

Cowan (2004), collected data from four field studies (including Jacobs et al 2003), investigating 503 rooftop units in 181 commercial buildings, across five states in the United States. Their data were similar to those of Jacobs et al. and the issues in the units operating in the field occurred with similar frequencies as those originally reported in Jacobs et al. Thus, Cowan confirmed the challenges related to field operation due to refrigerant charge, sensors, thermostats, airflow and economizers. 42% of all units had airflow rate lower than 300 cfm/ton and this was considered too low airflow rate. Considering that AHRI standards base their ratings on a 400 cfm/ton ratio, energy savings related with optimizing airflow rate were estimated at an average of 10% considering all the units studied. It is interesting how 64% (same percentage found by Jacobs et al 2003) of the total number of studied economizers presented problems. Problems with economizers include broken, frozen or missing drive components, outside air or mixed air sensor failure, faulty repairs, low changeover temperature set point and the use of a single-stage cooling thermostat. Energy savings related with either repairing or replacement economizers, varied from 14% to 40%. Where

14% was associated to adjustments to a working economizer and 40% was associated with repairing or replacing a broken one.

An economizer focused paper by Hart et al (2006), reviewed several field studies, including some of the previously mentioned ones. In their review, they indicate how only about a third of the potential savings estimated with simulations are being found in field studies. For this reason, they decided to investigate 10 units that use economizers in Eugene, Oregon. Half of the units tested had their economizers retrofitted to meet the “Western Premium Economizer” specification developed by the Eugene Water & Electric Board (EWEB). Improvements from the typical economizer installation to the “premium” one include two-stage cooling, differential dry-bulb control and alternating integration. Differential dry-bulb control allows using outside air for economizing, whenever it is below the return indoor air temperature. This configuration, makes better use of the colder outside air to provide cooling, therefore, increasing the savings. Another improvement is the alternating integration. When alternating integration is used, the economizer is the first stage of cooling. Then, in the second stage of cooling, the compressor is activated and the economizer damper reduces the percentage of outside air to avoid comfort problems from too cold supply air. The study found that several of the economizers had problems, including the “premium” ones due to technician mistakes. In addition, a comparison between the best functioning standard economizer and the best functioning premium one indicated that the unit equipped with the premium economizer required 18.1% less mechanical cooling than the standard one. This is a result in favor of the premium economizer, but the sampling set is too small to establish such conclusion. One of the recommendations of the study is that larger sample of units equipped with “premium” economizers should be tested in order to really assess the energy savings.

2.6 The need for an additional testing protocol for RTUs

A recent paper by Hart et al (2008) suggested the need to develop an additional testing protocol for RTUs in order to be able to use the results from laboratory tests for models development of RTUs integrated with buildings and in the actual field service operation and for verification of the simulation results. Kavanaugh (2002) and Jacobs et al (2003) also pointed out interest in developing such new testing protocol for RTUs. Hart et al 2008 indicated that potential savings outside of the steady state efficiency measurements (SEER, EER, IEER, and HSPF) are not properly captured with current temperature-based methods of test. They emphasized the need for developing a load-based method of test that could isolate and quantify potential energy savings due to advanced controls or additional technologies in the RTUs that act during the cycling periods of the RTUs and during transitory periods of the RTUs when they are integrated in the actual buildings.

For example, in the Northwest sixth power plan report it was stated that relatively sophisticated HVAC engineering, smart control systems, and careful system operations are needed to reach low-cost HVAC energy savings for the commercial sector, savings which are in the order of 325MW (NPCC 2010). One of the ways of currently doing so is by increasing SEER and HSPF requirements by the US DOE. However, EER and SEER are being increased by lower amounts each time. The price of materials used for coil fabrication, restrictions in coil size and theoretical limitations in the refrigeration cycle are some of the main reasons for lower increases in efficiency.

For this reason, it was pointed out, again, the importance to carefully evaluate energy savings of small rooftop technologies beyond steady-state efficiency. Multiple strategies can provide non-steady energy savings, such as outside air economizers, control configuration, fan energy during ventilation, and cycling. The effects of these strategies on energy consumption is simply overlooked by current figures of merit coming from temperature-based methods of tests.

Hart et al 2008 presents results of simulations that evaluate the potential savings of some non-steady state efficiency improvements for rooftop units. The study, which covered eight cities in different climate zones in the United States, suggested that there was a potential for 30% to 48% energy savings from technology improvements in rooftop units. When compared to the 1.5% to 6.7% expected savings from upgrading SEER for example from 13 to 15 it is clear that investigating these technologies is of great importance. The paper also mentions that since current metrics for energy consumption do not account the savings potential of advanced technologies, there is little incentive for manufacturers to incorporate them in their units. A test procedure that evaluates total system performance and provides means for reliably comparing these technologies would allow equipment with better performance and energy savings to be well recognized and promoted. The paper recommends a comprehensive laboratory test that includes ventilation and other control improvements. These method would be able to account for economizer effectiveness, ventilation damper losses, control issues, cycling losses, ventilation operation during warm-up, the use of condenser pre-cooling, or the impact of resistance heat on heat pump effectiveness. It is also mentioned that this new testing protocol would benefit manufacturers, building owners and energy program administrators by providing a better measurement of packaged rooftop unit efficiency.

The American Society for Heating, Refrigerating, and Air Conditioning Engineers (ASHRAE), recognizing the broad impact that such load-based method of test will have among the HVAC community, proposed a research project that focused on developing new lab-based performance testing procedures to allow a range of control and other technologies to be tested and system performance determined for multiple climates using regression based hourly projections. The ASHRAE project, referred as to ASHRAE Project RP-1608 and entitled “Development of a Load-Based Method of Test for Light Commercial Unitary HVAC”, started approximately 2 years ago and focused on developing a standard test procedure in laboratory that can provides a figure of merit of packaged air-source RTUs similar to the miles per gallon figure of merit used in the

automotive industry. This thesis describes the work conducted for this project and highlight the main findings of the study.

CHAPTER III

III. OBJECTIVES

The main goal of this thesis was to investigate the feasibility a new method of test for assessing the comprehensive performance figure of merit of light commercial HVAC RTUs. The new method of test has to account for cycling effects, air circulation energy use, economizer operation, short-cycling issues of components of the RTUs and measure the potential energy savings that can come from additional technologies assembled in the RTUs, including additional (and sometimes costly) controls hardware components (for example VFDs) or innovative control strategies and algorithms. The new load-based method of test must be applicable in existing psychrometric chamber facilities with minor modifications, if any, of the instrumentation typically used in those facilities. A new load-based method of tests was experimentally investigated by using the environmental large-scale climate controlled psychrometric chamber at Oklahoma State University, which replicated various outdoor climates and realistic indoor building thermal loading conditions.

3.1 Specific Objectives of my thesis

While the overarching goal of the project is to develop a new standardize test procedure for measuring a more representative figure of merit of the next generation of Roof Top Units (RTUs) and that can potentially be used for projecting annual energy use based upon the lab testing results, this thesis is only the first step toward developing such standard. The specific objectives of this thesis were as follows:

1. To study the feasibility of a load-based method of test, and in particular to investigate the instrumentation required in the new method of test, protocols of preparing the testing units inside the lab, procedures for setting up the load conditions, and data recording and data reduction procedures.
2. To document and quantify the uncertainty and repeatability of the tests and the degree of confidence of the testing results when using a load-based method of test. These are the very first features on which a method of testing is based upon.
3. To provide a range of testing conditions that is broad enough to be realistic for representing RTUs integrated with light commercial buildings but also doable in conventional psychrometric chamber laboratory facilities available today.
4. To highlight the limitations and potential improvements of a first load-based method of test that can be used for supporting RTUs simulation model development and verification.

In summary, the project aimed to develop a new method of test for characterizing the performance of advanced unitary equipment for light commercial HVAC applications and in support of buildings and RTUs simulation models development and verification. The findings from the present study are expected to provide the basis to formulate guidelines and recommendations in order to develop further a standard protocol for a load-based method of test. In order to fulfill the objectives stated above, I conducted the following tasks:

- a. I validated the proposed method by testing two technologies on the same rooftop unit. The technologies are outside air economizer and supply air fan speed control. I ran eighty four (84) tests with outdoor ambient temperatures ranging from 37°F to 105°F (2.8°C to 40.6°C), six different indoor cooling loads and three different indoor heating loads. (Short-cycling digital scroll compressors were also tested in this project as an extra technology being studied).

- b. I conducted repetition tests to verify the accuracy and repeatability of the method of test. Repeatability and accuracy of the method were validated based at least on the following two parameters:

$$\text{Sensible Performance} = [\text{average delivered sensible MBH}] / [\text{average unit power input}]$$

$$\text{Total Performance} = [\text{average delivered total MBH}] / [\text{average unit power input}]$$

- c. I run tests on which perturbations were purposely introduced in the cooling load being set to determine the sensitivity of the finally reported figures of merit to the induced load variations.
- d. I adjusted external fan static pressures to more typical commercial values that are in agreement with field data available in the literature. The static pressure was higher than the set by the current testing standards such as ASHRAE 116-2010.
- e. I investigated the impact of testing time (and recording start time and recording period) on the resulting figures of merit by analyzing the recorded data based on different test durations (i.e. 30 minutes, 60 minutes, 90 minutes, and 120 minutes) and different cycle based approaches. That is, when ON-OFF controls are used, evaluate the performance figures of merit based on number of cycles and starting points (i.e. beginning of and on cycle, middle of and on cycle, beginning of and off cycle and middle of and off cycle). I
- f. I finally made some recommendations for what type of instrumentation, testing procedures, and data reduction methods should be used for setting building loads in the lab and measuring the associated figures of merit that are most accurate, repeatable, and representative of the RTU integrated with the building.

I would like to emphasize that the goal was to develop a method of testing for unitary HVAC equipment in order to provide useful data for simulation model development and verification. The data coming from the tests conducted in a laboratory characterize unit performance when it operates in the field as if the unit was installed in an actual building. The data describe a comprehensive

figure of merit of the entire system, that is, of the RTU with integrated technologies, in terms of power usage required to deliver a net capacity to the building. This means the testing units were integrated with the technologies during the experiments and they were run as one complex system. The load-based method of test provided a figure of merit for the entire system; this was a new approach for testing for RTUs and while it was simply to define and intuitive to understand, it was quite challenging to implement in a laboratory. The approach commonly taken today is to develop models and verify the simulation results for each individual RTU technology (for example only the economizer in specific economizer only tests) separately from each other and then derive a figure of merit for each individual technology (for example the effectiveness of the economizer). Then once each technology is assembled together in the RTU, the individual figures of merits of each technology are combined together in order to predict an overall figure of merit for the RTU with the specific technologies integrated in it (for example the simulations predict the COP of the RTU with the economizer). In addition, the boundary conditions for the RTU in the new method of tests were expected to be closer to the actual operating conditions of the RTU when it is integrated with building because outdoor temperature, outdoor humidity, and indoor thermal loads are what the RTU responds to in actual building applications. Setting these boundary conditions allows the unit to freely cycle reduce its delivered capacity in case of part load conditions, ramp up or turn down its compressors or fans, open or close its economizer, and to modulate its supply airflow and air temperature according to any control algorithm implemented in the RTU. Thus, data from a load-based test can be used for modeling specific non-steady state features of the equipment. What is required by the new load-based method of test is that the RTU and any technology integrated with the RTU, continuously provides a range indoor return air temperature and humidity that matches indoor environmental comfort conditions for the occupied space of a building (ASHRAE 2013, Cremaschi 2013).

3.2 Thesis organization and brief highlights of each chapter

This thesis is organized in eight chapters. Chapter I is introduction and motivations of the study. Chapter II is a review of state-of-the-art literature of this topic area. Chapter III states the objectives of the thesis and the main tasks conducted in the present study to fulfill the objectives. Chapter IV described the experimental facility, the instrumentation, and the Roof Top Unit that was integrated with economizer technology and variable fan speed technology and then was tested. Chapter V describes the methodology for load-based testing, the conditions tested and how they were derived from simulation data of typical small office building thermal loads. Chapter VI shows the data reduction process, main equations used, and the validation of the capacity measurements with OSU psychrometric chamber. Chapter VII shows the results of the experimental testing campaign, which included 64 tests with the RTU in cooling mode tests and 5 tests with the RTU in heating mode. In the same chapter, results from an experimental uncertainty analysis, alternative methods for data reduction and alternative test durations are discussed. Finally, Chapter VIII summarizes the main findings from the present work, provide the conclusions, and suggests some recommendations for future work.

CHAPTER IV

IV. EXPERIMENTAL SETUP

4.1 Psychrometric Chamber Facility

The experiments carried out for investigating the feasibility of the new method of test developed in the present thesis were conducted in a large-scale psychrometric chamber at Oklahoma State University. This psychrometric chamber was an environmental simulator that consisted of two adjacent rooms where air was conditioned to artificially reproduce a wide range of outdoor conditions as well as indoor environments by replicating indoor comfort conditions with or without live thermal load in it. In order to simulate these environments temperature, humidity, and air speed in the rooms are controlled over a wide range of conditions. The OSU psychrometric chamber is designed to test HVAC unitary equipment. It is intentionally oversized to minimize the interference of the testing equipment with the walls and the ceiling of the chamber and it is sufficiently large (each room dimensions are 19ft (5.8m) x 21ft (6.4m) x 16ft (4.9m)) to test split systems and RTU with capacity up to 20 ton of refrigeration.

The chamber is able to reproduce thermal loads of up to 20 tons of refrigeration with the outdoor room conditions ranging from 10°F to 120°F (-12.2 °C to 48.9 °C)/10% to 95% relative humidity and the indoor room from 55°F to 120°F (12.8°C to 37.8°C)/20% to 85% relative humidity. These conditions are achieved in each room by passing the air through conditioning loops which take the

air to the desired psychrometric states and then circulates it into the rooms through a raised perforated floor. This design ensures vertical airflow to be uniformly distributed across the footprint of the facility. The air in the room circulates back to the conditioning loops after it passes through filters located on the ceiling of the chamber. A schematic of OSU Psychrometric chamber facility is shown in Figure 1.

4.1.1 Conditioning Loops

The conditioning loops are installed inside vertical bays (bays 1 and 3 for outdoor room and 4 and 6 for indoor room) adjacent to each room as shown in Figure 1. The main components of the loops are cooling coils, electric resistance heaters, steam wands and fans for air circulation. Chilled water circulates inside the cooling coils, shown in Figure 2, and their capacity is controlled by variable speed pumps, electronic mixing valves and electro-mechanical bypass valves. The cooling capacity of the coils is controlled so that when air passes through them it is cooled and dehumidified below the desired room psychrometric state. The air passes then over electric resistance heaters that raise the air temperature up to the desired room temperature. The power to the heaters is controlled by a PID control algorithm that matches the room dry bulb temperature to the reference set point. After passing over the electric heaters, air passes over steam wands where moisture is added to the air, finally raising the humidity to the desired state. The wand is connected to a steam generator that is also controlled by a PID control algorithm that matches the room wet bulb temperature to the reference set point. This conditioning procedure is applicable for temperature based testing which are the traditional ASHRAE/AHRI standards.

The cooling coils have large thermal inertia and are slow to change temperature. This characteristic helps with the stability of the chamber when a live load is activated inside the room. The electric heaters and steam generator allow for quicker adjustments of the load in order to maintain process conditions close to the set points.

For load-based testing (the new method being presented), the outdoor room operates the same way as in temperature based operation, whereas the indoor room undergoes a different procedure. The indoor room is where the thermal load is set so that the unit being tested matches it in order to find the desired dry bulb set point. In load-based testing mode, the cooling coils are off time, which means, there is no chilled water circulating through them. The constant sensible load is set by controlling the electric resistance heaters to a value of the desired sensible load. The electric resistance heaters are not the only contributors to the sensible load because the air going through the conditioning loops also sees its energy increased by the power of the fans. The desired latent load is set by fixing the flow rate and temperature (enthalpy) values of the steam coming out of the wands.

4.1.2 Instrumentation of the facility

In order to assess a comprehensive performance figure of merit for unitary equipment, a set of sensors, probes, and flow nozzles are installed in the facility. These measuring devices are in compliance with the requirements of the air enthalpy method in standard ANSI/ASHRAE 116-2010. The schematic of the psychrometric chamber with the position of the relevant instrumentation is shown in Figure 1

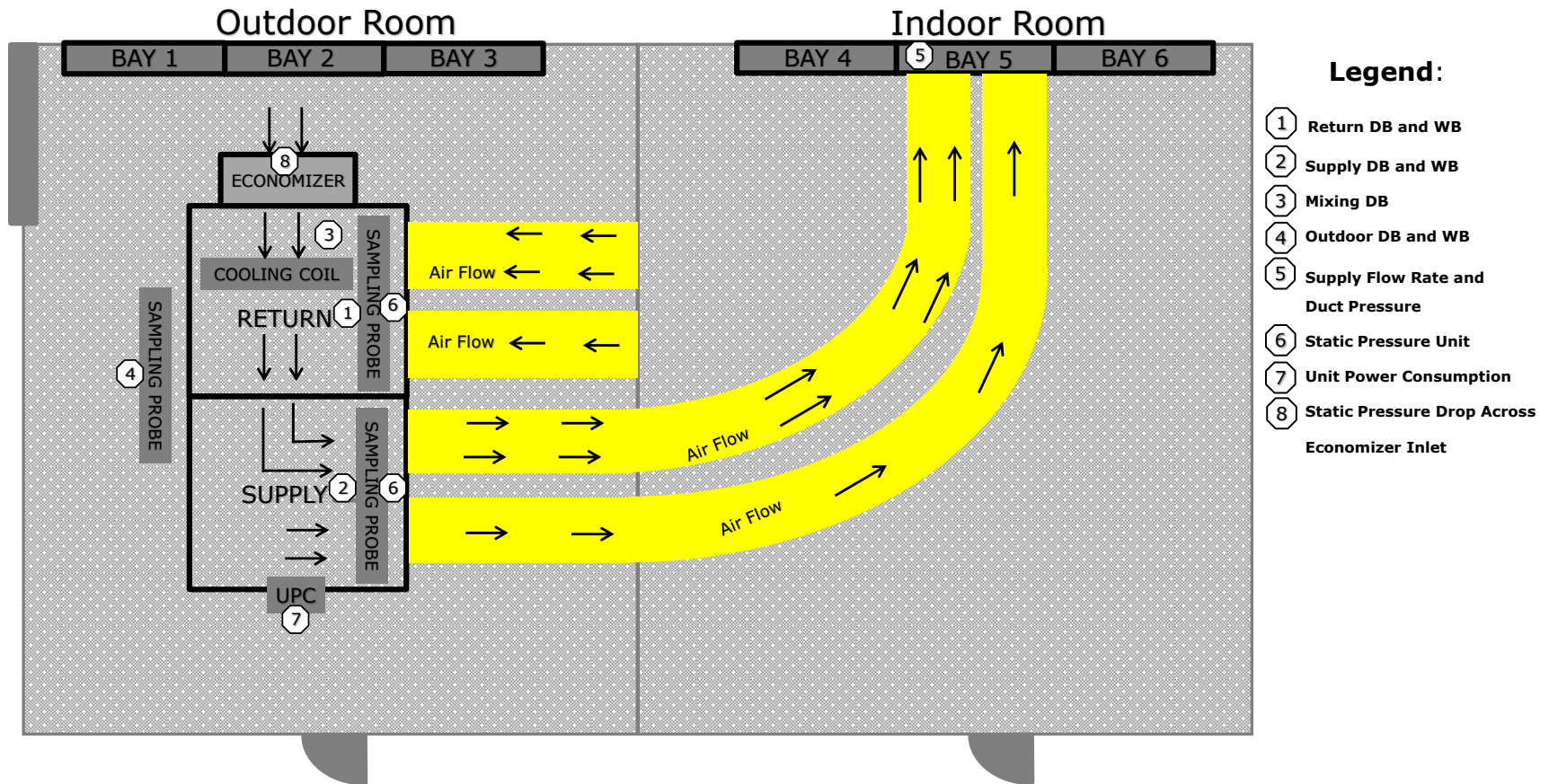
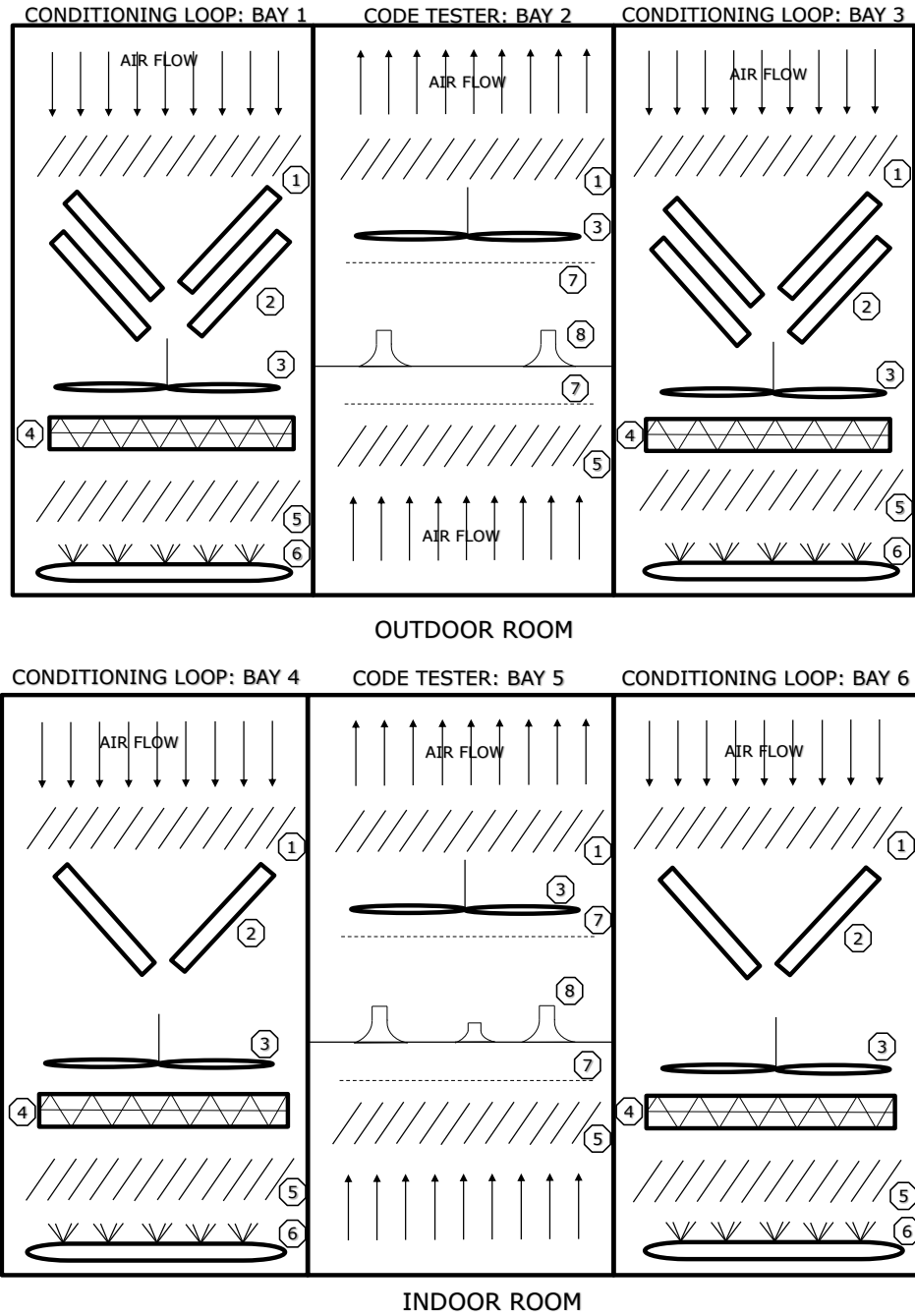


Figure 1: Schematic floor layout of the RTU under testing when it was installed inside the OSU psychrometric chamber facility; locations of the main measuring sensing points, and definition of the conditioning bays of the chamber



Legend:

- | | | | |
|--------------------|--------------------------------------|----------------|-------------------|
| ① Upper Air Damper | ② Cooling and Dehumidification Coils | ③ Blower | ④ Electric Heater |
| ⑤ Low Air Damper | ⑥ Humidifier | ⑦ Air Diffuser | ⑧ Flow Nozzles |

Figure 2: Schematic representation of the conditioning bays (bay 1 and 3, bay 4 and 6) and code tester bays (bay 2 and bay 5) for outdoor and indoor rooms.

The humidity, air temperature, and pressure are measured directly at the unit supply and return locations and at the indoor room supply air stream (see Figure 1). This is achieved with temperature sampling devices and pressure taps installed immediately at the beginning of the duct system that connects the unit to the indoor room. With this configuration the pressure drop and heat transfer through the connecting ducts are excluded from the measurement. Indoor room air stream is characterized by using a flow nozzle measuring device referred in this guidelines document as to code tester. Table 1 shows a summary of OSU chamber most relevant instrumentation.

Table 1: Summary of OSU psychrometric chamber main instrumentation

Parameter	Manufacturer	Model	Nominal Value	Uncertainty
Differential Pressure Across Nozzles	Setra	Model 264	0 to 3(747) InWC (Pa)	±0.25% full scale
Differential Pressure Across Unit	Setra	Model 265	0 to 3(747) InWC (Pa)	±0.25% full scale
Pressure at Nozzle Inlet	Setra	Model 266	-1.5(-374) to 1.5(374) InWC (Pa)	±0.25% full scale
Pressure of Indoor Room	Setra	Model 267	-1.5(-374) to 1.5(374) InWC (Pa)	±0.25% full scale
Unit Supply Dry Bulb RTD	Omega	PR-10	5(-15) to 140(60)°F(°C)	±0.2(0.1)°F(°C)
Unit Supply Wet Bulb RTD	Omega	PR-10	5(-15) to 140(60)°F(°C)	±0.2(0.1)°F(°C)
Unit Return Dry Bulb RTD	Omega	PR-10	5(-15) to 140(60)°F(°C)	±0.2(0.1)°F(°C)
Unit Return Wet Bulb RTD	Omega	PR-10	5(-15) to 140(60)°F(°C)	±0.2(0.1)°F(°C)
Nozzle Dry Bulb RTD	Omega	PR-10	5(-15) to 140(60)°F(°C)	±0.2(0.1)°F(°C)
Barometer	Valsala	PTB110	0.002(500) to 0.004(1100) InWC(hPa)	±0.12(30)InWC(Pa)
Unit Power Watt Transducer	Flex Core	AGW	0 to 45000 Watts	.2% Rdg
Refrigerant High Pressure	Setra	Model 206	0 to 500 (3447) psig (kPa)	±0.13% full scale
Refrigerant Low Pressure	Setra	Model 206	0 to 500 (3447) psig (kPa)	±0.13% full scale
Humidity Sensor	Omega	HX71-MA	15% to 85% RH	±3.5% RH

4.1.2.1 Temperature measurements

In the indoor room, temperature-sampling probes are designed to mix the airflow and average mechanically the temperature of the air in several points through the cross section of the supply and return ducts. The characteristic temperature of the outdoor room was measured in the vicinity of the condenser and with a dry bulb and wet bulb sample probe mounted right at the front of the condenser as shown in figure 3. The probe sampled the air in several locations and mechanically averaged the samples into one mixed air stream. Then one RDT measured the dry bulb temperature of the mixed air stream and one RDT with wet sock wrapped around it measured the wet bulb temperature of the air stream coming from the probe.

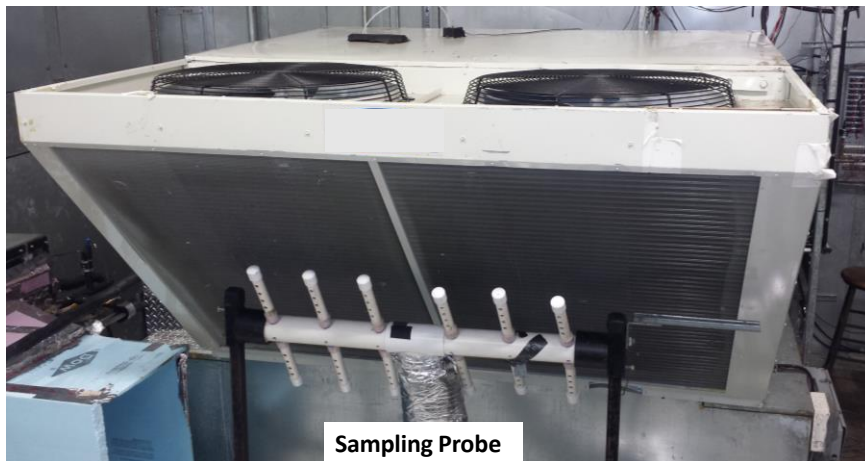


Figure 3: Outdoor sampling probe

The sampling probes are in compliance with ASHRAE Standard 41.1 for temperature measurement. A low speed fan is used to transfer the mixed air stream to remote dry and wet bulb sensors, which are in a fixed position and are connected to the sampling probe by using flexible air ducts that are impermeable to water vapor. The fan is located downstream of the instruments so that the heat generated by the fan does not affect the temperature measurements. The dry bulb and wet bulb temperatures are measured by using high precision Platinum RTDs that are calibrated periodically in-house and in-situ to 0.2°F (0.1°C) by using a temperature bath and a high precision

NIST traceable thermometer. For better accuracy, the RTDs were calibrated to two different ranges for cooling tests and one for heating. Table 2 summarizes the ranges of calibration used. The calibrations were verified using

Table 2: RTDs calibration ranges

	Low Cooling Load		High Cooling Load		Heating	
	Low Limit	High Limit	Low Limit	High Limit	Low Limit	High Limit
T_{nozzle} , °F (°C)	55.3 (12.9)	76.6 (24.8)	44.5 (7.0)	65.9 (18.8)	55.3 (12.9)	104.2 (40.1)
$T_{db,supply}$, °F (°C)	55.3 (12.9)	76.6 (24.8)	44.5 (7.0)	65.9 (18.8)	55.3 (12.9)	104.2 (40.1)
$T_{wb,supply}$, °F (°C)	49.9 (10.0)	74.0 (23.3)	41.9 (5.5)	63.4 (17.4)	49.9 (10.0)	89.8 (32.1)
$T_{db,return}$, °F (°C)	72.4 (22.5)	79.5 (26.4)	74.2 (23.5)	84.7 (29.3)	67.4 (19.7)	104.9 (40.5)
$T_{wb,return}$, °F (°C)	58.0 (14.5)	74.2 (23.5)	58.0 (14.5)	68.9 (20.5)	53.0 (11.7)	74.2 (23.5)
$T_{db,out}$, °F (°C)	46.1 (7.8)	105.9 (41.0)	46.1 (7.8)	105.9 (41.0)	15.0 (-9.4)	105.9 (41.0)
$T_{wb,out}$, °F (°C)	46.1 (7.8)	73.0 (22.8)	46.1 (7.8)	105.9 (41.0)	32.1 (0.04)	73.0 (22.8)

The wet bulb RTD was wrapped by a soft cotton tubing with a fine mesh wave referred to as “wick”. The wick is dipped in a water container filled with distillate water that evaporates as the air passes through the bulb, therefore providing a measurement corresponding to the thermodynamic wet bulb temperature. As water in the container evaporates, make up water flows from a reservoir located on top of the water container due to hydrostatic pressure difference. The dry bulb sensor is located upstream of the wet bulb sensor so that moisture evaporation from the wet bulb does not affect the dry bulb measurement. During steady state test period, the dry bulb temperatures in each room are maintained within $\pm 0.3^{\circ}\text{F}$ (0.1°C) of the desired set point, and the indoor wet bulb temperatures are maintained within $\pm 0.4^{\circ}\text{F}$ (0.2°C) of the set point for wet bulb (Worthington 2011).

In addition to the dry and wet bulb probes, a relative humidity sensor is installed in the arrangement as a secondary measurement for verification and diagnosis of the primary sensors. The relative

humidity sensor is a thin film polymer capacitor whose capacity is proportional to the amount of moisture in the air. Figure 4 shows the dry bulb, wet bulb and RH sensor arrangement.

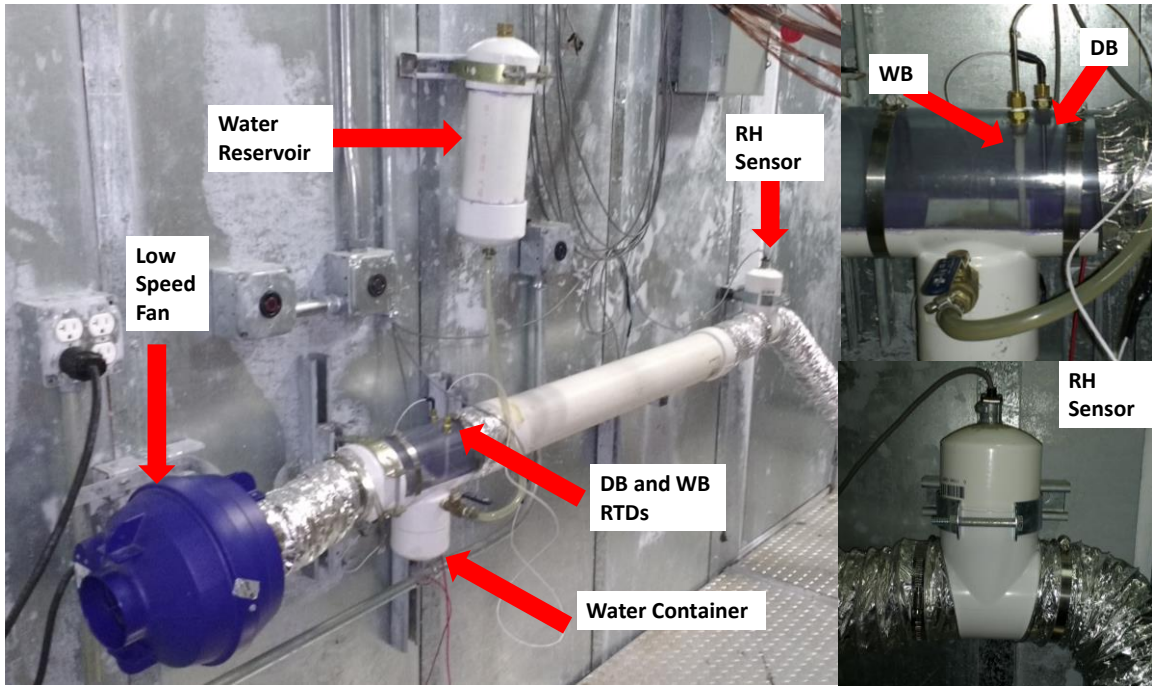


Figure 4: Example of an OSU in-house custom-made dry and wet bulb probe located in the outdoor room of the psychrometric facility

4.1.2.2 Supply Airflow Measurement

The code tester for the indoor room is located in bay 5 and for the outdoor room in bay 2 (see Figure 2) and it is composed by a nozzle bench of flow nozzles that induce pressure drop in the air stream in order to measure airflow rates. The code tester arrangement is in compliance with ASHRAE Standard 37, ASHRAE Standard 37, Section 6.2, “Nozzle Airflow Measuring Apparatus,” and Section 6.3, “Nozzles.”. The pressure drop across the flow nozzles is directly measured with static pitot tubes located before and after the nozzle bank. The pitot tubes are located in the center of each one of the faces of the squared cross section of the code tester according to figure 7a of ASHRAE Standard 37. There are four pitot tubes upstream and four downstream of the nozzle bank. The pitot tubes are manifolded according to figure 9 of ASHRAE Standard 37 and connected to a differential

pressure transducer. The airflow rate is calculated based on the diameter and number of flow nozzles used for the measurement and based on the air density at the inlet of the flow nozzle. The air temperature and static pressure are measured at the inlet of the flow nozzle to estimate the air density. A platinum RTD is used to measure the nozzle inlet temperature and a low-pressure differential pressure transducer to measure the nozzle inlet pressure. Additionally, a type T (copper – constantan) thermocouple wire is used as a secondary measurement for air inlet temperature. This measurement is used for verification and diagnosis of the RTD. The code tester design is based on the same concept as the wet outdoor room wet bulb probes where it is fixed in a remote location and it is connected to the unit using large flexible air duct. A variable speed blower and a set of dampers are also installed inside each code tester to balance the static pressure and pressure losses in the connecting air ducts. To minimize the measurement error of the airflow rate, the nozzle configuration in the code tester is selected such that the pressure difference across the nozzles during the actual test is at least 1 in H₂O (~249 Pa) whenever operating conditions allow it. Because the differential pressure transducer has 3 inch H₂O (~747 Pa) full scale and accuracy 0.25% of the full scale, when the actual pressure difference is 1 in H₂O (~249 Pa) the resulting uncertainty error in the airflow rate measurement is within 0.35%. Worthington (2011) developed an algorithm for nozzle configuration selection, which is built into the data acquisition software of the chamber. The nozzle bank is composed of ten different diameter nozzles. Six of 5.5”, two of 4”, one of 3” and one of ½”. The nozzle configuration selected for this project is shown in figure 5 along with the other components of the code tester. In this configuration, the 4” and the ½” nozzles are closed. This configuration optimizes airflow uncertainty in the full fan speed only, but the airflow uncertainty when the fan is operated at low speeds increases to 0.75% because the pressure difference across the nozzle decreases to approximately 0.5 in H₂O (~125 Pa). In this project, the supply air fan is operated at both low and high speeds within the same test. An ideal configuration for low speed fan operation is not suitable, because the pressure drop across the nozzle can be higher than the differential pressure transducer range when the supply air fan operates at higher speeds.

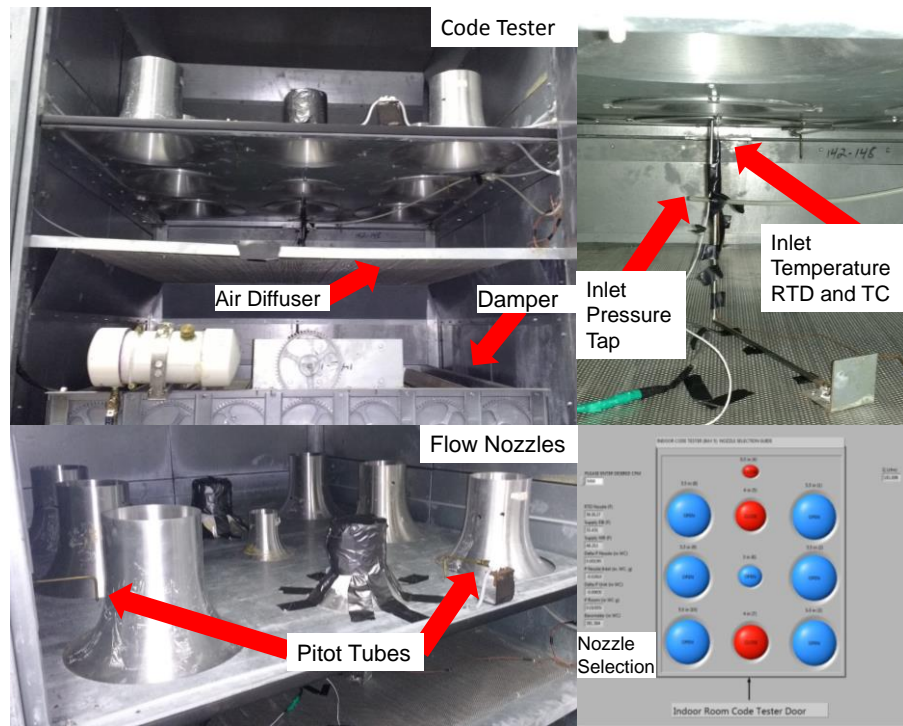


Figure 5: Indoor room code tester showing the airflow nozzles, RTDs, pitot tubes, and the corresponding LabVIEW data acquisition graphic user interface for the selection of the nozzle configuration

4.1.2.3 External resistance to airflow measurements

The external resistance to airflow is the drop in pressure of the supply air as it goes through the ducting system, the building (chamber indoor room) and returns to the unit. This quantity, also known as Unit Static Pressure Difference has a direct impact in supply air fan power consumption. A differential pressure transducer was used to measure this quantity. The instrument range is 0 to 3 in H₂O (0 to 747 Pa) and the uncertainty is $\pm 0.25\%$ of the full scale. Pressure taps were located exactly at the supply and return points in the unit, therefore excluding pressure drop and heat transfer through the connecting ducts from the measurement. This configuration complies with ASHRAE 116-2010 section 6.8 requirements.

4.1.2.4 Economizer Airflow Measurements

An outside air economizer is installed in the heat pump unit used in this project. Economizer specifications will be described in section 4.2.3. A procedure to measure outside airflow through the economizer was developed. The procedure is intended to be as little unit-invasive as possible by relying on the chamber instrumentation with some minor instrument additions to the unit itself. The airflow rate measuring method is very similar to the one used to measure the supply airflow rate with the code tester nozzle bank arrangement. For this procedure, the economizer inlet opening can be thought of as the nozzles in the code tester. An electronic differential pressure transducer is used to measure the static pressure difference at the economizer inlet opening with a 0-1 in H₂O (0-249 Pa) of range and an accuracy of $\pm 1\%$ of full scale. A series of pitot tubes are arranged around the economizer inlet opening to obtain a mechanical average of the pressure drop of the air stream going through the economizer. One side of the pressure measuring device is connected to four manifolded static pressure taps installed within the most inner side of the inlet opening of the economizer. The other side of the pressure transducer is open to the outdoor room ambient, therefore capturing the atmospheric pressure. The four static pressure taps are manifolded in a similar way to figure 9 of ASHRAE Standard 37. There are pressure taps in three out of four sides

of the economizer opening due to accessibility reasons for installation. Figure 6 shows the Pitot tube manifold and the differential pressure transducer. A correlation is used to calculate the flow rate going into the unit through the economizer. The procedure to obtain this correlation is described in chapter V.

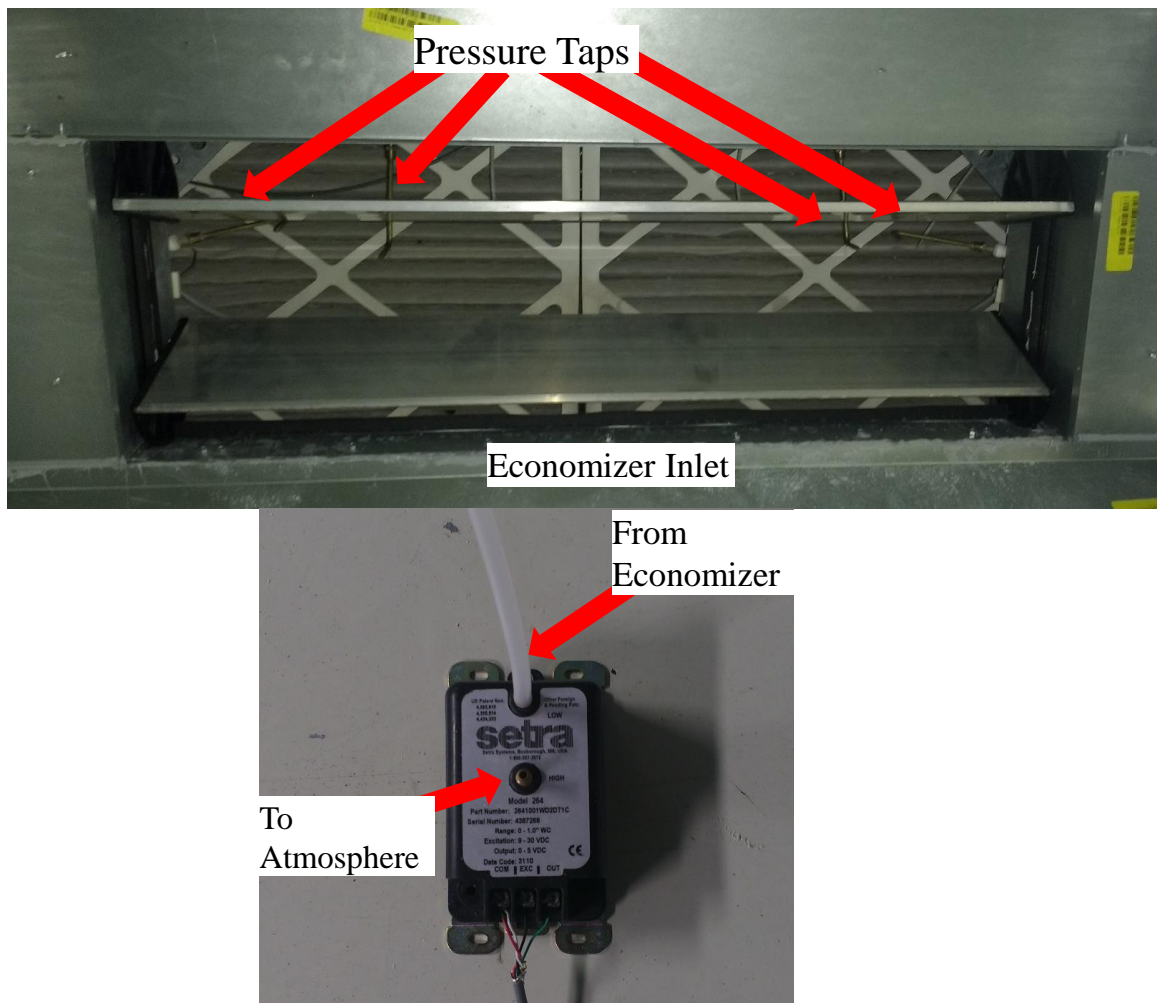


Figure 6: Installation of the pressure taps across the economizer in order to estimate the airflow rate entering the economizer

4.1.2.5 Unit Power Consumption

The unit power is measured by using a high precision AC watt transducer. Voltage and current of the three phases that power the unit are inputs to the watt transducer. In an AC circuit, the power

consumed is the product of the current times the voltage, times the cosine of the phase angle between current and voltage. The cosine of this angle is known as power factor. The watt transducer, sometimes also referred to as wattmeter has an accuracy of 0.2% of the reading, including the combined effects of voltage, current, load and power factor. The instrument can measure power between 0 and 45000 Watts and has an output of 4 to 20 mA.

4.1.2.6 Data Acquisition and Control System

Overall, the chamber currently has 384 sensors that are used to determine the response, behavior, and adjustments needed to maintain indoor and outdoor room set points as well as monitor the experiments in the facility. Sensors for the testing equipment currently include 256 thermocouples, 32 high accuracy RTDs, 4 relative humidity probes, 8 differential air pressure transducers, 1 barometer, 1 watt transducers and 81 analog inputs. A National Instruments PXI (open, PC-based platform for test, measurement, and control) with LabVIEW Real Time software is the platform for the data acquisition and control of the chamber. The built-in data acquisition system acquires all the data from the sensors and transducers and sends them to the chamber process and control main computer. The custom-built LabVIEW interface shows the status of the equipment and the conditions of the process air in real time (see figure 7). Parameters are adjusted automatically using 192 analog outputs that control different components within the conditioning loops. The user can choose to operate the chamber in manual or automatic mode. In manual mode, the user can control each component independently, while in automatic mode the chamber adjusts the components to maintain a user defined temperature and humidity. The process control program is also capable of combining both manual and automatic controls. This capacity is of great relevance for this project since it allows automatic control of the temperature and humidity in the outdoor room of the chamber, while manually setting sensible and latent loads in the indoor room. During recording periods, the sample rate from the sensors is typically set to 2 seconds but it can reach a maximum sample rate of 0.25 seconds for transient tests such as cycling on/off tests. For more information

on the Psychrometric Chamber installed at Oklahoma State University, refer to Cremaschi and Lee (2008) and Worthington (2011).

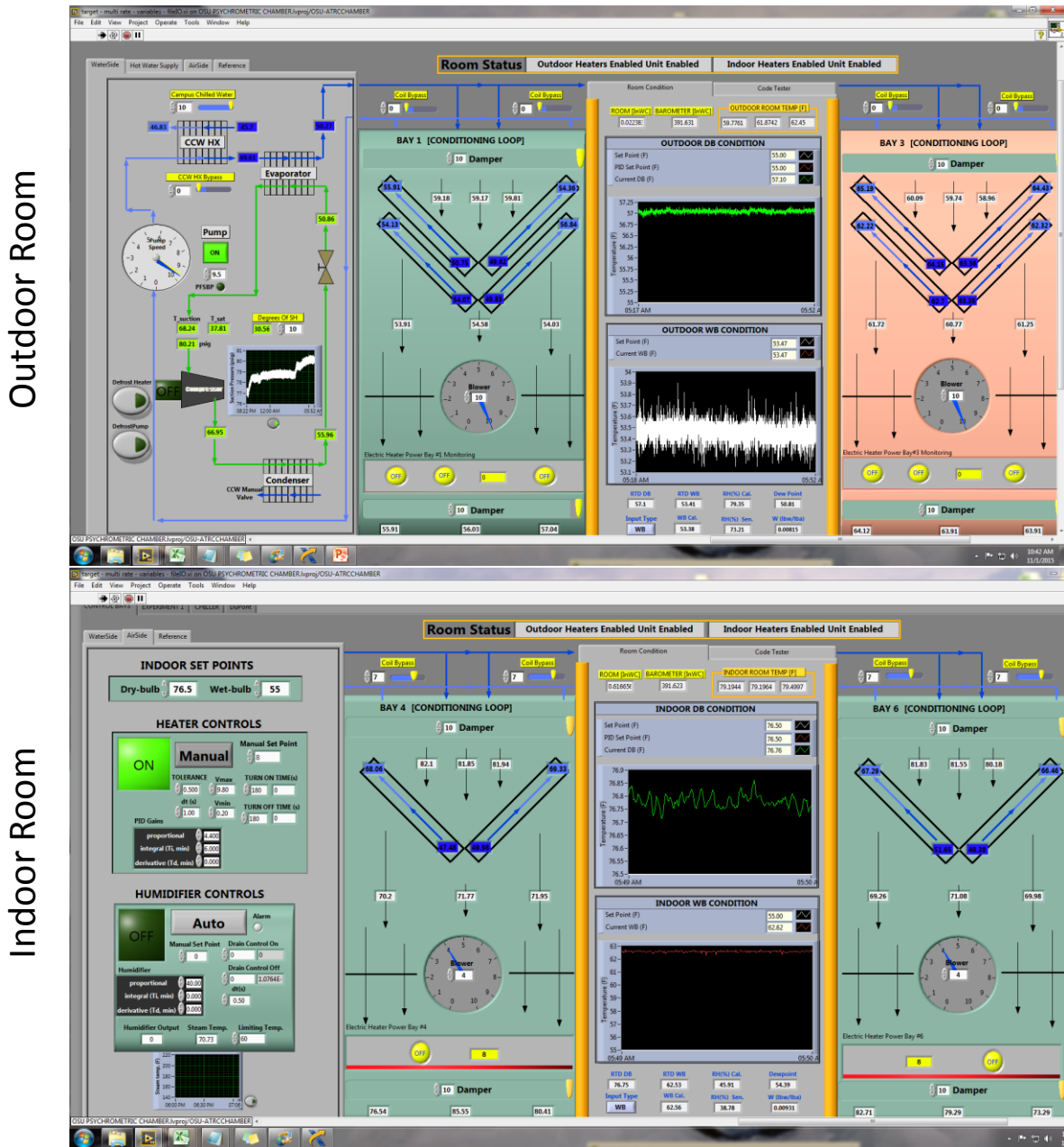


Figure 7: Example of the in-house custom-made Real Time LabVIEW graphic user interface used to monitor and control the psychrometric conditions of the outdoor and indoor rooms during the tests

4.2 Experimental test bed: 15-ton Rooftop Unit

The equipment used for the experiments was an electrically driven rooftop air-to-air heat pump with 15-ton nominal capacity. The unit is supported by an 8-wheeler cart wagon, which is also designed to accommodate the unit supply and return plenums, and the air sampling probes. The cart supply and return plenums are connected to the door that separates indoor and outdoor rooms and then to the code tester by using a series of flexible 24-inch diameter neoprene ducts (see ducts represented in yellow in Figure 1). The rooftop unit has two digital scroll compressors, a variable speed supply air blower, variable speed condenser fans, and associated variable speed drives. 80 kW (272971 BTU/h) of auxiliary electric heat to supplement the heat pump. The unit includes a controller that allows adjusting the compressors, fans and blowers speed for partial load conditions.

Table 3 shows a summary of the unit specifications, and Figure 8 shows several views of the 15-TON RTU installed in OSU psychrometric chamber for this project.

Table 3: Specifications of the Roof Top Unit (RTU) used in the present work

Unit Type	Roof Top Unit/Air-to-Air Heat Pump, Electrically Driven
Nominal capacity	15-tons of refrigeration
Refrigerant	R-410A
Nominal airflow rate	3600 cfm
Supply air fan	460 VAC – 3 phase – 5hp (3.73 kW) (Variable Speed)
Condenser fans	2 – 460 VAC – 3-phase – 560 W
Compressor	2 x Digital Scroll compressor. Nominal Power: 6 hp
Expansion valve	1 thermal expansion valve per stage (2 for each stage of heating and 2 for each stage of cooling)
Economizer	Gear driven, sensible controlled, opposing blades, with manometric exhaust



Figure 8: Photos of the 15-ton nominal capacity air-to-air RTU used in the present work and installed inside OSU psychrometric chamber

4.2.1 RTU custom-made controller

The unit counts with a Java-based controller. The controller is capable of integrating a variety of devices and protocols allowing the unit to be remotely controlled in real-time over the Internet. The controller has a user interface, which is installed in a separate computer from the one controlling the psychrometric chamber. The software also has a web version for the unit to be controlled over a standard internet browser. The controller collects a series of signals such as supply air temperature, return air temperature, supply-static pressure, indoor room thermostat, air-flow-

switch, coil temperature and variable frequency drive signals for supply air and condenser fans. The controller has its own built-in logic, which mainly responds in normal operation to supply and return air temperature settings and the room thermostat. This logic can be by-passed in the controller software by overriding several of the automatic settings. Hence, compressor percentage capacity, supply air fan speed and condenser fan speed can be controlled independently from the unit thermostat and independently from each other. This provides an advantage during the verification of the load-based method of testing in case of parametric investigation of each component operation by applying user imposed control logics. Figure 9 shows the controller and its user interface.

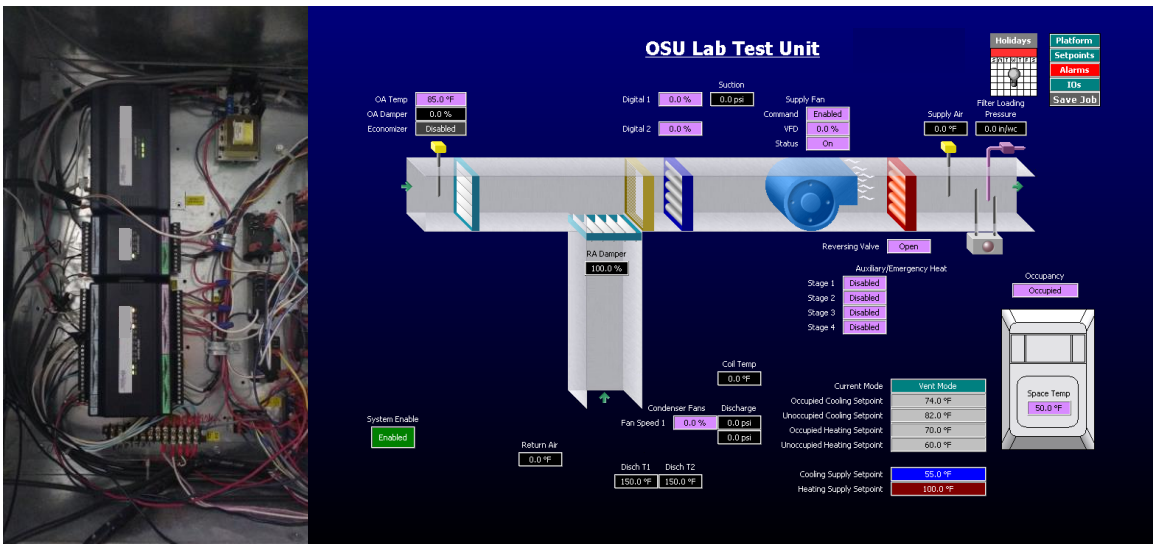


Figure 9: Photo and graphic user interface of the RTU custom-made controller

4.2.2 Digital Scroll Compressors of the RTU

Two 7.5-ton (90000 BTU/h) digital scroll compressors, which operated in tandem, were installed in the rooftop unit. The compressors provide variable capacity outputs ranging from 10% to 100% in a very smooth and quick way. Among the advantages of this type of compressor is the ability to match varying heating and cooling loads, while providing precise temperature and humidity control.

Scroll compressors use two interleaving scrolls to compress the refrigerant vapor. One scroll is fixed; while the other orbits eccentrically, compressing the refrigerant pockets that are trapped between the two scrolls. Load modulation is achieved by utilizing axial scroll compliance. That is, the scrolls are forced to separate, causing compression of the refrigerant to stop without stopping the compressor motor. When the scrolls are separate, the output capacity is 0%. When the scrolls are engaged compressor output capacity is 100%. The period of time that the scrolls are engaged or separated are equal or less than 30 seconds. The average compressor-capacity output is the result of the ratio of the ON and OFF cycling times. That is, if the compressor is ON for 15 seconds and then OFF for 15 seconds, the average output capacity is 50%. This allows the compressor to achieve infinite capacity modulation between 10% and 100%. Corti and Marelli (2013) thesis provides more information on the digital scroll compressors installed in the RTU used in the present work at Oklahoma State University.

4.2.3 Economizer

An outside air economizer is a set of components that allows the use of outside air for cooling instead of, or in addition to operating a mechanical refrigeration compressor (Hart et al 2006). Using outside air for cooling decreases the capacity that the unit compressor must provide in order to achieve indoor, therefore providing energy savings. For this project, an economizer was installed on the left side of the unit. The economizer outside air damper has opposed blades, which provide a better modulation of the outside airflow. The return air damper has parallel blades. Both dampers are gear driven, which avoids the excess play and bind that occurs with linkage economizers. When the outside air damper opens, the return air closes and vice versa.

Figure 10 shows a schematic for the economizer configuration used in this project. When cooling is required and the outside air temperature is at sufficiently low value, the outside air damper opens to provide “free” cooling. When cooling is not required, the outside air damper remains at a position

that provides minimum outside air ventilation. In addition, when the outside air damper opens, the supply air fan is increased to take better advantage of the cold outside air. The excess return air is exhausted through a barometric damper. This damper operates based on the pressure difference between the return air and the atmospheric pressure. In the outdoor room of the chamber, walls and other surfaces close to the relief damper can cause the exhausted air to recirculate back to the economizer inlet opening. For this reason, an open duct was installed to deviate the warm exhaust air from the economizer inlet (see figure 8).

The type of control sequence used in this project can be referred to as single sensor temperature changeover. The changeover sequence is the one that determines when the outside air is too cold, too hot or too humid for the economizer to open. Changeover sequences are classified by mode and by sensor type. The sensor can be either temperature or enthalpy type. The changeover mode can be single sensor or differential. The single sensor mode only looks at the outdoor air temperature or enthalpy to determine if the air is suitable for “economizing”. The differential mode looks at the temperature difference (or enthalpy difference) between the return and the outside air. Temperature sensors are sufficient for western US, while enthalpy sensors are suitable for more humid eastern US. Differential changeover provides more savings, since the economizer is activated whenever the outside air is colder than the return air instead of a single established outside air temperature value. The mixed air temperature is also monitored. Very low mixed air temperature results in extremely low supply air temperatures, which can cause occupants to feel discomfort. When this is the case, the economizer returns to the minimum outside air position (Hart et al 2006).

In summary, supply, return, mixed and outside air temperatures are monitored to properly control the economizer. Sensors are placed in the positions shown in figure 10 to monitor these values. Outside and mixed air temperature signals are fed to the economizer controller.

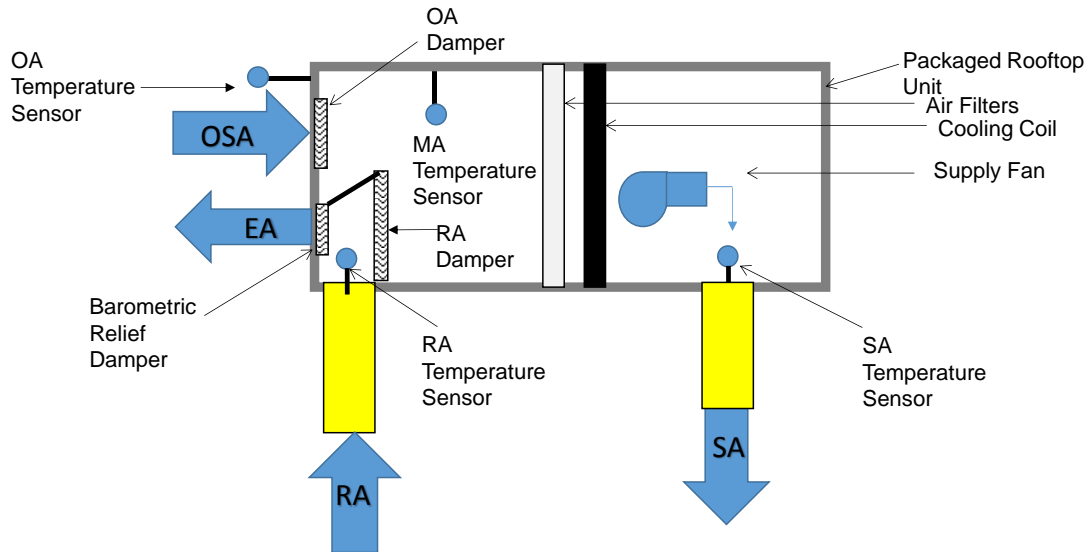


Figure 10: Side view schematic the RTU with economizer when it was installed in the OSU outdoor room chamber for the tests of the present study (RA: return air, SA: supply air, OA: outside air, MA: mixed air)

The controller an expandable economizer control system. The model of the controller is JADE and its input power is 24 Vac. The JADE also requires a 24 Vac input signal that indicates if cooling is required. A thermostat normally provides this signal, however, in this project the thermostat is simulated with the laboratory control equipment. The operator determines whether cooling is required and activates a relay that sends the 24 Vac input to the controller. When conditions for economizing are present, the controller sends a 2-10V signal to the economizer actuator, which opens the damper until a desired mixed air temperature is reached. Figure 11 shows the relevant input and outputs of the JADE controller. Specific thermostatic settings for economizer operation used in this project are explained in the following chapter.



Figure 11: Photo of the economizer controller (standard commercially available JADE model controller) used in the RTU for the tests of the present work

CHAPTER V

V. TEST CONDITIONS AND EXPERIMENTAL METHODOLOGY

The new testing protocol for unitary HVAC equipment developed in this project departs from current standards, ASHRAE 116-2010, ASHRAE 37-2009, AHRI 210/240 and AHRI 340/360. In these standard methods of test, the RTU is typically tested at steady-state full- or part-load operation conditions and at specified indoor and outdoor dry and wet bulb temperatures. The new testing approach developed in the present work aims to characterize the unit performance at specified outdoor dry and wet bulb temperatures and specified building space sensible and latent loads. These were generated by using the conditioning equipment of the indoor room of the psychrometric chamber facility. Test conditions used in the present work represented common outdoor dry and wet bulb temperatures for two different climate zones in the United States. The specified sensible and latent loads were obtained from simulations and they were based on ASHRAE Standard 90.1 of typical building requirements. The climate zones used for the simulations were zone 4C – Salem, OR and zone 3A – Memphis, TN. These two locations were selected because the resulting loads from the simulations allowed testing the RTU under part-load conditions for a broad range of outdoor temperatures. The building loads were set in the indoor room of the chamber and a target indoor return dry bulb temperature was selected as representative set point of the occupied space of the building that the chamber laboratory aimed to mimic. Then the RTU was run in the chamber and it simply reacted to these external boundary conditions as it would when it is integrated in a building in order to continue to provide the desired indoor environmental room temperature.

The method developed in this work characterized the unit performance and efficiency during this reaction period and for two specific technologies that are commonly integrated in RTUs, that is, economizer and variable indoor fan (or blower) speed.

A thermostat sequence was developed and implemented in the data acquisition system (DAQ) of the facility. The program in the DAQ mimic a thermostat operating in a building with no set back temperature. This program controlled the RTU compressors, economizer and indoor fan (or blower) speed in order to cool or heat the indoor room at specific rates. Consequently, the indoor room temperature (which was measured at the return air temperature location of the RTU) continuously varied in time and gradually changed between the minimum and maximum temperature limits of the thermostat set points. This meant that the load-based tests were transient cycling tests or sometimes quasi-steady state test but they were never steady state tests.

Two constraints of the project were that the new load-based method of test must be (i) feasible to conduct, that is, the testing time must be reasonable and practical, and (ii) it must not be too costly to implement in existing psychrometric chamber laboratories. This meant that the new method of test must introduce as few as possible modifications of the existing laboratory hardware and instrumentation and each test must be completed in one or two hours if possible. This chapter describes how the test conditions of the present work were selected in order to develop the load-based method of test that would respect these two constraints.

5.1 Indoor Room Load Setting Principle

For load-based testing, sensible and latent loads were set in the psychrometric chamber indoor room by adjusting the parameters of the components of the room conditioning loops and the code tester. Electric resistance heaters, fans on each one of the conditioning loops and the code tester fan were the major contributors to the sensible load. The steam introduced in the room set the latent load of the test due to people building occupancy, but it also had some contributions on the sensible load of the test.

First principle thermodynamic analysis of the work and heat transfer rates present in the indoor room during a typical load based test

To clarify the interactions among the various heat transfer rates and work rates during a load-based test, figure12 presents a schematic of the indoor room with the corresponding main conditioning equipment. It is helpful to apply the first law of Thermodynamics, that is, the conservation of energy in the indoor room. The thermodynamic control volume on which a first law, steady-state, energy balance analysis was applied is delimited in figure12 by the walls, floor and ceiling of the indoor room plus the control surfaces surrounding the fans in bays 4, 5 and 6 and the heaters and humidifiers in Bays 4 and 5. The boundaries of the system were represented by dotted lines. Blue arrows indicate the energy interactions entering and leaving the system. There is mechanical power introduced by the fans in Bay 4, 5 and 6, electrical power introduced by the heaters in Bays 4 and 6, latent heat introduced in the form of vapor through the steam wands and mass flow interactions due to the air entering (supply air) and leaving (return air) the indoor room. A steady state, open system, first law energy balance is presented in equation (2), where all the energy interactions of the same type have been grouped together for simplicity:

$$\dot{m}_{air}(h_{return} - h_{supply}) = \dot{W}_{Fans} + \dot{W}_{Heaters} + \dot{Q}_{lat,humidifier} \quad (2)$$

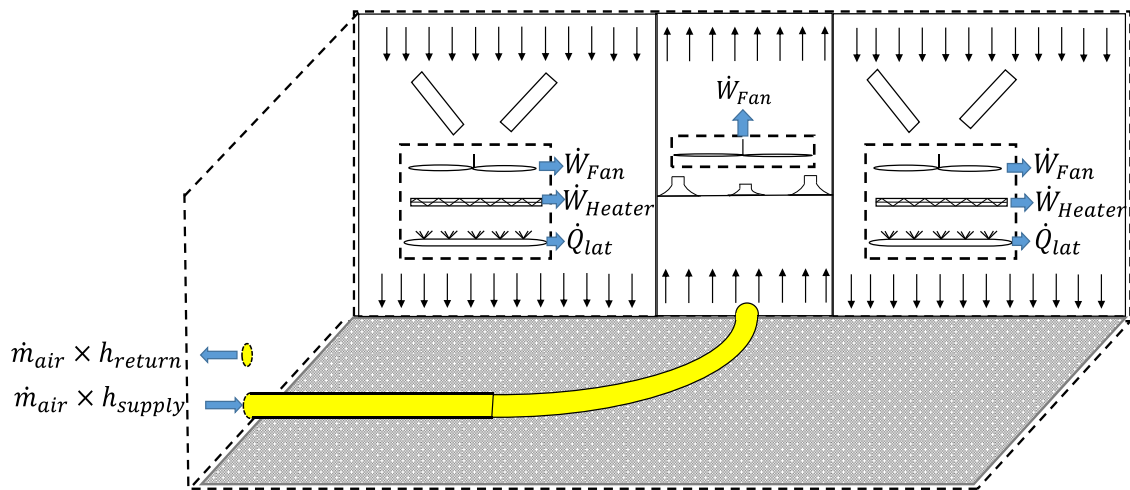


Figure 12: Indoor room energy balance during a typical load-based test

Notice that the left hand side of equation (2) represents the total capacity of the equipment that was tested.

5.2 Test Conditions

Table 4 shows the tests conditions for the experimental campaign of present work. Tests 1, 2, 28 and 29 were steady state “ordinary” temperature-based cooling and heating tests (ordinary here means as indicated in ASHRAE Standard 116-2010). They were used to (1) verify that the measured cooling capacity and COP of the RTU were in agreement with the manufacturer specifications and (2) to characterize the RTU performance for temperature-based boundary conditions according to currently used ASHRAE Standard 116. These tests (3) also provided the baseline results on which the PNNL load profiles were scaled up or down for the specific RTU installed in the OSU chamber during the present work. The remaining 34 tests in Table 4 were load-based transient tests and they were conducted with the boundary conditions for the RTU set as summarized in the Table. From left to right, table 4 header provides test No., test type, indoor room temperature settings (applicable only for steady state temperature-based tests), total load, sensible load and space latent load settings, outdoor dry bulb and wet bulb settings, test main objective, whether the economizer operates or not during the test, fan speed setting, test duration and the climate zone for the particular test.

Table 4: Details of the experimental test conditions of the tests of the present work

Test No.	Test Type	Indoor		Total Load, (Btu/h)	Sensible Load, (Btu/h)	Space Latent Load, (Btu/h)	Outdoor		Objective	Economizer or Min OA	Variable Speed Fan	Duration (minutes)	Location
		DB, (°F)	WB, (°F)				DB, (°F)	WB, (°F)					
<i>A: 2 steady state standard cooling tests- determine unit capacity in cooling mode as per ASHRAE 116-2010</i>													
1	Cooling	80	67	----	----	----	95	----	SS Full Load (Baseline)	No OA	Full	90	----
2	Cooling	80	67	----	----	----	82	----	SS Full Load (Baseline)	No OA	Full	90	----
<i>B: 6 cooling tests with min OA & Full fan, marine climate (Salem, zone 4C)</i>													
3	Cooling	----	----	113215	105465	7750	105	72 - 73	Cooling Full Load	Min OA	Full Speed	90	Salem (zone 4C)
4	Cooling	----	----	99567	91817	7750	95	68 - 69	Cooling Full Load	Min OA	Full Speed	90	Salem (zone 4C)
5	Cooling	----	----	92743	84993	7750	82	63 - 64	Cooling Partial Load	Min OA	Full Speed	90	Salem (zone 4C)
6	Cooling	----	----	79095	71345	7750	72	59 - 60	Cooling Partial Load	Min OA	Full Speed	90	Salem (zone 4C)
7	Cooling	----	----	51799	44049	7750	65	56 - 56.8	Cooling Partial Load	Min OA	Full Speed	90	Salem (zone 4C)
8	Cooling	----	----	35046	27296	7750	57	52 - 52.6	Cooling Partial Load	Min OA	Full Speed	90	Salem (zone 4C)
<i>C: 3 cooling tests with fan control, marine climate (4C)</i>													
9	Cooling	----	----	99567	91817	7750	95	68 - 69	Cooling Full Load	Min OA	Speed Control	120	Salem (zone 4C)
10	Cooling	----	----	92743	84993	7750	82	63 - 64	Cooling Partial Load	Min OA	Speed Control	120	Salem (zone 4C)
11	Cooling	----	----	79095	71345	7750	72	59 - 60	Cooling Partial Load	Min OA	Speed Control	120	Salem (zone 4C)
<i>D: 3 cooling tests with economizer, marine climate (4C)</i>													
12	Cooling	----	----	79095	71345	7750	72	59 - 60	Econom. + fan control	Economizer	Speed Control	120	Salem (zone 4C)
13	Cooling	----	----	51799	44049	7750	65	56 - 56.8	Econom. + fan control	Economizer	Speed Control	120	Salem (zone 4C)
14	Cooling	----	----	35046	27296	7750	57	52 - 52.6	Econom. + fan control	Economizer	Speed Control	120	Salem (zone 4C)
<i>E: 3 cooling tests with fan control and economizer, moist climate (3A) outdoor dry bulb temperature and, loads from (4C) zone</i>													
15	Cooling	----	----	79095	79087	7750	72	61 - 62	Impact of OA humidity	Economizer	Speed Control	120	Memphis (zone 3A)
16	Cooling	----	----	51799	51791	7750	65	53 - 54	Impact of OA humidity	Economizer	Speed Control	120	Memphis (zone 3A)
17	Cooling	----	----	35046	35038	7750	57	48 - 49	Impact of OA humidity	Economizer	Speed Control	120	Memphis (zone 3A)
<i>F: 5 Repeat selected partial load tests with econ and fan (65 °F OA)</i>													
18	Repeat test 13	----	----	51799	44049	7750	65	56 - 56.8	Verify repeatability	Economizer	Speed Control	120	Salem (zone 4C)
19	Repeat test 13	----	----	51799	44049	7750	65	56 - 56.8	Verify repeatability	Economizer	Speed Control	120	Salem (zone 4C)
20	Repeat test 13	----	----	51799	44049	7750	65	56 - 56.8	Verify repeatability	Economizer	Speed Control	120	Salem (zone 4C)
21	Repeat test 13	----	----	51799	44049	7750	65	56 - 56.8	Verify repeatability	Economizer	Speed Control	120	Salem (zone 4C)
22	Repeat test 13	----	----	51799	44049	7750	65	56 - 56.8	Verify repeatability	Economizer	Speed Control	120	Salem (zone 4C)

Table 4: Detail of the experimental test conditions of the present work (continued)

Test No.	Test Type	Indoor		Total Load, (Btu/h)	Sensible Load, (Btu/h)	Space Latent Load, (Btu/h)	Outdoor		Objective	Economizer or Min OA	Variable Speed Fan	Duration (minutes)	Location
		DB, (°F)	WB, (°F)				DB, (°F)	WB, (°F)					
<i>G: 7 repeating tests: three from series B, two from series C and two from series D, marine climate (4C)</i>													
23	Repeat test 5	----	----	92743	84993	7750	82	63 - 64	Cooling Partial Load	Min OA	Full Speed	90	Salem (zone 4C)
24	Repeat test 6	----	----	79095	71345	7750	72	59 - 60	Cooling Partial Load	Min OA	Full Speed	90	Salem (zone 4C)
25	Repeat test 7	----	----	51799	44049	7750	65	56 - 56.8	Cooling Partial Load	Min OA	Full Speed	90	Salem (zone 4C)
26	Repeat test 10	----	----	92743	84993	7750	82	63 - 64	Cooling Partial Load	Min OA	Speed Control	120	Salem (zone 4C)
27	Repeat test 11	----	----	79095	71345	7750	72	59 - 60	Cooling Partial Load	Min OA	Speed Control	120	Salem (zone 4C)
28	Repeat test 12	----	----	79095	71345	7750	72	59 - 60	Econom. + fan control	Economizer	Speed Control	120	Salem (zone 4C)
29	Repeat test 13	----	----	51799	44049	7750	65	56 - 56.8	Econom. + fan control	Economizer	Speed Control	120	Salem (zone 4C)
<i>H:2 cooling tests with fan control, marine climate (4C), with load variations (82 °F OA)</i>													
30	Cooling	----	----	92743	84993	7750	82	63 - 64	+/- 15% Load 20min	Min OA	Speed Control	120	Salem (zone 4C)
31	Cooling	----	----	92743	84993	7750	82	63 - 64	+/- 15% Load 10min	Min OA	Speed Control	120	Salem (zone 4C)
<i>I: 2 Heating steady state standard tests – determine unit capacity in heating mode as per ASHRAE 116-2010</i>													
32	Heating	70	----	----	----	----	47	43	Standard (baseline)	No OA	Full	60	----
33	Heating	70	----	----	----	----	62	56	Standard (baseline)	No OA	Full	60	----
<i>J: 3 heating tests with constant load</i>													
34	Heating	----	----	32831	32831	----	37	34	Part Load	Min OA	Full	120	Salem (zone 4C)
35	Heating	----	----	15450	15450	----	47	43	Part Load	Min OA	Full	120	Salem (zone 4C)
36	Heating	----	----	1544	1544	----	55	50	Minimum Part Load	Min OA	Full	120	Salem (zone 4C)
<i>K: 2 cooling tests with fan control and economizer, moist climate (3A) load and temperatures</i>													
37	Cooling	----	----	26374	18624	7750	65	53 - 54	Impact of OA humidity	Economizer	Speed Control	120	Memphis (zone 3A)
38	Cooling	----	----	9281	1531	7750	57.1	48 - 49	Impact of OA humidity	Economizer	Speed Control	120	Memphis (zone 3A)

5.3 Example of a load-based cooling test

For load-based tests, the indoor and outdoor rooms of the chamber and the rooftop unit were operated in cooling mode until equilibrium conditions were attained but not for less than thirty minutes. During these first thirty minutes, the outdoor room dry bulb and wet bulb temperatures were at steady state according to the test conditions in table 4. During this period, the indoor room dry bulb temperature was set to 77°F (25°C) and the wet bulb temperature to 66°F (18.9°C). The economizer was set to minimum outside air position (min OA). The condition and operating tolerances during this period were the same of ASHRAE 116-2010 steady state tests.

Following the first thirty minutes, the control of the humidifier and electric heaters were set to manual mode in order to provide constant latent load and sensible load to the indoor room. The cooling coils of the indoor room were closed so the equipment under testing directly controlled the sensible and latent loads from this point forward. After both sensitive and latent loads were set, the room underwent a period of 60 minutes of transitory operation before the start of the actual testing period for performance characterization of the tested equipment. Acceptable return air temperatures ranged from 75°F (23.9°C) to 77.5°F (25.3°C). Whenever the return dry bulb temperature reached those boundaries, the unit was cycled on/off according to a simulated thermostat setting sequence used in this project.

Figure 13 shows the indoor return dry bulb temperature vs. time in the three periods explained above for tests 12 of table 4. During the first thirty minutes, the RTU and the room were temperature controlled so that the return temperature was steady at 77°F (25°C). At the thirtieth minute, indoor room controls were varied from automatic mode used to control the temperature to manual mode to set the sensible and latent loads. At this time, the temperature decreased sharply because the power the heaters required to control indoor room temperature at 77°F (25°C) was higher than the sensible load setting of the test (71345 BTU/h). From this time and onwards, the unit was cycled on/off according to the thermostat setting sequence. The purpose of the transition period between

the thirtieth and the ninetieth minute was used to allow the RTU controls to balance the change in inertia that occurred when the switch from temperature control to load control took place. Data for the load-based test was recorded during the last 120 minutes period (from the ninetieth minute and onwards). The data recorded during this period was then used to determine the RTU capacity and performance.

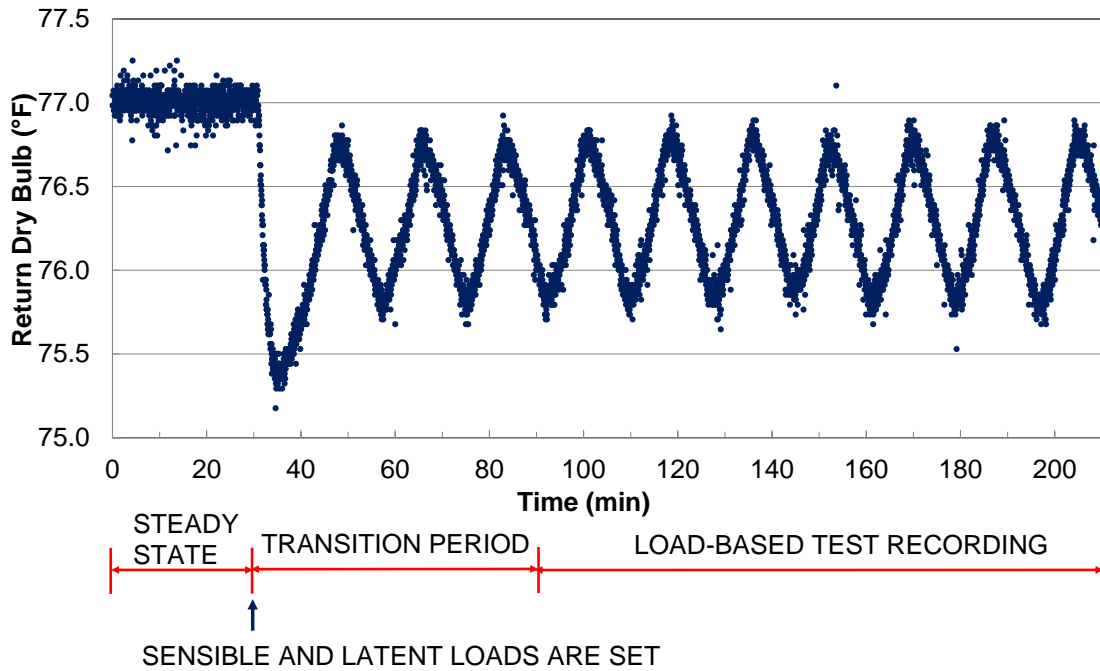


Figure 13: Example of complete load-based cooling test from startup of the RTU (both outdoor and indoor rooms were temperature controlled during the initial steady state part of the test, then the indoor room was switched to load controlled mode at the beginning of the transition period; the actual recording period started at the end of the transition period, referred as to “load-based test recording” section)

5.4 Initial Definition of the Test Conditions

Test conditions were initially defined by 11 categories from series “A” to series “K” as summarized in table 5. Series “A” and “T” were steady state cooling and heating tests as described in ANSI/ASHRAE Standard 116-2010. The remaining tests were based on TMY3 data for two representative climate zones of ASHRAE Standard 90.1 Building Envelope Climate Criteria: one

marine climate, and the location of Salem, OR was selected for representing Zone 4C, and one moist climate, and the location of Memphis, TN was chosen to represent Zone 3A. Pacific Northwest National Laboratory (PNNL) collaborated in this project by providing prototype simulations for a small office building that were used for estimating the cooling and heating loads. Salem, OR (4C) and Memphis, TN (3A) TMY3 data for a one year period (2006) were applied as boundary conditions to an ASHRAE 90.1 prototype small office building of approximately 5500 ft² (511 m²) to simulate hourly cooling and heating loads. From these loads, the steady state tests in series A and I were used as baseline tests to scale up or down the cooling and heating loads for the other series. In other words, the offsets of the building load profiles obtained from the PNNL simulations were shifted in order to approximately match the RTU capacity when the outdoor temperature was 95°F (35°C) for the cooling tests and 47°F (8.3°C) for the heating tests. Then the slope of the building load profiles obtained from the PNNL simulations were used to determine the loads to be set in the psychometric chamber indoor room for the other outdoor temperatures. Salem, OR (4C) and Memphis, TN (3A) were selected for the present work because the resulting simulation loads allowed testing the RTU under part-load conditions for a broad range of outdoor temperatures. When part-load conditions were present, the RTU thermostat cycled the compressors, economizer and indoor fan (or blower) speed in order to provide the cooling or heating capacities that matched the thermal load demands set by the indoor room. It should be highlighted in here that the RTU thermostat was mimicked by a series of command sequences programmed into the DAQ of the chamber facility, which controlled the RTU and was connected to the RTU in the same way as of a programmable thermostat would have. The RTU thermostat sequence of commands will be described in details later in this thesis.

Table 5: Definition of test conditions and summary of the tests for each series

Series	Description of the series	No. of Tests in this series	Test no.
A	Cooling tests steady-state standard cooling - determine unit capacity in cooling mode as per ASHRAE 116-2010	2	1, 2
B	Cooling tests load-based with min OA & full speed fan, marine climate (4C)	6	3, 4, 5, 6, 7, 8
C	Cooling tests load-based with fan control, marine climate (4C)	3	9, 10, 11
D	Cooling tests load-based with fan control and with economizer, marine climate (4C)	3	12, 13, 14
E	Cooling tests load-based with fan control and economizer, moist climate (3A) outdoor dry bulb temperature, loads from (4C) zone	3	15, 16, 17
F	Repeat selected partial load tests with econ and fan (65°F OA)	5	18, 19, 20, 21, 22
G	Repeat tests: three from series B, two from series C and two from series D, marine climate (4C)	7	23, 24, 25, 26, 27, 28, 29
H	Cooling tests load-based with fan control, marine climate (4C), with load variations (82°F OA)	2	30, 31
I	Heating steady-state standard tests - determine unit capacity in heating mode as per ASHRAE 116-2010	2	32, 33
J	Load-based heating tests	3	34, 35, 36
K	Cooling tests load-based with fan control and economizer, moist climate (3A) load and temperatures	2	37, 38
Total		38	

Test conditions for each series referred by letters in Table 5 were determined as described in details next.

A. 2 steady state standard cooling tests- determine unit capacity in cooling mode as per ASHRAE 116-2010

Conditions for these tests were based on ANSI/AHRI 340/360 and ASHRAE116-2010 standards. The unit was operated at full load, steady state cooling and no outside air. The return air dry bulb temperature was representative of the indoor room conditions. The indoor room dry bulb temperature was set to 80°F (26.7 °C) and the indoor room wet bulb temperature was set to 67°F

(19.4°C). The economizer was set to the closed position. The unit static pressure was set to 0.3 in wg. The objective of these two tests was to determine unit actual capacity and COP according to current standards. The unit actual capacity measured from these tests was used to scale the loads in the series B to H (i.e. load-based tests in unit cooling mode). These two tests also served to provide baseline data to characterize the unit according to the current standards.

B. 6 cooling tests with min OA & Full fan, marine climate (Salem, OR, zone 4C)

Determination of the outside DB and WB Temperatures for Salem, OR

Six outdoor dry bulb temperatures ranging from 57°F (13.9°C) to 105°F (40.6°C) were selected for testing the RTU at different outdoor conditions that would yield six different indoor cooling loads. The dry bulb temperatures and their corresponding wet bulb temperatures were obtained from TMY3 climate zone data for Salem, OR, which is representative for climate zone 4C (that is, marine climate zone). TMY3 stands for Typical Meteorological Year data sets derived from the 1991-2005 National Solar Radiation Data Base (NSRDB) update (Wilcox and Marion 2008). The unit static pressure was set to 1.0 in wg. (~249 Pa), which is higher than the ones set in the standard ANSI/AHRI 340/360. The reason for this deviation is that field studies such as Jacobs et al (2003) reported that average static pressure drop across typical rooftop units is higher than 0.3 in wg.

Determination of Total Cooling Loads for Salem, OR

The occupied total cooling loads were selected for a small office space of approximately 5500 ft² (511 m²) floor area. PNNL simulations were available for occupied cooling hours of a small office space without economizer operation in Salem, OR. The simulations were conducted based on climate data of year 2006. Figure 14 shows the plot of the occupied total cooling load, $Q_{\text{total,cooling}}$ in BTU/h (kW) vs outside dry bulb temperature, $T_{\text{db,out}}$ in °F (°C).

A linear regression of the occupied cooling load with dry bulb temperature for Salem, OR (that is, climate zone 4C) provided the equation shown in figure 14. The temperatures at loads equal to 0 were not considered in the regression in order to obtain a better representation of the load profile.

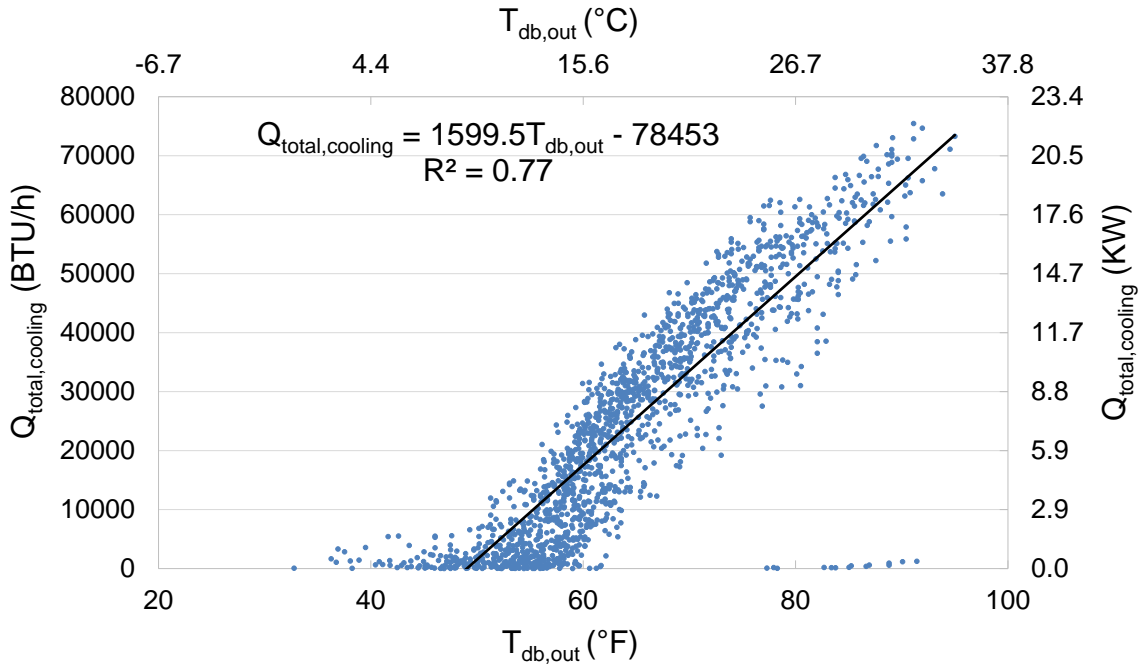


Figure 14: Total cooling Load ($Q_{total,cooling}$) versus outside dry bulb temperature ($T_{db,out}$) for the location of SALEM, OR (ZONE 4C) (results from PNNL simulations of a small office building of approximately 5500 ft² (511 m²)).

Substituting the values of the selected outdoor dry bulb temperatures $T_{db,out}$ (obtained from TMY3 for Salem, OR and reported in table 4) in the linear regression equation (equation (3)) yielded the total cooling loads as a function of temperature that would later be scaled up or down to better match the capacity of the RTU tested.

$$\dot{Q}_{total,cooling} \left[\frac{Btu}{h} \right] = 1599.5 T_{db,out} [F] - 78453 \quad (3)$$

Determination of the space latent load

The latent load was selected for the same office space. PNNL prototype simulations were available for the office space and the latent load was calculated based on the number of people present in the office. The data showed that 31 people occupied the office during 8am to 5pm. ASHRAE Handbook of Fundamentals 2009 recommends a latent load per person of 250 Btu/h for an office with moderately active office work (when the indoor design temperature is 80°F (26.7°C). Thus, the total latent load was estimated according to equation (4) and was constant throughout the test conditions table 4.

$$\dot{Q}_{latent,space} = 31[people] \times 250 \left[\frac{BTU}{h - person} \right] = 7750 \frac{Btu}{h} \quad (4)$$

Determination of the sensible cooling load

The sensible cooling load was calculated as difference of the total cooling load and the latent cooling load and it is also reported in the test conditions table (table 4):

$$\dot{Q}_{sens,cooling} = \dot{Q}_{total,cooling} - \dot{Q}_{lat,cooling} \quad (5)$$

C. 3 cooling tests with fan control, marine climate (4C)

Outside air temperatures and loads of the tests 9, 10, and 11 were the same as in tests 3, 4, and 5. The tests 9, 10, and 11 introduce fan speed control (see column labeled “Variable Speed Fan” on table 4).

D. 3 cooling tests with economizer, marine climate (4C)

Outside air temperatures and loads of tests 12, 13, and 14 were the same as the ones in tests 6, 7, and 8. Tests 12, 13, and 14 introduce economizer operation (see column labeled “Economizer or Min OA” on table4) in addition to the fan speed control.

E. 3 cooling tests with fan control and economizer, moist climate (Memphis, TN, zone 3A) outdoor dry bulb temperature and, loads from (4C) zone

Loads and outdoor dry bulb temperatures for tests 15, 16, and 17 were the same as the ones of tests 12, 13, and 14 but the corresponding wet bulb temperatures were selected for climate zone 3A TMY3 data (i.e. moist climate zone). The objective of tests 15, 16, and 17 was to measure the impact of the outside air relative humidity on the new method of testing

F. 5 Repeat selected partial load tests with econ and fan (65°F (18.3°C) OA)

Tests 18, 19, 20, 21 and 22 in this series were repetitions of test 13. The objective of these five tests was to verify repeatability of the measured performance with the new method of tests for one test condition. Results from these tests were also used to assess the experimental uncertainty of the facility and of the equipment arrangement.

G. 7 repeating tests: three from series B (easy to set and execute), two from series C (moderate to set and execute), and two from series D (difficulty to set and execute), marine climate (4C)

Tests in this series focused on assessing the repeatability of test results for three levels of difficulty of set and execution of the test, that is, easy, moderate, and difficult to set and execute the test.

- Three Series B cooling tests with min OA & Full fan, marine climate (Salem, OR, zone 4C): tests 23, 24 and 25 were repetitions of tests 5, 6 and 7 respectively and they had the lowest difficulty for load setting in the psychrometric chamber and lowest difficulty of execution of the load based test.
- Two Series C cooling tests with fan control, marine climate (Salem, OR, Zone 4C): tests 26 and 27 were repetitions of tests 10 and 11, which were of moderate difficulty for load setting in the psychrometric chamber and of moderate difficulty in the execution of the load-based test.

- Two Series D cooling tests with economizer, marine climate (Salem, OR, Zone 4C): tests 28 and 29 were repetitions of tests 12 and 13 that had highest difficulty for load setting in the psychrometric chamber and the highest difficulty of execution of the load-based test.

H. 2 cooling tests with fan control, marine climate (4C), with load variations (82°F (27.8°C) OA)

The objective of tests 30 and 31 in this series was to study the effect of perturbation and fluctuation of the indoor load due to the effectiveness of the controls of the chamber and due to the instrumentation experimental uncertainty and human operator error. The purpose of these tests was to determine if the figures of merit resulting from a test with fluctuating loads, but yet with the same average load during the test, can still be used as representative figures of merit of the RTU during the RTU model development and verification. In other words, these tests were meant to simulate conditions in which the loads cannot be controlled properly due to chamber limitation or human operator error. In such cases, the question that these tests addressed was if the load-based method of test was still valid and provided realistic results for the figures of merit. The two tests conducted in the present work to explore this issue were:

- One Section C cooling test with fan control, marine climate (Salem, OR, Zone 4C): Test 30 is a repetition of test 10 but the load was intentionally varied from -15% to +15% of the average load every 20 minutes period. The average load was basically set by the electric heaters of the chamber and thus the electric heaters output was manually varied every 20 minutes to simulate a quite large fluctuation of the load set in the indoor room. This might be the case when the chamber laboratory is not able to match the response time of the RTU due to thermal inertia issues.
- One Section C cooling test with fan control, marine climate (Salem, OR, Zone 4C): Test 31 is a repetition of test 10 but the load was intentionally varied from -15% to +15% of the average load every 10 minutes period. Again, the average load was basically set by the electric heaters

of the chamber and thus the electric heaters output was manually varied every 10 minutes to simulate a fast fluctuation of the load set in the indoor room. This might be the case when the control parameters of the chamber are not properly calibrated and tuned to the specific test and thus the control hunts the set point during a test by continuously changing the heaters output.

I. 2 Heating steady state standard tests – determine unit capacity in heating mode as per ASHRAE 116-2010

Conditions for tests 32 and 33 were based on high and low temperature tests respectively with full load, steady state heating and no outside air as described by ANSI/AHRI 340/360. The objective of these two tests was to determine unit actual capacity and COP according to current standards.

J. 3 heating tests with constant load

Determination of the outside DB and WB Temperatures for Salem, OR Heating Tests

Three outdoor dry bulb temperatures ranging from 37°F (2.8°C) to 55°F (12.8°C) were selected testing the RTU at different outdoor conditions that would yield three different indoor heating loads. The dry bulbs and their corresponding wet bulb temperatures were obtained from climate zone data TMY3 for Salem, OR, which is representative for climate zone 4C (that is, marine climate zone). TMY3 stands for Typical Meteorological Year data sets derived from the 1991-2005 National Solar Radiation Data Base (NSRDB) update (Wilcox and Marion 2008). The unit static pressure was set to 1.0 in wg. (~249 Pa).

Determination of Heating Loads for Salem, OR

The occupied total heating loads were selected for a small office space of approximately 5500 ft² (511 m²) floor area. PNNL simulations were available for occupied heating hours of a small office space in Salem, OR. The simulations were conducted based on climate date of year 2006. Brown points in Figure 15 represent the occupied total heating load, $Q_{\text{total,heating}}$ in BTU/h (kW) versus the outside dry bulb temperature, $T_{\text{db,out}}$ in °F (°C) for the year 2006. The blue circles, green triangles

and red squares represent specific load profiles for only three days during the heating season, that is, for February 2nd, November 29th and December 21st 2006. These three series are highlighted in Figure 15 because they were used as examples to describe how the distribution of the data points shown in Figure 15 was obtained when starting from the PNNL simulation results.

A linear regression of the occupied heating load with dry bulb temperature for Salem, OR (that is, climate zone 4C) provided the equation shown in figure 15. The temperatures at loads equal to 0 were not considered in the regression in order to obtain a better representation of the load profile.

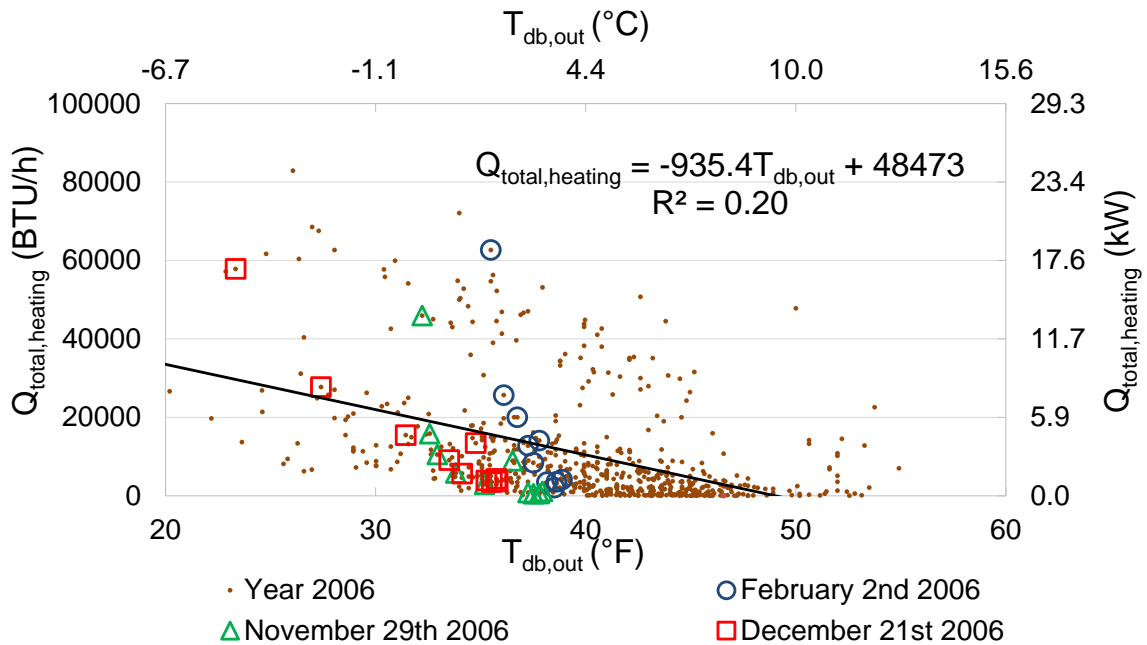


Figure 15: Heating load ($Q_{total,heating}$) versus outside dry bulb temperature ($T_{db,out}$) for the location of SALEM, OR (ZONE 4C) (results from PNNL simulations of a small office building of approximately 5500 ft² (511 m²))

Substituting the values of the selected outdoor dry bulb temperatures $T_{db,out}$ (obtained from TMY3 for Salem, OR and reported in table 4) in the linear regression equation (equation (6)) yielded the total heating loads as a function of temperature that would later be scaled up or down to better match the capacity of the RTU tested.

$$\dot{Q}_{total,heating} \left[\frac{Btu}{h} \right] = -935.4 T_{db,out} [F] + 48473 \quad (6)$$

The load profile in figure 15 is very scattered, that is, for similar values of temperature very different values of load can be found. The reason for this is that for similar values of outdoor temperatures different values of solar radiation were found in the northern climate of Salem, OR. In order to understand this better, a time series of occupied hours for three days in the heating season are shown in figures 16 and 17. For example it is observed in the time series for February 2nd (represented by the blue circles) that an outdoor temperature during the occupied hours of the day (8am to 5pm) varied only from 35.5°F to 38.6°F (1.9°C to 3.7°C). While the heating load varied from 63000 BTU/h (at 8am) to 4300 BTU/h (at 5pm).

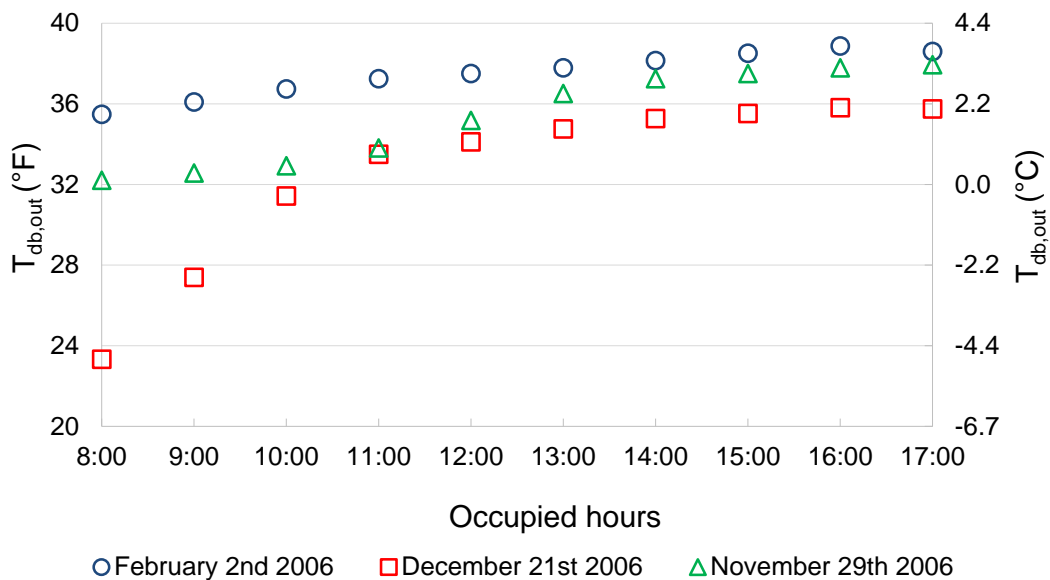


Figure 16: Outdoor Temperature ($T_{db,out}$) vs. Time (h) for three heating season days in Salem, OR (ZONE 4C)

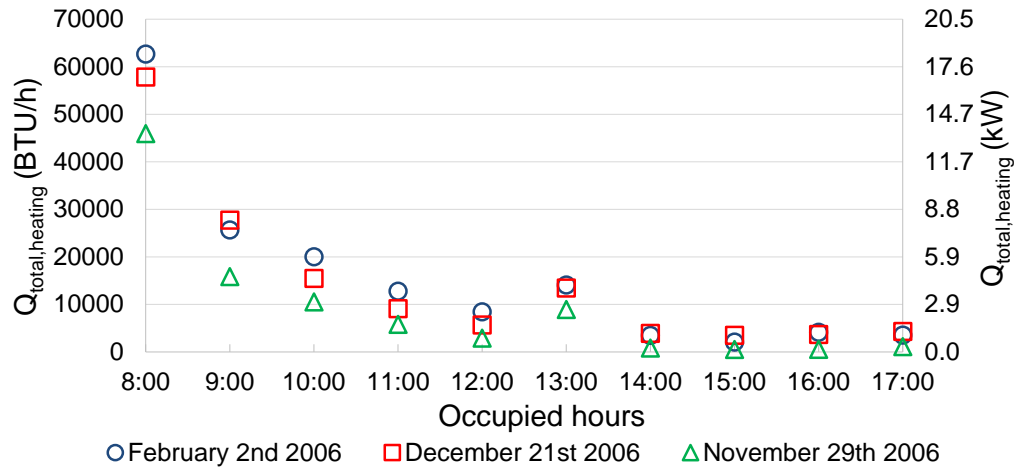


Figure 17: Total heating load ($Q_{total,heating}$) vs Time (h) for three heating season days in Salem, OR (Zone 4C)

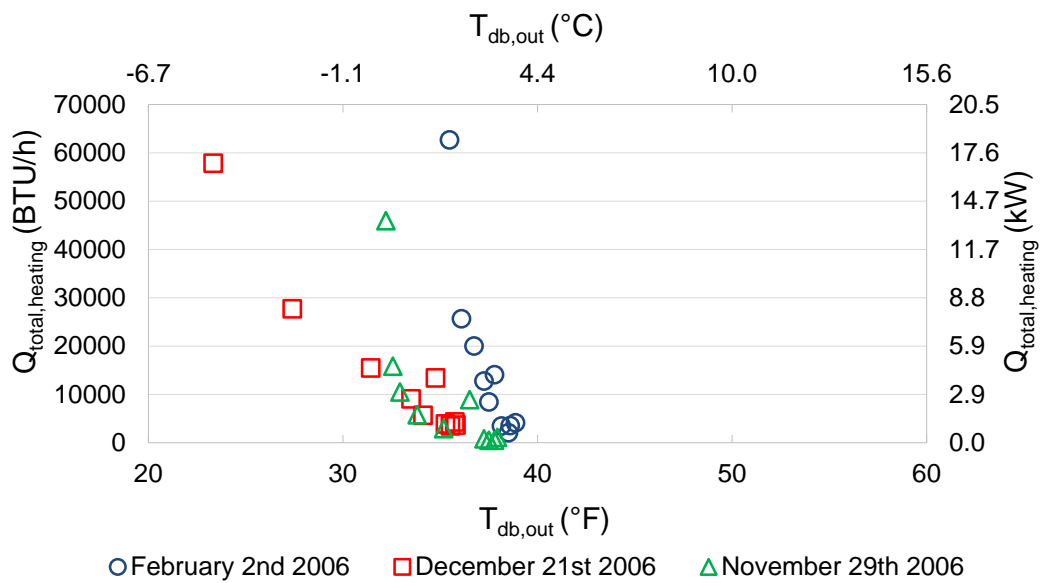


Figure 18 Heating load ($Q_{total,heating}$) versus outside dry bulb temperature ($T_{db,out}$) for three heating season days in the location of SALEM, OR (ZONE 4C) (results from PNNL simulations of a small office building of approximately 5500 ft² (511 m²))

Figure 18 shows the load profiles for three heating season days of the year 2006 in Salem, OR (Zone 4C). This figure, which is basically a zoom out of Figure 15, provides a better understanding for how the distribution of the data points shown in Figure 15 was obtained when starting from the

PNNL simulation results shown in Figures 16 and 17. In particular, the comparison of the data points from these three series clarify that different heating load values for the building are possible when the outdoor dry bulb temperatures were the same. This result might be due to the different values of solar radiation throughout the heating season, different minimum outdoor temperatures for each month, and the various hours during the day at which the specific load occurred. For example, for the February 2nd series, the outdoor temperature during occupied hours was fairly constant while the heating load had a fairly large variation. This variation could be due to the effect of solar radiation on the building envelope surfaces, outdoor temperature during the non-occupied hours (especially the minimum outdoor temperature during the night and early morning), and the effect of internal loads (i.e., lights, people, and equipment) on decreasing the load profile drastically as soon as the building became occupied.

K. 2 cooling tests with fan control and economizer, moist climate (Memphis, TN, zone 3A) load and temperatures

Tests 37 and 38 have the same outside dry bulb and wet bulb temperatures of tests 16 and 17, which are representative of climate zone 3A (i.e., moist climate). In contrast to tests 16 and 17, the loads in tests 37 and 38 are also representative of zone 3A and they were calculated based on the load profile of a small office in this climate zone with a respective load scaling based on steady state tests.

Determination of Total Cooling Loads for Memphis, TN (tests 37 and 38 in table 4)

The occupied total cooling loads were selected for a small office space of approximately 5500 ft² (511 m²) floor area. PNNL simulations were available for occupied cooling hours of a small office space without economizer operation in Memphis, TN. The simulations were conducted based on climate data of year 2006. Figure 19 shows the plot of the occupied total cooling load, $Q_{\text{total,cooling}}$ in BTU/h (kW) vs outside dry bulb temperature, $T_{\text{db,out}}$ in °F (°C).

A linear regression of the occupied cooling load with dry bulb temperature for Memphis, TN (that is, climate zone 3A) provided the equation shown in figure 19. The temperatures at loads equal to 0 were not considered in the regression in order to obtain a better representation of the load profile.

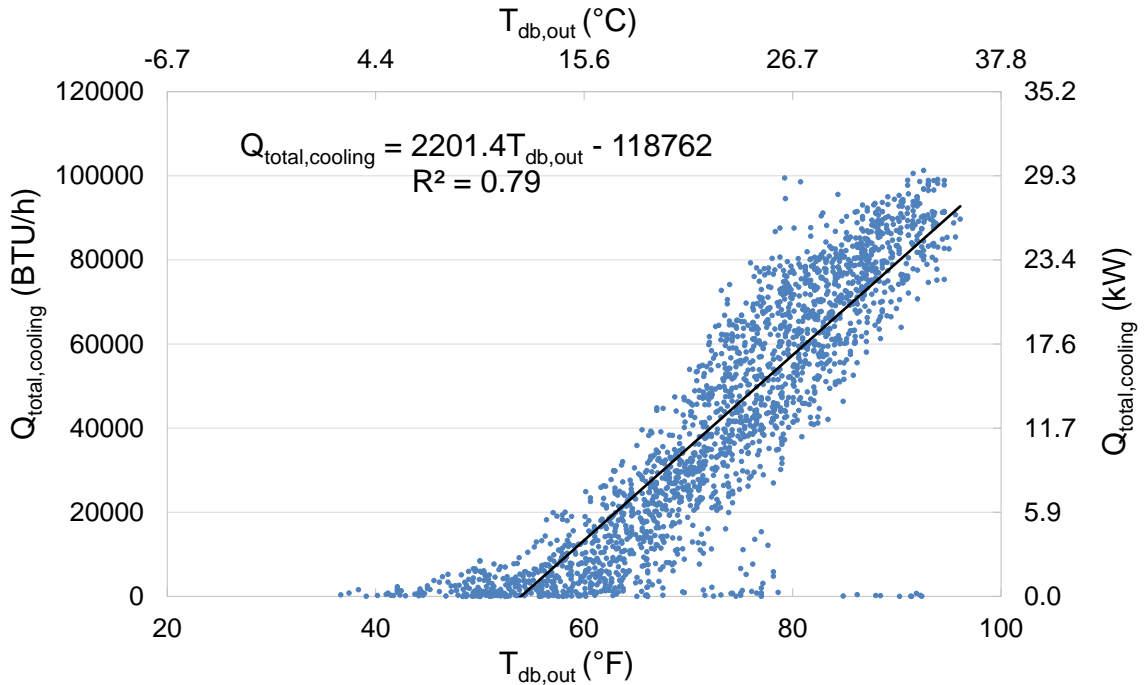


Figure 19: Total cooling load ($Q_{total,cooling}$) versus outside outdoor temperature ($T_{db,out}$) for the location of MEMPHIS, TN (ZONE 3A) (results from PNNL simulations of a small office building of approximately 5500 ft² (511 m²))

Substituting the values of the selected outdoor dry bulb temperatures $T_{db,out}$ (obtained from TMY3 for Memphis, TN and reported in table 4) in the linear regression equation (equation (7)) yielded the total cooling loads as a function of temperature that would later be scaled up or down to better match the capacity of the RTU tested.

$$\dot{Q}_{total,cooling} \left[\frac{Btu}{h} \right] = 2201.4 T_{db,out} [F] - 118762 \quad (7)$$

5.5 Experimental Methodology

In the experimental campaign of the present study, the indoor air enthalpy method was used for measuring the RTU airflow rate, capacity and COP. The procedures used for carrying out the tests listed in table 4 are explained in the following subsections. For the steady state tests, the ASHRAE 116-2010 and ASHRAE 37-2009 testing procedures were followed and they will not be repeated here. For the load-based tests, we followed new procedures that were gradually developed during this project and only the final sequence of the procedures is reported in this thesis. In addition to the load-based tests, a series of calibration tests were carried out to estimate the contributions of chamber components on the loads that needed to be set. For example, the heat rejected to the indoor room from the air fans of the conditioning bays and of the code tester had to be estimated before the actual load-based test is commenced because the heater outputs must be adjusted to account for this contribution of the fans to the indoor load. Thus, calibration tests were conducted to characterize the heat rejection from the fan circulating the air in the chamber. In addition, a non-standard procedure to measure the outside airflow rate through the economizer at minimum and full opening position of the economizer dampers and at full and part fan speeds was also conducted in the present work prior to the actual load-based test. This procedure is described next.

5.5.1 Calibration tests to characterize the effect of the chamber conditioning equipment on the RTU external cooling and heating loads set in the indoor room

5.5.1.1 Procedure for estimating the outside airflow rate through the economizer

An empirical correlation was developed to estimate the outside airflow rate through the economizer from the measured pressure drop of the air stream flowing through the economizer dampers. A series of preliminary tests were conducted to develop the flow characteristic curves of the economizer dampers. Three degrees of damper opening position were considered for these measurements based on the operating conditions to be set during the experimental campaign. These

conditions were economizer fully open, minimum outside air with high fan speed and minimum outside air with low fan speed. A correlation was required for each one of the economizer opening position and fan speed level. Each economizer opening position generated a unique characteristic curve of the dampers of the economizer and thus the characteristic flow rate vs. pressure drop curve of the economizer and fan system of the RTU was determined. Three economizer flow characteristic curves were empirically generated for the RTU tested in the present work and they were obtained by varying the speed of the supply air fan while keeping the economizer opening position controlled and fixed to a specified position.

Temperature Setting

The indoor and outdoor room dry bulb temperatures were set to a mid-range temperature of the experimental test conditions to diminish the effects of density variations in the correlation. This is not critical since air density variation does not have a great impact in final measurements. However, 65°F (18.3°C) was the selected mid-range temperature based on the experimental test conditions used in this project (see table 4).

Unit and ducts settings

The roof top unit was set up to work at a 100% outside air condition; this means no return air flows back to the unit. In this way, the entire volume of the air that enters the unit through the economizer opening flows through the supply ducts reaching the “code tester”. The airflow rate as a function of the static pressure drop across the nozzle bank was then calculated using a Bernoulli type equation. Since the OSU chamber is set up to work with the indoor air enthalpy method, this equation is readily available. Equation (20) was used as a reference to obtain the correlation for outside airflow rate measurement. When carrying out these operations, ambient air was admitted into the outdoor room while also releasing air from the indoor room. Otherwise, the outdoor room pressure goes into a vacuum state while also over-pressuring the indoor room, which could be unsafe for personnel and certain components such as the conditioning loop fans and the unit blower.

Selecting economizer positions

For this project, three positions were used: economizer fully open, minimum outside air with high fan speed and minimum outside air with low fan speed. The minimum outside airflow rate at both low and high fan speeds was the same. This led to two different damper opening positions besides the fully open damper one. These positions depended on the economizer control approach used. The logic used to control economizer operation is explained in the thermostatic settings for cooling tests.

a) Economizer damper fully open

The economizer damper was set to fully open position. The unit fan was run for at least four different speeds allowing a minimum of 30 minutes for stabilizing, and recordings were taken for a minimum of 10 minutes. Each speed setting constituted a recording. Every one of the speed settings were selected to develop a curve of flow rate as a function of static pressure difference across the economizer inlet. The curve was developed in such a way that the expected outdoor airflow rate was in between the points obtained during the calibration tests.

b) Economizer damper at minimum outdoor air position with full speed fan

A mechanical position for minimum outdoor air with full speed fan was selected and the procedure in part a) was repeated, taking at least three recordings to develop the curve. This process required some iteration. The iteration consisted on operating the unit under normal flow conditions (with return air involved), to determine the actual outside airflow rate. If the resulting outside airflow rate was not the one desired, another mechanical damper position was selected until the desired outside airflow rate was obtained.

c) Economizer damper at minimum outdoor air position with half speed fan

A mechanical position for minimum outdoor air with low speed fan was selected and the procedure described in b) was repeated. At least three recordings were taken to develop the curve. Iterations were performed until the desired outside airflow rate for low speed fan was obtained.

d) Development of the RTU economizer and fan characteristic curves

Flow characteristic curves for each one of the economizer positions were obtained. The curves consist of the recorded points plus the point of zero static pressure difference for the no flow case.

A regression to obtain a quadratic correlation of Airflow rate vs. $\Delta P_{\text{static,economizer}}$ was performed using Excel. Figure 20 shows the three curves obtained for each one of the economizer openings with their respective correlations.

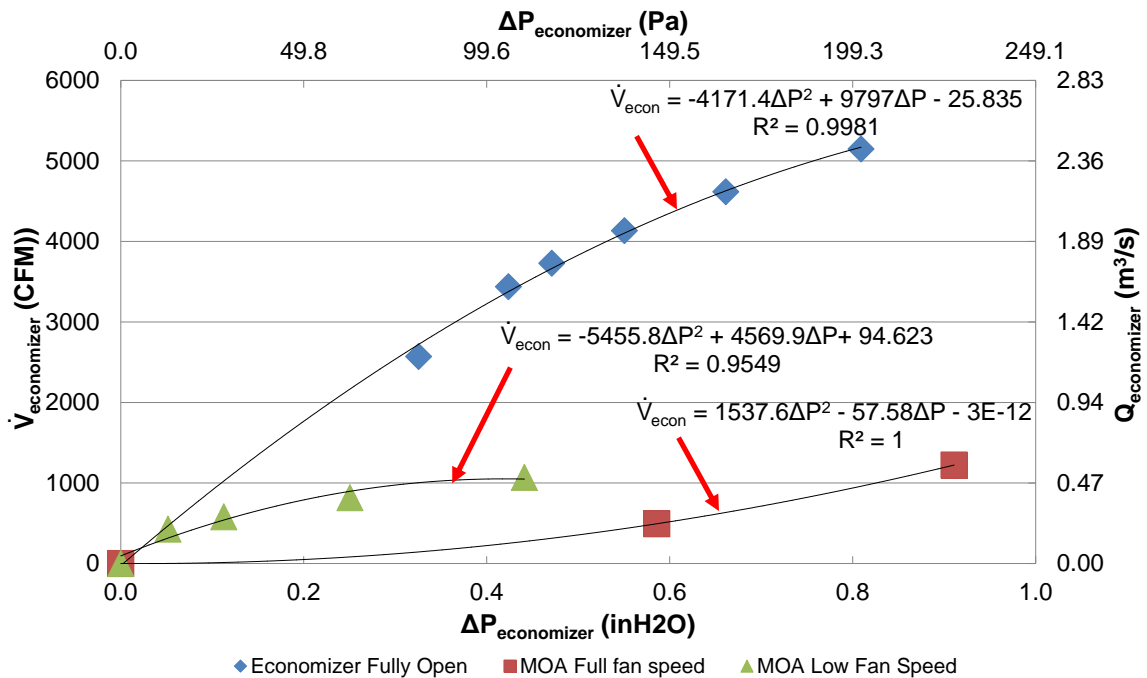


Figure 20: Economizer and fan characteristic curves for the RTU tested in the present work

5.5.1.2 Procedure for determining sensible heat transfer reject from the fans circulating air to the indoor room of the chamber

When it comes to load setting, the power given by electric heaters in Bay 4 and Bay 6 of the chamber indoor room used for developing this method could be adjusted to a determined fixed set point in kW. Similarly, the steam mass flow rate (lb/h) provided by the humidifier and the steam temperature could also be fixed. This capability allowed these components to be used independently from their corresponding PID controllers, making it possible to set sensible and latent load in the indoor room as desired. Yet, other components increased the sensible energy of the air circulating in the indoor room and the amount of this energy needed to be accounted for towards the experimental campaign. Such components were the air circulating fans in the conditioning loops (Bays 4 and 6) and the fan used to control static pressure across the flow nozzle bank or code tester (Bay 5). Fans power contribution needed to be assessed in order to get the complete value of sensible load to be set in the indoor room. To determine the power from the fans inside the conditioning bays, a calculation approach based on electrical theory of three phase motors was also considered. A test was done prior to the actual tests of the calibration procedure described in this section in order to verify if this approach was accurate enough for estimating the fan power in load-based tests. In the calibration test, the three fans of the conditioning bays 4, 5, and 6 of the indoor room were run at full speed, that is, the frequency of the controlling VFDs was set to 60Hz. The total sensible heat rejected from the fans into the indoor room air was estimated based on air side measurements of temperatures across the fans in bay 4 and bay 6 and of airflow rate measured with the flow nozzle in bay 5. The calibration test yielded a total sensible heat rejected in the indoor room by the three fans of 81,226 BTU/h (16.5 kW). Since three identical fans and the same full speed were run to circulate the air in the indoor room and no other equipment was on during the test, the result was that approximately 5.5 kW were transferred from each fan to the air stream if the fan in the conditioning bay was at full speed. This value was then compared to the estimated

power given to the fan when the input voltage and current values to the VFD controllers were known. Three-phase electric motor fan power was calculated using the following equation:

$$\dot{W}_{fan,electric} [kW] = \sqrt{3} \times V_{L-L} \times I \times \cos \phi / 1000 \quad (8)$$

Where the V_{L-L} is the line-to-line RMS voltage and $(\cos \phi)$ is the power factor of the electric motor of the fan. The V_{L-L} was varied between 460V and 480V and the current was approximately 13A. The power factor $(\cos \phi)$ was varied parametrically from 0.5 to 0.9. Table 6 shows the resulting power by assuming those power factors.

Table 6: Estimation of fan power for one bay based on VFD current and voltage values

	$V_{L-L} = 460V$ AC, 3 phase, 60 Hz	$V_{L-L} = 480V$ AC, 3 phase, 60 Hz
$\cos \phi$	$\dot{W}_{fan,electric} (kW)$	$\dot{W}_{fan,electric} (kW)$
0.5	5.2	5.4
0.6	6.2	6.5
0.7	7.3	7.6
0.8	8.3	8.6
0.9	9.3	9.7

These values indicate that the power factor of the fan and VFD system (when combined together as a whole device) might have been between 0.5 and 0.6. However, what is more important was that there was a large variation of the estimated fan power based on electric side based on the power factor of the fan and VFD system device. Using VFD current and voltage values, which were given by the VFD displays, might lead to overestimate the sensible heat that the fans put into the indoor room air by as much as 87%. For this reason, in this section, a procedure used for determining fan power contribution is presented. This procedure is also referred to in this project as “Fan Calibration”.

Fan calibrating test conditions, settings and procedure

The load set by the fans depended on fan flow rate (fan speed) and the static pressure drop across them. These variables were not measured by the developed testing method (except for the flow rate

of the code tester fan). It is also important to notice that the static pressure drop across the fans changed depending on the opening of the economizer. Remembering fan laws and typical fan and system curves, different economizer openings yielded different system curves. Hence, a calibration table of fan setting vs. power given was developed for each economizer opening.

a) Economizer damper fully open

The sequence of steps in the procedure to estimate the heat transfer rates from the chamber fans with economizer damper fully open were as follows:

- 1) The conditioning loops fans were set to the same speed they run during the experimental testing campaign. Such speed was the minimum one required to provide enough airflow for all the equipment functioning inside the conditioning loops (i.e. electric heaters) to operate at safe temperatures. In this project, the conditioning loop fans were set to operate at 40% of their full speed.
- 2) Water flow rate to the cooling coils was off.
- 3) The outdoor room was set to the same dry bulb temperatures at which the economizer operated under fully open conditions. 72°F, 65°F and 57°F were the outside air temperatures used in series D and E, economizer with fan speed control tests (see table 4). Each temperature constituted a different calibrating point in this procedure.
- 4) The economizer damper was set to fully open position.
- 5) The indoor room dry bulb temperature was set at 76.5°F and the heaters ran in automatic mode.
- 6) The rooftop unit was run in cooling mode and the unit supply-air fan set to full speed.
- 7) The code tester fan was run at full speed. This speed allowed to control the static pressure across the rooftop unit to 0.4 inH₂O.
- 8) Once the rooms were operating under steady state conditions for at least 30 minutes data was recorded for a minimum of 20 minutes. Steps 1) through 8) were repeated for all the temperatures indicated in step 3).

b) Economizer damper at minimum outdoor air position with full speed fan

The sequence of steps in the procedure to estimate the heat transfer rates from the chamber fans with economizer damper at minimum OA position and with full speed fan were as follows:

- 1) The conditioning loops fans were set to the same speed they run during the experimental testing campaign. Such speed was the minimum one required to provide enough airflow for all the equipment functioning inside the conditioning loops (i.e. electric heaters) to operate at safe temperatures. In this project, the conditioning loop fans were set to operate at 40% of their full speed.
- 2) Water flow rate to the cooling coils was off.
- 3) The outdoor room was set to the same dry bulb temperatures at which the economizer operated under minimum outside air position with full fan speed. 105°F, 95°F, 82°F, 72°F, 65°F and 57°F were the outside air temperatures used in series B, full fan speed with minimum outside air tests (see table 4). Each temperature constituted a different calibrating point in this procedure.
- 4) The economizer damper was set at minimum outdoor air for full speed fan position.
- 5) The indoor room dry bulb temperature was set at 76.5°F and the heaters ran in automatic mode.
- 6) The rooftop unit was run in cooling mode and the unit supply-air fan set to full speed.
- 7) The code tester fan was run at full speed. This speed allowed to control the static pressure across the rooftop unit according to 1 inh₂O.
- 8) Once the rooms were operating under steady state conditions for at least 30 minutes, data was recorded for a minimum of 20 minutes. Steps 1) through 8) were repeated for all the temperatures indicated in step 3).

c) Economizer damper at minimum outdoor air position with low speed fan

The sequence of steps in the procedure to estimate the heat transfer rates from the chamber fans with economizer damper at minimum OA position and with low speed fan were as follows:

- 1) The conditioning loops fans were set to the same speed they run during the experimental testing campaign. Such speed was the minimum one required to provide enough airflow for all the equipment functioning inside the conditioning loops (i.e. electric heaters) to operate at safe temperatures. In this project, the conditioning loop fans were set to operate at 40% of their full speed.
- 2) Water flow rate to the cooling coils was off.
- 3) The outdoor room was set to the same dry bulb temperatures at which the economizer operated under minimum outside air position with half fan speed. 95°F, 82°F, 72°F, 65°F and 57°F were the outside air temperatures used in series C, D and E tests. Series C were the fan speed control tests, and series D were the economizer with fan speed control tests (see table 4). Each temperature constituted a different calibrating point in this procedure.
- 4) The economizer damper was set at minimum outdoor air for low speed (66% of the total speed) fan position.
- 5) The indoor room dry bulb temperature was set at 76.5°F and the heaters ran in automatic mode.
- 6) The rooftop unit was run in cooling mode and the unit supply-air fan set to low (66% of the total) speed.
- 7) The code tester fan was run at 60% speed. This speed allowed to control the static pressure across the rooftop unit according to 0.4 inH₂O.
- 8) Once the rooms were operating under steady state conditions for at least 30 minutes data was recorded for a minimum of 20 minutes. Steps 1) through 8) were repeated for all the temperatures indicated in step 3).

Procedure to calculate the heat rejected by the fans to the indoor room from the calibration test results

Once the heater power was known, applying equation (9) to calculate fan power yielded:

$$\dot{W}_{Fans} = \dot{Q}_{sens} - \dot{W}_{Heaters} \quad (9)$$

Where the term \dot{Q}_{sens} was the sensible cooling provided by the rooftop unit and was calculated according to equation (28). The following example illustrates the calculation for one case encountered in this project.

Example of calibration for power that is rejected to the air as sensible heat:

- Airflow rate was calculated with equation (20) resulting in: $\dot{V}_{supply} = 5075 \text{ cfm}$.
- Return and supply temperatures were: $T_{db,return} = 76.5 \text{ }^\circ\text{F}$ and $T_{db,supply} = 66.2 \text{ }^\circ\text{F}$.
- Return and supply specific heats were: $c_{p,return} = 0.2419 \text{ BTU/lbm}^\circ\text{F}$ and $c_{p,supply} = 0.2417 \text{ BTU/lbm}^\circ\text{F}$.
- Moist air density at the nozzle: $\rho_{nozzle} = 0.0726 \text{ lb/ft}^3$.
- Using equation (28) to calculate the sensible heat capacity of the unit:

$$\dot{Q}_{sens} = \dot{V}_{supply} \rho_{nozzle} (c_{p,return} T_{db,return} - c_{p,supply} T_{db,supply})$$

$$\dot{Q}_{sens} = 5075 \text{ cfm} \left(\frac{60 \frac{\text{ft}^3}{\text{h}}}{1 \text{ cfm}} \right) \times 0.0726 \frac{\text{lb}}{\text{ft}^3} \left(0.2419 \frac{\text{BTU}}{\text{lbm}^\circ\text{F}} \times 76.5 \text{ }^\circ\text{F} - 0.2417 \frac{\text{BTU}}{\text{lbm}^\circ\text{F}} \times 66.2 \text{ }^\circ\text{F} \right)$$

$$\dot{Q}_{sens} = 55373 \frac{\text{BTU}}{\text{h}} \quad (16.23 \text{ kW})$$

- The heater power, determined from the PID controller signals was: $\dot{W}_{Heaters} = 8.6 \text{ kW}$
- Finally equation (9) was used to determine conditioning fans power:

$$\dot{W}_{Fans} = 55373 \frac{\text{BTU}}{\text{h}} - 8.6 \text{ kW} \left(\frac{3412 \text{ BTU}}{1 \text{ kW}} \right) = 26030 \frac{\text{BTU}}{\text{h}} \quad (7.63 \text{ kW})$$

This procedure was used to estimate the sensible load that the lab fans put in the indoor room for a particular fan and economizer configuration of the testing campaign. Sensible loads above this value were provided by the electric heaters to meet the requirements of table 4.

Figure 21 shows the sensible load provided by indoor room chamber fans estimation. The economizer fully open and the minimum outside air with full fan speed values were very close to each other. On the other hand, it was observed that the fan sensible loads for the minimum outside air with low fan speed cases were approximately half of the sensible load provided by the fans at minimum outside air with full fan speed and economizer fully open position.

Both, the economizer fully open and minimum outside air with full fan speed tests were run with supply air fan at 100% and code tester fan at 100%. Moreover, the minimum outside air with low fan speed tests were run with the supply air fan at 66% of the total and the code tester fan at 60%. It was observed that the difference in fan speeds translated into more significant differences in sensible load (fan power) than the ones caused by different economizer positions (which changes the pressure drop of the system) and differences in outside air temperature. In summary, figure 21 indicates that whenever the economizer was at minimum outside air and the supply air fan was operating at low speed (66%) the difference in sensible load (fan power) between this economizer position and the other two, had to be compensated by adjusting the electric heaters in the indoor room.

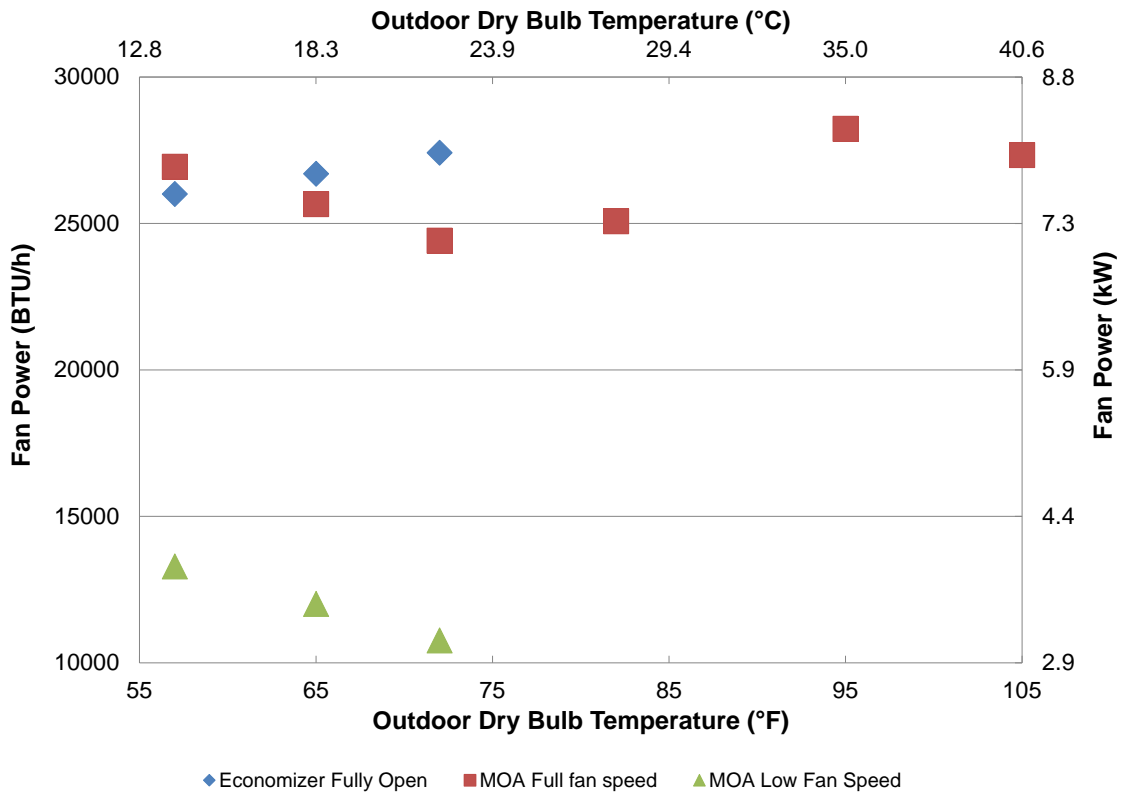


Figure 21: Results of the sensible heat transfer rate rejected by the chamber conditioning equipment air circulating fans at various outdoor dry bulb temperatures and for the case of economizer fully open (blue diamond points) and for the cases of economizer in MOA position with full speed (red square points) and low speed fan (green triangle points).

5.5.1.3 Minimum cooling load case

For tests that required a load setting lower than the minimum one provided by the fans alone, additional cooling needed to be provided by the indoor room cooling coils. The effect of that additional cooling was to decrease the net load set in the room. The procedure used to determine the sensible cooling removed from the indoor air by the cooling coils is described in this section. This procedure is also referred to in this project as “Coil calibration”.

The procedure to determine sensible cooling removed from the air by the chamber indoor room coils for minimum load cooling tests was as follows:

- 1) The conditioning loops fans were set to the same speed they run during the experimental testing campaign. Such speed was the minimum one required to provide enough airflow for all the equipment functioning inside the conditioning loops (i.e. electric heaters) to operate at safe temperatures. In this project, the conditioning loop fans were set to 40%.
- 2) The outdoor room was set to the dry bulb temperature(s) for which the load was less than that provided by the fans. In this project, that temperature was 57°F.
- 3) The economizer damper was set at the same positions at which the load-based test was to be performed according to the thermostatic settings for cooling tests. Since there were 57°F tests in series B, C, D and E. A coil calibration test was ran for each one of the economizer positions.
- 4) The indoor room dry bulb temperature was set at 76.5°F and the heaters ran in automatic mode.
- 5) The rooftop unit was run in cooling mode and the unit fan was set to the speeds at which the load-based test would be run later. That is, the unit supply air fan ran at full speed at minimum outside air and fully open economizer positions and at low speed for the (other) minimum outside air position. Economizer position and fan speed combinations are the same as explained at the thermostatic settings for cooling tests.
- 6) The code tester fan ran at the speed required to control the static pressure across the rooftop unit to 1 inH₂O for full speed tests and 0.4 inH₂O for the low speed tests. That is, the code tester fan ran at 100% for the unit supply air full speed tests and at 60% for the supply air low speed tests.
- 7) The room cooling coils were run at a fixed mass flow rate, the inlet water (refrigerant) temperature to the coils was less than the room dew point at all times, this was to ensure that no dehumidification occurred and therefore the entire load being removed by the coils was sensible.

- 8) Once the rooms were operating under steady state conditions for at least 30 minutes, data was recorded for a minimum of 20 minutes. Steps 1) through 8) were repeated for all different fan operating speeds and economizer damper settings.

Procedure to calculate sensible cooling removed from the air by the chamber indoor room coils from the calibration tests results for minimum load case tests

The calibration procedure was based on the application of a first law of thermodynamics energy balance to the indoor room as explained in 5.3. In this case, the desired outcome of the calibration was the cooling load provided by the coils, which was calculated by equation (10).

$$\dot{Q}_{Coils} = \dot{W}_{Fans} + \dot{W}_{Heaters} - \dot{Q}_{sens} \quad (10)$$

Where \dot{W}_{Fans} was previously determined in the fan calibration tests , using the same supply air fan, conditioning loop fans, economizer opening and dry bulb temperature settings as the coil calibration test. $\dot{W}_{Heaters}$ was obtained from the PID controller set point and \dot{Q}_{sens} was calculated with equation (28).

Example:

- The sensible capacity of the unit was calculated using equation (28).For this example:

$$\dot{Q}_{sens} = 18169 \text{ BTU/h } (5.33 \text{ kW})$$

- The heater power, determined from the PID controller signals was: $\dot{W}_{Heaters} = 2 \text{ KW}$
- Assuming the same fan configuration used in the example in page 79, the fan power was:

$$\dot{W}_{Fans} = 26030 \frac{\text{BTU}}{\text{h}} (7.63 \text{ kW})$$

- Finally equation (10) was used to determine the heat removed by the coils:

$$\dot{Q}_{Coils} = 26030 \frac{\text{BTU}}{\text{h}} + 2 \text{ KW} \left(\frac{3412 \text{ BTU}}{1 \text{ KW}} \right) - 18169 \frac{\text{BTU}}{\text{h}} = 14685 \frac{\text{BTU}}{\text{h}} (4.30 \text{ kW})$$

This procedure was used to estimate the sensible load removed by the cooling coils from the indoor room for a particular fan and economizer configuration of the testing campaign. This sensible cooling balanced the power provided by the fans plus the heaters.

5.5.1.4 Heating Load case

For load-based heating tests, the load set in the room was also a product of an energy balance in the indoor room. In this case, the more important contribution to the indoor room load came from the cooling coils. The rooftop unit matched the sensible load set by the coils in the room to find the desired target indoor temperature. Indoor room conditioning fans and heaters impose a heating load into the room, therefore decreasing the load the unit had to match. To find the balance between the cooling fans, cooling coils and heaters, “Coil calibration” tests were performed. These tests were in principle and in execution quite similar to the coil calibration tests for the minimum cooling load case presented in 5.5.1.3. The specifics of the heating load case are presented in this section

Procedure to determine sensible cooling removed from the air by the chamber indoor room coils for heating tests

- 1) The conditioning loops fans were set to the same speed they run during the experimental testing campaign. Such speed was the minimum one required to provide enough airflow for all the equipment functioning inside the conditioning loops (i.e. electric heaters) to operate at safe temperatures. In this project, the conditioning loop fans were set to 40%.
- 2) The outdoor room was set to the dry bulb temperature(s) for which the heating load based tests would run later.
- 3) All heating tests used the economizer damper at minimum outside air position.
- 4) The indoor room dry bulb temperature was set at 76.5°F and the heaters ran in automatic mode.

- 5) The rooftop unit was run in heating mode and the unit fan was set to the speed at which the load-based test would be run later. For heating tests, the unit supply air fan ran at full speed at minimum outside air
- 6) The code tester fan ran at the speed required to control the static pressure across the rooftop unit according to 1 inH₂O. That is, the code tester fan ran at 100%, since for all heating tests, the unit supply air fan always ran at full speed.
- 7) The room cooling coils were run at a fixed mass flow rate, the inlet water (refrigerant) temperature to the coils was less than the room dew point at all times, this was to ensure that no dehumidification occurred and therefore the entire load being removed by the coils was sensible.
- 8) Once the rooms were operating under steady state conditions for at least 30 minutes, data was recorded for a minimum of 20 minutes. Steps 1) through 8) were repeated for the different outside air temperatures used in load-based heating tests (table 4).

Procedure to calculate sensible cooling removed from the air by the chamber indoor room coils from the calibration tests results for heating tests

The calibration procedure was based on the application of a first law of thermodynamics energy balance to the chamber indoor room. In this case, the desired outcome of the calibration was the cooling load provided by the coils, which was calculated by equation (11).

$$\dot{Q}_{Coils} = \dot{W}_{Fans} + \dot{W}_{Heaters} + \dot{Q}_{sens} \quad (11)$$

Where \dot{W}_{Fans} was previously determined in the fan calibration tests, using the same supply air fan, conditioning loop fans, economizer opening and dry bulb temperature settings as the coil calibration test for heating tests. $\dot{W}_{Heaters}$ was obtained from the PID controller set point and \dot{Q}_{sens} was calculated with equation (31).

5.5.2 Procedures for load setting during experimental testing campaign

5.5.2.1 Load setting for cooling tests

During actual load-based testing, sensible load provided by the humidifier, thermal inertia and other transient factors influence the actual load measured, therefore, results obtained with the procedure described in 5.5.1.2 were considered a means for estimating fan power contribution. Precise tuning of the load setting could only be made during the actual load-based test and differences between the desired and the calculated load were adjusted by increasing or decreasing electric heaters settings until the desired load was reached within the desired tolerances. Having to adjust the electric heaters made the load setting process an iterative one. During load-based testing, rooftop unit fan and conditioning fan were run at the same speeds as the ones used for the calibration process. Whenever the fan speed and/or economizer opening changed during a test due to the control logic of the economizer (explained in thermostatic settings for cooling tests), the heater settings were adjusted accordingly to obtain the desired load.

5.5.2.2 Load setting for minimum cooling load case tests

The procedure for load setting was the same as in 5.5.2.1 except for the additional sensible cooling provided by the cooling coils. Settings of the cooling coil (i.e. water/refrigerant coil entering temperature and flow rate) were the same as in the coil calibration test. Setting the indoor room load during the experimental testing campaign was an iterative process (even more so than 5.5.2.1). The reason for this was that the load from the coil determined with the calibration procedure was not the same when an actual load was being set in the room. That is, the temperature of the air entering the coil was not the same as the steady state calibration test. Therefore, the heaters needed to be adjusted until the desired load was found. The coil calibration procedure gave a good starting point for the iteration process. Nonetheless, it could be found sometimes that no amount of heater adjustment could lead to the desired load. In this case, the steady state coil calibration needed to be repeated with a different coil setting and the iteration process had to start again

5.5.2.3 Load setting for heating tests

The procedure for load setting for heating tests was in general, the same as the minimum cooling load case. Water/refrigerant coil entering temperature and flow rate were the same as in the calibration tests. The process to find the desired load required also several iterations because of the different air temperature in the calibration and the actual load-based test. Again, the results of the calibration provided a good starting point for the iteration process on which the heaters were increased to decrease the load the unit handled and decreased when the opposite outcome was desired. If obtaining the desired heating load with a particular coil setting was not possible, the coil calibration test needed to be repeated with different coil settings, to then repeat the iteration process again.

5.5.3 Testing tolerances

5.5.3.1 Tolerances for steady state tests

All steady state tests, including ASHRAE 116-2010 heating and cooling tests, fan calibration and coil calibration tests were run within the tolerances prescribed by table 3A of ASHRAE 116-2010. This table establishes test condition tolerance and test operating tolerances for heating and cooling steady state tests. A summary of these tolerances is presented next.

Test condition tolerance

Defined as the maximum permissible variation of the full-length test average value of the measurement under specified conditions. Test condition tolerance for the most relevant measurements are as follows:

- Indoor dry bulb entering the unit (indoor return air dry bulb temperature): 0.5°F (0.3°C)
- Indoor wet bulb entering the unit (indoor return air wet bulb temperature): 0.3°F (0.2°C) (this condition is only required for cooling tests).
- Outdoor dry bulb air temperature: 0.5°F (0.3°C)
- Outdoor wet bulb air temperature: 0.3°F (0.2°C)

- External resistance to airflow (unit static pressure difference): 0.02 inH₂O (5 Pa)
- Electrical voltage: $\pm 2\%$

Test operating tolerance

Defined as the maximum permissible deviation of any measurement from the full-length test average value.

- Indoor dry bulb entering the unit (indoor return air dry bulb temperature): 2.0°F (1.1°C)
- Indoor dry bulb leaving the unit (supply air dry bulb temperature): 2.0°F (1.1°C) for cooling and 3.0°F (1.7°C)
- Indoor wet bulb entering the unit (indoor return air wet bulb temperature): 1.0°F (0.6°C) (this condition is only required for cooling tests).
- Indoor wet bulb leaving the unit (supply air wet bulb temperature): 1.0°F (0.6°C) (this condition is only required for cooling tests).
- Outdoor dry bulb temperature: 2.0°F (1.1°C)
- Outdoor wet bulb temperature: 1.0°F (0.6°C)
- External resistance to airflow (unit static pressure difference): 0.05 inH₂O (12.5 Pa)
- Electrical voltage: $\pm 2\%$.

5.5.3.2 Tolerances for load-based tests

For load-based tests, since cycling was present, there were no tolerance requirement for indoor room dry bulb and wet bulb temperature tolerances for both heating and cooling tests. However, the indoor room cycled within certain boundaries established in the thermostatic settings. For the same reason, there were no tolerance requirements for the supply air dry and wet bulb temperatures. Compressor cycling caused the outdoor room dry and wet bulb temperatures to cycle as well, hence the tolerance indicated in table 7. Unit static pressure difference and electrical voltage tolerance are also indicated in table 7. The tolerance for load setting indicated in the table is 1.25 kW, or 4265

BTU/h. The reason for this value is that the heaters in the indoor room chamber can be adjusted up or down by a minimum of 2kW at a time.

Table 7: Test Tolerances for Load-based Tests

	Test Operating Tolerance – IP units	Test Condition Tolerance – IP units	Test Operating Tolerance – SI units	Test Condition Tolerance – SI units
Indoor dry-bulb	--	--	--	--
Entering	--	--	--	--
Leaving	--	--	--	--
Indoor wet-bulb	--	--	--	--
Entering	--	--	--	--
Leaving	--	--	--	--
Outdoor dry-bulb	4.00 °F	0.80 °F	2.20 °C	0.40 °C
Outdoor wet-bulb	4.00 °F	2.60 °F	2.20 °C	0.40 °C
External resistance to airflow	0.05 inH2O	0.02 inH2O	12.50 Pa	5.00 Pa
Electrical voltage, ±%	2.00	2.00	2.00	2.00
Capacity	--	4265 BTU/h	--	1.25 kW

5.5.4 Testing Procedures

5.5.4.1 Test Procedure for ASHRAE 116-2010 Steady-State Heating and Cooling Tests

Test Procedure for ASHRAE 116-2010 Steady-State Heating and Cooling Tests were as follows:

1. Indoor and outdoor rooms were set to the dry and wet bulb conditions indicated in table 4.
2. At the same time, the rooftop unit was run at full capacity, that is, full supply air fan speed, full condenser fan speed and both compressors running at 100% capacity (full load).
3. Unit static pressure difference was controlled to 0.3 inches of water.
4. When conditions were steady for at least one hour according to the tolerance for steady state tests, recordings were taken for 60 minutes, with a 2-second sampling time.

5.5.4.2 Test Procedures for Load-Based Constant Cooling Load Tests

A general description of the procedure steps is as follows:

- 1) The indoor and outdoor rooms of the chamber and the rooftop unit were operated in cooling mode until equilibrium conditions were attained but not for less than thirty minutes. During this first thirty minutes, the outdoor room dry bulb and wet bulb temperatures were at steady state according to the test conditions in table 4 for a particular test. The return air dry bulb temperature was representative of the indoor room conditions. During this period, the indoor room dry bulb temperature was set to 77°F (25°C) and the wet bulb temperature to 66°F (18.9°C). The economizer was set to minimum outside air position (min OA). The condition and operating tolerances during this period were the same of ASHRAE 116-2010 steady state tests.
- 2) Following the first thirty minutes, the control of the humidifier and electric heaters were set to manual mode in order to provide constant latent load and sensible load to the indoor room. The cooling coils of the indoor room were closed so the equipment under testing directly controlled the sensible and latent loads from this point forward. For the minimum cooling load case only, the cooling coils remained open providing the same water/refrigerant flow rate and inlet water/water temperature as the one used in the coil calibration tests. After both sensitive and latent loads were set, the room should underwent a period of 60 minutes of transitory operation before the start of the actual testing period for performance characterization of the tested equipment. Acceptable return air temperatures for the purpose of developing the method of test ranged from 75°F (23.9°C) to 77.5°F (25.3°C). Whenever the return dry bulb temperature reached those boundaries, the unit was cycled on/off according to the thermostat setting sequence described in 5).
- 3) Unit Static Pressure Difference (External resistance to airflow): The unit static pressure difference was set to 1.0 in H₂O (~249 Pa) for full speed fan operation and 0.4 in H₂O (~100

Pa) for low speed operation, which is higher than the ones set in the standards ANSI/AHRI 210/240 and 340/360. This is based on findings by Jacobs 2003 and Kavanaugh 2002 who indicated that average static pressure drop across typical rooftop units was 0.48 in H₂O (~120Pa) which is higher than the average pressure drop of the units mentioned in the standards.

- 4) Fan control requirements: Two fan speeds were used in cooling tests. Full speed and low speed. Low speed was set at 66% of the total full speed used. Low or minimum speeds were used for the speed control and economizer with speed control tests. The minimum ventilation air was set at 10% of the volumetric supply airflow rate at high fan speed. At low fan speed (66%), the economizer damper was set at a position to provide the same minimum volumetric outside airflow rate as at high fan speed.
- 5) Thermostat settings: An electro-mechanical multi-stage thermostat was simulated by using the programming software of the laboratory data acquisition and control system. The following sequence was used to simulate an electro-mechanical multi-stage thermostat without anticipator. The sequence was included in the method of test as the default testing control approach because an actual thermostat was not being tested. The simulated thermostat was used to provide the following cooling set points based on indoor dry bulb return temperature for the testing equipment.

a) Minimum outside air with full fan speed tests

Return temperature is increasing

- Mechanical cooling stage 1 on: turn on compressor stage 1 if the return temperature is > 76.5°F (24.7°C); the supply air fan operates at full speed with the economizer set at minimum outside air for full fan speed position.

- Mechanical cooling stage 2 on: turn on compressor stage 2 if the return temperature is $> 77.5^{\circ}\text{F}$ (25.3°C); the supply air fan operates at full speed with the economizer set at minimum outside air for full fan speed position.

Return temperature is decreasing

- Mechanical cooling stage 2 off: turn off compressor stage 2 if the return temperature is $< 77.0^{\circ}\text{F}$ (25°C); the supply air fan operates at full speed with the economizer set at minimum outside air for full fan speed position.
- Mechanical cooling stage 1 off: turn off compressor stage 1 if the return temperature is $< 76.0^{\circ}\text{F}$ (24.4°C); the supply air fan operates at full speed with the economizer set at minimum outside air for full fan speed position.

Figure 22 shows a graphical representation of the thermostatic settings for minimum outside air with full fan speed tests.

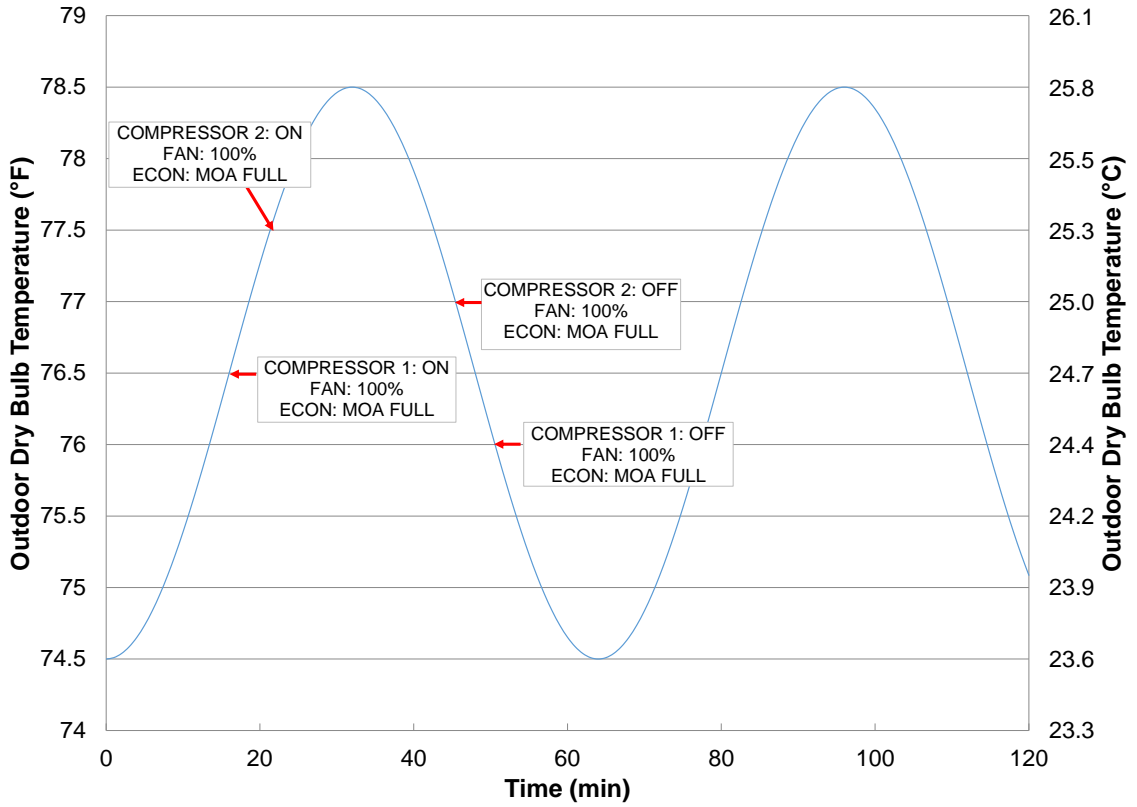


Figure 22: Example of the thermostatic settings used in the present work for the cooling mode load-based tests with minimum outside air and with full fan speed tests

b) Speed control tests

Return temperature is increasing

- Mechanical cooling stage 1 on: turn on compressor stage 1 if the return temperature is $> 76.5^{\circ}\text{F}$ (24.7°C); the supply air fan operates at low speed with the economizer set at minimum outside air for low fan speed position.
- Mechanical cooling stage 2 on: turn on compressor stage 2 if the return temperature is $> 77.5^{\circ}\text{F}$ (25.3°C); the supply air fan operates at low speed with the economizer set at minimum outside air for low fan speed position.

Return temperature is decreasing

- Mechanical cooling stage 2 off: turn off compressor stage 2 if the return temperature is $< 77.0^{\circ}\text{F}$ (25°C); the supply air fan operates at low speed with the economizer set at minimum outside air for low fan speed position.
- Mechanical cooling stage 1 off: turn off compressor stage 1 if the return temperature is $< 76.0^{\circ}\text{F}$ (24.4°C); the supply air fan operates at low speed with the economizer set at minimum outside air for low fan speed position.

Figure 23 shows a graphical representation of the thermostatic settings for speed control tests.

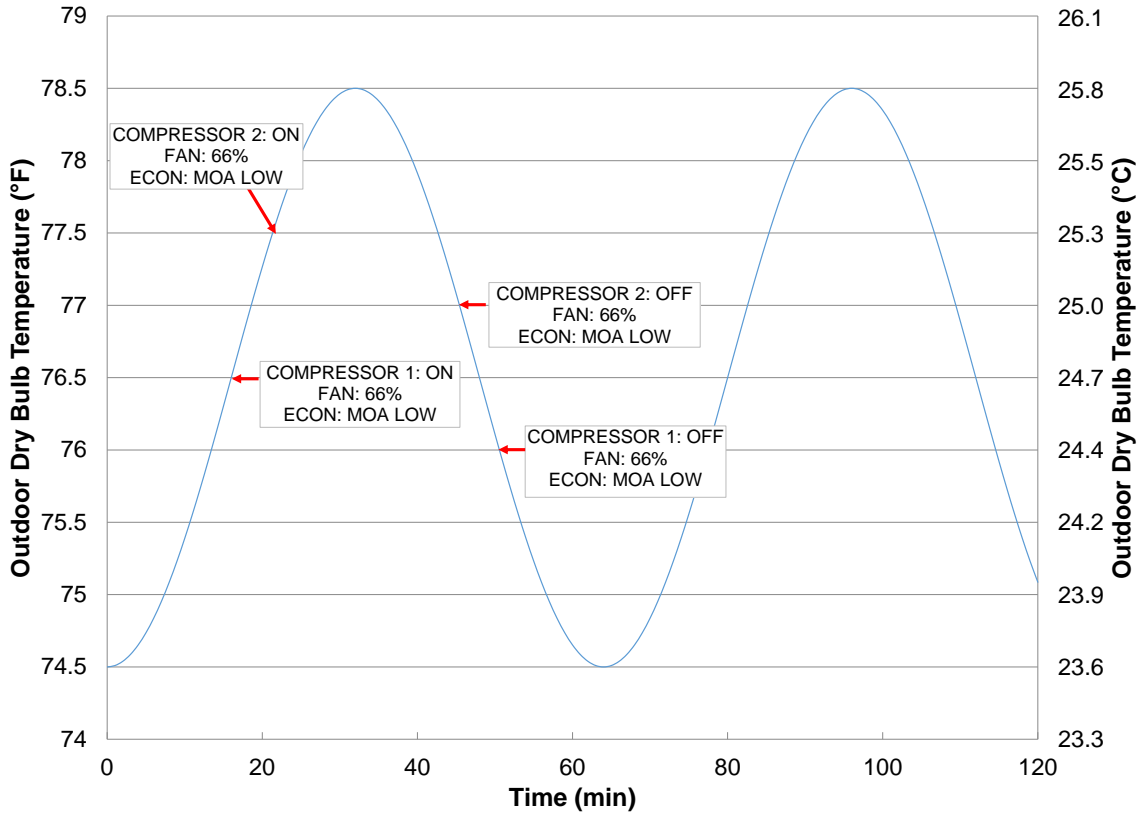


Figure 23: Example of the thermostatic settings used in the present work for the cooling mode load-based tests with fan speed control technology integrated in the RTU.

c) Economizer Tests

Return temperature is increasing and outside temperature is below economizer high limit

When return air temperature is $\leq 75^{\circ}\text{F}$ (23.9°C), the unit operates at low speed (66%) with the economizer damper set at low speed position.

- Economizer on: turn on economizer if the return temperature becomes $> 75.5^{\circ}\text{F}$ (24.2°C); the supply air fan operates at full speed with the economizer set at 100% open position.
- Mechanical cooling stage 1 on: turn on compressor stage 1 if the return temperature is $> 76.5^{\circ}\text{F}$ (24.7°C); the supply air fan operates at full speed with the economizer set at 100% open position.

- Mechanical cooling stage 2 on: turn on compressor stage 2 if the return temperature is $> 77.5^{\circ}\text{F}$ (25.3°C); the supply air fan operates at full speed with the economizer set at 100% open position.

Return temperature is decreasing and outside temperature is below economizer high limit

- Mechanical cooling stage 2 off: turn off compressor stage 2 if the return temperature is $< 77.0^{\circ}\text{F}$ (25°C); the supply air fan operates at full speed with the economizer set at 100% open position.
- Mechanical cooling stage 1 off: turn off compressor stage 1 if the return temperature is $< 76.0^{\circ}\text{F}$ (24.4°C); the supply air fan operates at full speed with the economizer set at 100% open position.
- Economizer off: turn off economizer if the return temperature is $< 75.0^{\circ}\text{F}$ (23.9°C); the supply air fan operates at minimum or low speed (66%) with the economizer damper set at minimum outside air for low speed position.
- During combined economizer and mechanical cooling operation, should the supply air temperature fall below 45°F (7.2°C), the economizer outside air damper closes until the supply air is 53°F (11.7°C) for the remainder of the mechanical cooling cycle.

Return temperature is increasing and outside temperature is above economizer high limit

When the return air temperature is $\leq 75.5^{\circ}\text{F}$ (24.2°C), the unit operates at low speed (66%) with the economizer damper set at minimum outside air for low speed position.

- Mechanical cooling stage 1 on: turn on compressor stage 1 if the return temperature is $> 76.5^{\circ}\text{F}$ (24.7°C); the supply air fan operates at low speed (66%) with minimum outside air set at minimum outside air for low speed position..
- Mechanical cooling stage 2 on: turn on compressor stage 2 if the return temperature is $> 77.5^{\circ}\text{F}$ (24.7°C); the supply air fan operates at low speed (66%) with minimum outside air set at minimum outside air for low speed position.

Return temperature is decreasing and outside temperature is above economizer high limit

- Mechanical cooling stage 2 off: turn off compressor stage 2 if return temperature is $< 77.0^{\circ}\text{F}$ (25°C); the supply air fan operates at minimum or low speed (66%) with the economizer damper set at minimum outside air for low speed position.
- Mechanical cooling stage 1 off: turn off compressor stage 1 if return temperature is $< 76.0^{\circ}\text{F}$ (24.4°C); the supply air fan operates at minimum or low speed (66%) with the economizer damper set at minimum outside air for low speed position.

The economizer high limit was set as follows

- Climate Zone 4C Economizer high limit: If the outdoor temperature becomes $> 75.0^{\circ}\text{F}$ (22.2°C), the economizer must go into minimum outside air position.
- Climate Zone 3A Economizer high limit: If the outdoor temperature becomes $> 65.0^{\circ}\text{F}$ (18.3°C), the economizer must go into minimum outside air position.

Figure 24 shows a graphical representation of the thermostatic settings for economizer tests.

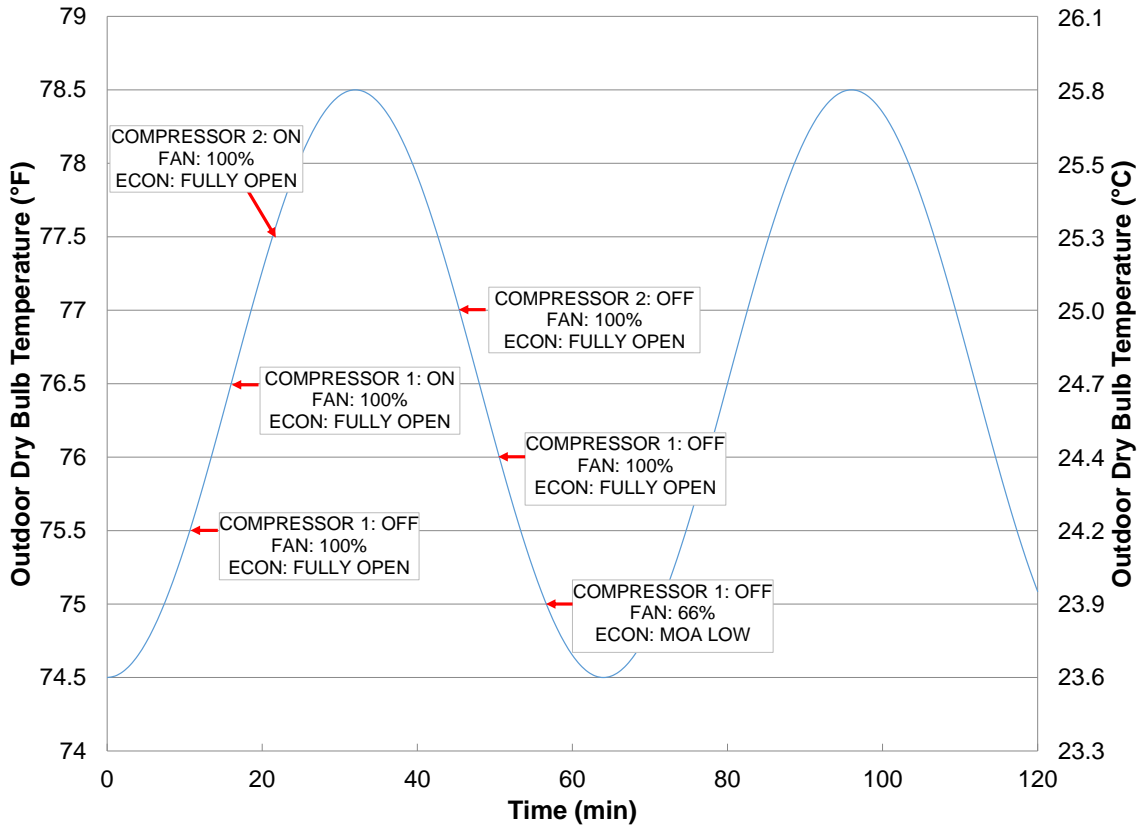


Figure 24: Example of the thermostatic settings used in the present work for the cooling mode load-based tests with economizer technology integrated in the RTU.

5.5.4.3 Test Procedures for Load-Based Variable Cooling Load Tests

The procedure and requirements for variable cooling load tests were the same as constant load tests described in 5.5.4.2 with the exception of the way the indoor heaters were controlled. For the constant load tests, the heaters remained constant throughout a test if no fan or economizer damper position changes were made. For the economizer tests, the heaters were modified in coordination with the changes in supply air fan speed and economizer opening to keep a constant load setting in the indoor room. For the variable load tests, the heaters were “cycled” periodically to a percentage above the nominal value of the load for a particular time frame, and then the same percentage below the nominal value of the load for the same period of time. For instance, for one of the

variable load tests, load settings were 115% of the nominal load during 10 minutes, and then 85% of the nominal load during the subsequent 10 minutes until the full time of the test was completed.

5.5.4.4 Test Procedures for Load-Based Constant Heating Load Tests

A general description of the procedure is as follows:

- 1) The indoor and outdoor rooms of the chamber and the rooftop unit were operated in heating mode until equilibrium conditions were attained but not for less than thirty minutes. During this first thirty minutes, the outdoor room dry bulb and wet bulb temperatures were at steady state according to the test conditions in table 4 for a particular test. The return air dry bulb temperature was representative of the indoor room conditions. During this period, the indoor room dry bulb temperature was set to 77°F (25°C). The economizer was set to minimum outside air position (min OA). The condition and operating tolerances during this period were the same of ASHRAE 116-2010 steady state tests described in 5.5.3.
- 2) Following the first thirty minutes, the control of the electric heaters were set to manual mode in order to provide constant sensible load to the indoor room. The cooling coils of the indoor room remained open providing the same water/refrigerant flow rate and inlet water/water temperature as the one used in the coil calibration tests for heating tests. After the sensible load was set, the room should underwent a period of 60 minutes of transitory operation before the start of the actual testing period for performance characterization of the tested equipment. Acceptable return air temperatures for the purpose of developing the method of test ranged from 75°F (23.9°C) to 77.5°F (25.3°C). Whenever the return dry bulb temperature reached those boundaries, the unit was cycled on/off according to the thermostat setting sequence described in 5).

- 3) Unit Static Pressure Difference (External resistance to airflow): The unit static pressure difference was set to 1.0 in H₂O (~249 Pa) since the supply air fan operated at full speed at all times.
- 4) Fan control requirements: The supply air fan was run at 100% (full) speed for all tests. The minimum ventilation air was set at 10% of the volumetric supply airflow rate at high fan speed.
- 5) Thermostat settings: Like in the cooling tests, a multi-stage thermostat was simulated by using the programming software of the laboratory data acquisition and control system. The sequence was included in the method of test as the default testing control approach because an actual thermostat was not being tested. The simulated thermostat was used to provide the following heating set points based on indoor dry bulb return temperature for the testing equipment.

Return temperature is decreasing

- Mechanical heating stage 1 on: turn on compressor stage 1 if the return temperature is < 76.5°F (24.7°C); the supply air fan operates at full speed with the economizer set at minimum outside air for full speed position.
- Mechanical heating stage 2 on: turn on compressor stage 2 if the return temperature is < 75.5°F (24.2°C); the supply air fan operates at full speed with the economizer set at minimum outside air for full speed position.

Return temperature is increasing

- Mechanical heating stage 2 off: turn off compressor stage 2 if the return temperature is > 76.5°F (24.7°C); the supply air fan operates at full speed with the economizer set at minimum outside air for full speed position.
- Mechanical heating stage 1 off: turn off compressor stage 1 if the return temperature is > 77.5°F (25.3°C); the supply air fan operates at full speed with the economizer set at minimum outside air for full speed position.

Figure 25 shows a graphical representation of the thermostatic settings for heating tests.

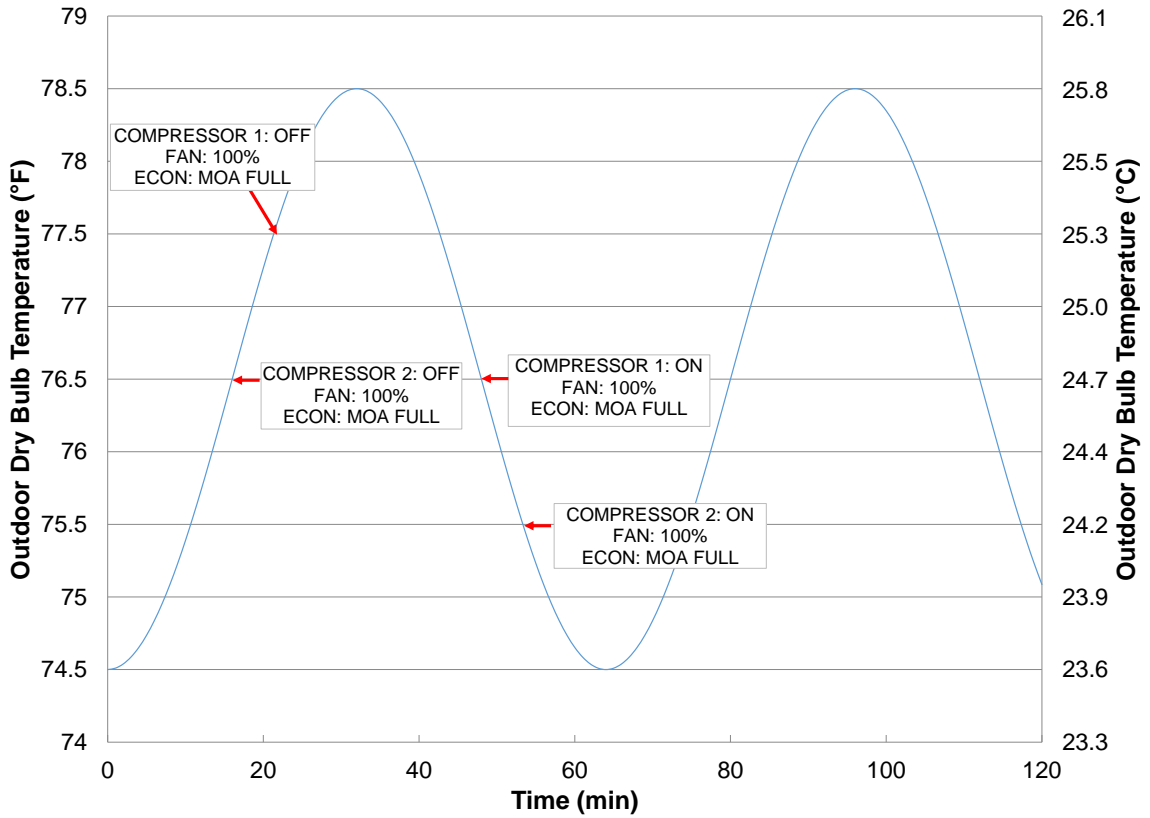


Figure 25: Example of the thermostatic settings used in the present work for the heating mode load-based tests

5.5.5 Recordings

Recordings for load-based tests were taken for the time periods indicated in table 4 and with a 2-second sampling rate. The data were within the tolerances indicated in table 7.

CHAPTER VI

VI. DATA REDUCTION

The Oklahoma State University psychrometric chamber facility used 384 sensors to determine the response, behavior, and adjustments needed in order to maintain indoor and outdoor room set points as well as monitor all the experiments ongoing within the facility. The majority of these sensors were used to control the facility and make sure equipment and components such as the cooling coils, the conditioning fans, the heaters, and the cooling coil water/refrigerant circulating pumps were operating properly and within safe limits. Signals from all these sensors, as well as all the analog inputs and outputs of the chamber controls from and to the transducers and actuators were recorded with a sample rate of every 2 seconds and for a recording period of up to 3 hours during each test. Each recording produced an output text file that was saved and archived in the hard disk memory of the data acquisition and process control computer. The text files were then converted to Excel files. Each Excel file contains two sheets, one with all the raw data as they were loaded from the original text file and the second spreadsheet containing the signals filtered, translated into values for the variables of interest, and reduced to psychrometric quantities according to the data reduction procedure presented in this thesis. The reduced data included all the information necessary to calculate the figures of merit that characterized the RTU, as well as all the variables that were commonly reported in the output test result summary document.

During this conversion process, the original text file with the raw data in it remained unchanged in case that future post-processing process are needed. The reduced data were then exported to a program written by using Engineering Equation Solver software (EES). The program in EES had built-in libraries that estimated moist air thermo-physical properties. These calculated moist air properties were then imported back to Excel spreadsheet file where all the relevant variables were obtained and the figures of merit were calculated for each test. Average quantities were calculated and statistical analysis of the data was conducted as explained next in this chapter.

6.1 Variables to be recorded and calculated

Table 8 shows all the measured and calculated variables required for each load-based test. Table 8 includes all the data required by ASHRAE 116-2010 standard plus a series of parameters inherent to the load-based method of test and the technologies that were tested in this project.

Table 8: Variables to be recorded and calculated

Item	Units
Date	
Barometric pressure	in. water (Pa)
Times	
Power input to equipment(a)	W
Frequency	Hz
External resistance to airflow or coil pressure drop	in. water (Pa)
Fan speed(s)	Rpm
Dry-bulb temperature of indoor return air entering equipment	°F (°C)
Wet-bulb temperature of indoor return air entering equipment	°F (°C)
Dry-bulb temperature of supply air leaving equipment	°F (°C)
Wet-bulb temperature of the supply air leaving equipment	°F (°C)
Dry-bulb temperature of outdoor return air entering the economizer	°F (°C)
Wet-bulb temperature of outdoor return air entering the economizer	°F (°C)
Throat diameter of nozzle(s)	In (cm)
Static pressure difference across nozzle (s)	in. water (Pa)
Temperature at nozzle throat	°F (°C)
Pressure at nozzle throat	in. water (Pa)
Static Pressure difference across economizer inlet	in. water (Pa)
Power to electric heaters	kW
Steam output from the humidifier	lb/h (kg/s)
Cycling time (if any cycling is present)	min
Supply airflow rate	CFM (m ³ /s)
Outside airflow rate through economizer	CFM (m ³ /s)
Total Capacity of the unit	BTU/h (kW)
Sensible Capacity of the unit	BTU/h (kW)
Total Capacity of the unit without outdoor air ventilation effects	
Total Coefficient of Performance	
Sensible Coefficient of Performance	
Total Coefficient of Performance without outdoor air ventilation effects	
Temperature Control Figure of Merit	°F (°C)

6.2 Moist air properties estimation

ASHRAE Standard 116-2010 formulas used to calculate airflow rate and unit capacity on the air side, are based on air-water vapor mixture properties presented in the ASHRAE Handbook of Fundamentals (ASHRAE 2009b), Psychometrics chapter. Hyland and Wexler (1983a, 1983b) originally developed the air-water vapor mixture properties equations presented in the Handbook. The Engineering Equation Solver software (EES) has a built-in library called AIRH2O, which allows estimating air-water vapor mixture properties. EES AIRH2O library also uses the thermodynamic properties equations developed by Hyland and Wexler 1983. This library consolidates in a single tool, formulations for the thermodynamic properties of saturated phases of water from 173.15K to 473.15K (311.67R to 851.67R), dry air from 173.15K to 373.15K (311.67R to 671.67R) and saturated moist air from 173.15K to 372.15K (311.67R to 669.87R) at pressures up to 5 MPa (725.2 psi). In other words, the correlations are valid for moist air temperatures up to 210.2 °F (99 °C). EES reference state for dry air enthalpy at 0°F and 0°C is zero, which is consistent with most psychrometric charts (Klein and Alvarado 2015). EES functions facilitate the data reduction process allowing to determine moist air properties such as humidity ratio, enthalpy, density and specific heat.

6.3 Main equations used during the data reduction

The equations used to calculate unit capacity (indoor room load), COP efficiency, supply airflow rate, economizer airflow rate and the temperature control figure of merit are presented next.

6.3.1 Air properties

$$P_{supply} = P_{barometer} + \Delta_{p,unit} \quad (12)$$

Where:

P_{supply} : Absolute supply air pressure, inH₂O (Pa)

$P_{barometer}$: Atmospheric air pressure, inH2O (Pa)

Δp_{unit} : Static pressure difference across the unit (external resistance to airflow), inH2O (Pa)

$$P_{nozzle,absolute} = P_{barometer} + P_{nozzle,gage} \quad (13)$$

Where:

$P_{nozzle,absolute}$: Absolute air pressure at code tester nozzle inlet, inH2O (Pa)

$P_{nozzle,gage}$: Measured manometric air pressure at nozzle inlet, inH2O (Pa)

$$\omega_{supply} = f(T_{db,supply}, T_{wb,supply}, P_{supply}) \quad (14)$$

Where:

ω_{supply} : Supply air humidity ratio as a function of supply air dry and wet bulb temperatures and supply air pressure (calculated with EES), lb_{H2O}/lb_{dry air} (kg_{H2O}/kg_{dry air})

$T_{db,supply}$: Supply air dry bulb temperature, °F (°C)

$T_{wb,supply}$: Supply air wet bulb temperature, °F (°C)

$$\rho_{nozzle} = f(T_{nozzle}, P_{nozzle,absolute}, \omega_{supply}) \quad (15)$$

Where:

ρ_{nozzle} : Air density at nozzle as a function of dry bulb temperature at the nozzle, pressure at nozzle inlet and supply air humidity ratio (calculated with EES), lbm/ft³ (kg/ m³)

T_{nozzle} : Dry bulb temperature at the nozzle, °F (°C)

It is assumed that the humidity ratio remains constant between the supply air and nozzle inlet points of measurement.

$$h_{supply} = f(T_{db,supply}, T_{wb,supply}, P_{supply}) \quad (16)$$

Where:

h_{supply} : Supply air enthalpy as a function of supply air dry and wet bulb temperatures and supply air pressure (calculated with EES), BTU/lbm (kJ/kg)

$$h_{return} = f(T_{db,return}, T_{wb,return}, P_{barometer}) \quad (17)$$

Where:

h_{return} : Return air enthalpy as a function of return air dry and wet bulb temperatures and atmospheric air pressure (calculated with EES), BTU/lbm (kJ/kg)

$$c_{p,supply} = f(T_{db,supply}, T_{wb,supply}, P_{supply}) \quad (18)$$

Where:

$c_{p,supply}$: Supply air specific heat at constant pressure as a function of supply air dry and wet bulb temperatures and supply air pressure (calculated with EES), BTU/lbm (kJ/kg)

$$c_{p,return} = f(T_{db,return}, T_{wb,return}, P_{barometer}) \quad (19)$$

Where:

$c_{p,return}$: Return air specific heat at constant pressure as a function of return air dry and wet bulb temperatures and atmospheric air pressure (calculated with EES), BTU/lbm (kJ/kg)

6.3.2 Airflow rate

6.3.2.1 Supply airflow rate

$$\dot{V}_{supply} = 1096 Y \sqrt{\frac{\Delta p_{nozzle}}{\rho_{nozzle}}} \sum (CA_{nozzle}) \left[\dot{V}_{supply} = Y \sqrt{2 \frac{\Delta p_{nozzle}}{\rho_{nozzle}}} \sum (CA_{nozzle}) \right] \quad (20)$$

Where:

\dot{V}_{supply} : Supply airflow rate, CFM (m³/s)

Y: Expansion factor, dimensionless

C: Nozzle coefficient of discharge, dimensionless

A_{nozzle} : Area of each nozzle, ft² (m²)

Δp_{nozzle} : Static pressure difference across the nozzle bank, inH₂O (Pa)

$$Y = 1 - 0.548(1 - \alpha) \quad (21)$$

Where:

α : Alpha ratio (ratio of absolute nozzle exit pressure to absolute pressure)

$$\alpha = 1 - 5.187 \frac{\Delta_{p,nozzle}}{\rho_{nozzle} T_{nozzle} R} \quad \left[\alpha = 1 - \frac{\Delta_{p,nozzle}}{\rho_{nozzle} T_{nozzle} R} \right] \quad (22)$$

Where:

T_{nozzle} : Dry bulb temperature at the nozzle, R (K)

R: Ideal gas constant of air, ft-lbf/lbm-R (J/kg-K)

$$C = 2.2 \times 10^{-31} Re^5 - 6.1 \times 10^{-25} Re^4 + 6.8 \times 10^{-19} Re^3 - 3.9 \times 10^{-13} Re^2 + 1.3 \times 10^{-7} Re + 0.97 \quad (23)$$

Where:

Re : Reynolds number at the nozzle

Equation (23) is a polynomial regression of the coefficients of discharge for airflow nozzles in table 4 of ASHRAE Standard 41-2 1987 Standard Methods for Laboratory Airflow Measurements (ASHRAE 1992).

$$Re = 1.636 \times 10^6 D_{nozzle} \sqrt{\frac{\Delta_{p,nozzle}}{\rho_{nozzle}}} \quad Re = 70.9 \times 10^3 D_{nozzle} \sqrt{\frac{\Delta_{p,nozzle}}{\rho_{nozzle}}} \quad (24)$$

Where:

D_{nozzle} : Nozzle diameter, ft (m)

6.3.2.2 Economizer airflow rate

$$\dot{V}_{econ,fo} = -4171.4 \Delta_{p,econ}^2 + 9797 \Delta_{p,econ} - 25.835 \quad (25)$$

$$[\dot{V}_{econ,fo} = -3.17 \times 10^{-5} \Delta_{p,econ}^2 + 1.86 \times 10^{-2} \Delta_{p,econ} - 4.89 \times 10^{-5}]$$

$$\dot{V}_{econ,moa,f} = 1537.6 \Delta_{p,econ}^2 - 57.58 \Delta_{p,econ} - 3 \times 10^{-12} \quad (26)$$

$$[\dot{V}_{econ,moa,f} = 1.17 \times 10^{-5} \Delta_{p,econ}^2 - 1.09 \times 10^{-4} \Delta_{p,econ} - 5.68 \times 10^{-18}]$$

$$\dot{V}_{econ,moa,l} = -5455.8 \Delta_{p,econ}^2 + 4569.9 \Delta_{p,econ} + 94.623 \quad (27)$$

$$[\dot{V}_{econ,moa,l} = -4.15 \times 10^{-5} \Delta_{p,econ}^2 + 8.66 \times 10^{-3} \Delta_{p,econ} + 1.79 \times 10^{-4}]$$

Where:

$\dot{V}_{econ,fo}$: Economizer airflow rate for fully open position, cfm (m³/s)

$\dot{V}_{econ,moa,f}$: Economizer airflow rate for minimum outside air with full fan speed position, cfm (m³/s)

$\dot{V}_{econ,moa,l}$: Economizer airflow rate for minimum outside air with low fan speed position, cfm (m³/s)

$\Delta_{p,econ}$: Static pressure difference across economizer inlet, inH₂O (Pa)

6.3.3 Unit Capacity (Indoor Room Load)

6.3.3.1 Cooling mode heat transfer rates

$$\dot{Q}_{sens} = \dot{V}_{supply} \rho_{nozzle} (c_{p,return} T_{db,return} - c_{p,supply} T_{db,supply}) \quad (28)$$

$$\dot{Q}_{total} = \dot{V}_{supply} \rho_{nozzle} (h_{return} - h_{supply}) \quad (29)$$

$$\dot{Q}_{lat} = \dot{Q}_{total} - \dot{Q}_{sens} \quad (30)$$

Where:

\dot{Q}_{sens} : Unit sensible cooling capacity or indoor room sensible cooling load, BTU/h (kW)

\dot{Q}_{total} : Unit total cooling capacity or indoor room total cooling load, BTU/h (kW)

\dot{Q}_{lat} : Unit latent cooling capacity or indoor room latent load, BTU/h (kW)

Equations (28), (29), (30) were calculated instantaneously, that is, for every recorded data point and then averaged throughout the entire length of the test.

6.3.3.2 Heating mode heat transfer rates

$$\dot{Q}_{sens} = \dot{V}_{supply} \rho_{nozzle} (c_{p,supply} T_{db,supply} - c_{p,return} T_{db,return}) \quad (31)$$

$$\dot{Q}_{total} = \dot{V}_{supply} \rho_{nozzle} (h_{supply} - h_{return}) \quad (32)$$

$$\dot{Q}_{lat} = \dot{Q}_{total} - \dot{Q}_{sens} \quad (33)$$

Where:

\dot{Q}_{sens} : Unit sensible heating capacity or indoor room sensible heating load, BTU/h (kW)

\dot{Q}_{total} : Unit total heating capacity or indoor room total heating load, BTU/h (kW)

\dot{Q}_{lat} : Indoor room latent load, BTU/h (kW)

Equations (31), (32) and (33) were calculated instantaneously, that is, for every recorded data point and then averaged throughout the entire length of the test.

6.3.4 Coefficient of Performance

6.3.4.1 Cooling mode COPs

$$COP = \frac{\dot{Q}_{total,average}}{\dot{W}_{unit,average}} \quad (34)$$

$$COP_{sens} = \frac{\dot{Q}_{sens,average}}{\dot{W}_{unit,average}} \quad (35)$$

Where:

COP : Unit total cooling coefficient of performance, dimensionless

COP_{sens} : Unit sensible cooling coefficient of performance, dimensionless

$\dot{Q}_{total,average}$: Unit total cooling capacity or indoor room total cooling load averaged throughout the entire length of the test, BTU/h (kW)

$\dot{Q}_{sens,average}$: Unit sensible cooling capacity or indoor room total cooling load averaged throughout the entire length of the test, BTU/h (kW)

$\dot{W}_{unit,average}$: Unit power consumption averaged throughout the entire length of the test, BTU/h (kW)

6.3.4.2 Heating mode COPs

$$COP = COP_{sens} = \frac{\dot{Q}_{sens,average}}{W_{unit,average}} \quad (36)$$

Where:

COP : Unit total heating coefficient of performance, dimensionless

COP_{sens} : Unit sensible heating coefficient of performance, dimensionless

$\dot{Q}_{sens,average}$: Unit sensible heating capacity or indoor room sensible heating load averaged throughout the entire length of the test, BTU/h (kW)

$W_{unit,average}$: Unit power consumption averaged throughout the entire length of the test, BTU/h (kW).

6.3.5 Temperature control figure of merit, $\sigma_{tdb,return}$

For the load-based tests, a temperature control figure of merit, $\sigma_{tdb,return}$ is introduced in this thesis for the return air dry bulb temperature and it was calculated as follows:

$$\sigma_{tdb,return} = \sqrt{\frac{\sum_i^n (T_{db,return} - T_{db,return,target})^2}{n}} \quad (37)$$

Where $T_{db,return,target}$ represents the target set point dry bulb return temperature (i.e. 76.5°F (24.7°C) for the tests of this project), and $T_{db,return}$, is the instantaneous measured return dry bulb temperature at each sampled time i , (the sampled time step was every 2 seconds for the tests conducted in this project), and n is the number of samples.

Total quantities in this project were averaged throughout the entire test length as indicated in table 4. However, in the following chapter, other methods of averaging that were studied in this project will be presented.

6.4 Verification of capacity measurements taken with the OSU psychrometric facility

The OSU psychrometric chamber airflow rates and heat transfer capacity measurements were verified in previous work. Using the same psychrometric facility, that is, identical instrumentation and configuration of the instrumentation within the chamber, Worthington (2011) conducted tests with an 11-ton (39 kW) unit at 95°F (35°C) and indoor conditions of 80°F (26.7°C) and 67°F (19.4°C) dry and wet bulb temperatures, respectively. The same unit was also tested at the manufacturer's laboratory and at a certified agency for energy performance rating of rooftop units. Measurements from OSU psychrometric chamber were within 5% of the capacity and 2% of the airflow rate obtained at the outside laboratories.

Corti and Marelli (2013) tested the 15-ton (53 kW) RTU of the present study at several indoor and outdoor temperature conditions. In their work, the authors operated only the first stage compressor and the first stage refrigerant circuit of the RTU was instrumented with additional refrigerant pressure transducers and in-line refrigerant temperature sensors. This additional instrumentation allowed the authors to conduct an order of magnitude heat balance analysis between the primary method of measurement of the unit heat transfer capacity, i.e. the air side heat transfer capacity measured from the instrumentation of the psychrometric chamber located externally to the RTU, and a secondary redundant method of measurement of the unit capacity, that is the refrigerant side heat transfer capacity measured from pressure, temperature, and mass flow meter sensors installed inside the RTU. In their work, they reported a heat balance between the air and refrigerant sides that ranged from -18.9% to 7.7%. The discrepancy between air side and refrigerant side was due to the fact the indoor coil outlet refrigerant temperature (i.e. the evaporator outlet refrigerant temperature when the RTU run in cooling mode) was assumed to be equal to the compressor suction line temperature. Only the latter was directly measured with an in-line T-Type thermocouple in their work.

Additional verification was conducted in this project to estimate the heat balance in the facility and the error in the primary method of measurement of the RTU capacity. It should be emphasized in here that in the present work the refrigerant circuitry of the RTU was not completely instrumented and thus a true heat balance between air and refrigerant side was not possible. In addition, the RTU was modified specifically for the tests of the present study and for accommodating the two technologies (economizer and variable fan speed) of interest of the present work. Thus, its components, layout, and controls were a little bit different than those of similar units but commercially available. Because the configuration of the RTU was unique, true manufacturer data for the performance of this RTU were not available, not even at the rated standard testing conditions. An order of magnitude analysis of the heat balance is provided here because it can be still meaningful in order to document the confidence level in the measured heat transfer capacities and COPs of the RTU during the experimental campaign of the present work. The first approach was to compare two tests conducted in the present work with the heat transfer capacity reported in Corti and Marelli (2013) work. Indoor conditions were 80°F (26.7°C) and 67°F (19.4°C) for both cases. Outdoor conditions were slightly different between the previous and the present project as shown in table 9. Tests performed in Corti and Marelli (2013) work only used the first stage compressor, while tests performed in this project used first and second stage compressors. The measured heat transfer capacity reported in Corti and Marelli (2013) study was then multiplied by two, with the assumption that both compressors of the RTU would deliver approximately the same refrigerating capacity. This assumption was reasonable in the present work because the second stage of the RTU was an exact replica of the first stage and the coils of the two stages had interlaced circuitry. When the capacities measured in the present work were compared against the extrapolated capacities of two times the capacities of the first stage as reported in Corti and Marelli work, the difference in the heat transfer capacities ranged from -3.4% to -1.6%. This similarity indicated that the measured heat transfer capacities from the present work were at the very least,

close to the expected capacities of the RTU and in line with the capacities previously measured for this RTU.

Table 9: Comparison of measured capacity with Corti and Marelli (2013) data

Corti and Marelli (2013)			Present Project		% Difference
$T_{db,out}$ (°F)	Load (ton) 1 st Stage Compressor	Load (ton) 1 st Stage Compressor x 2	$T_{db,out}$ (°F)	Load (ton) 1 st and 2 nd Stage Compressors	
85	6.39	12.78	82	12.57	-1.6
97	5.81	11.62	95	11.23	-3.4

In the present work, the refrigerant flow rate of the first stage was directly measured by using a Coriolis type mass flow meter and the suction and discharge temperatures and pressures of the first stage compressor were also measured directly. Unfortunately, the refrigerant temperature at the outlet of the condenser coil was not measured in the present work and the heat transfer rate from the refrigerant side were only roughly estimated. Refrigerant pressure drop in the condenser was neglected and the condenser outlet temperature approach, that is, the temperature difference between air entering the condenser and refrigerant exiting the condenser, was varied from 2°F (-16.7°C), 5°F (-15°C), 10°F (-12.2°C) and 15°F (-9.4°C) in a parametric fashion. This sensitivity analysis provided an estimated inlet temperature to the expansion device of the RTU and thus an estimated refrigerant side heat transfer capacity of the evaporator coil that was compared with the measured air side heat transfer capacity of the RTU. At the very minimum, this sensitivity analysis highlighted the effect of the condenser outlet temperature approach limit on the heat transfer balance of the RTU. The result was used to verify that the primary method of measurement of the heat transfer capacity were reasonable and did not violate the laws of physics. The sensitivity analysis was performed for three steady state tests, for which only one compressor of the first stage was run at outdoor temperatures of 82 °F (27.8°C), 72 °F (22.2°C), 65 °F (18.3°C). Table 10 shows the measured values of temperatures and pressures in the first stage refrigerant circuitry and the corresponding measured air side heat transfer capacities (in the last column of the table).

Table 10: Test conditions for heat balance

$T_{db,out}$ (°F)	\dot{m}_{ref} (lb/h)	$T_{suction}$ (°F)	$P_{suction}$ (psi)	$T_{discharge}$ (°F)	$P_{discharge}$ (psi)	$\dot{Q}_{air-side}$ (BTU/h)
82	1183	62.2	153.6	163.3	357.6	87647
72	1139	62.0	148.3	156.1	316.8	95329
65	1121	63.1	148.4	148.9	293.4	102590

Table 11 summarizes the results of the sensitivity analysis and the estimated refrigerant-side heat transfer capacities were compared to the corresponding measured air side heat transfer capacity of the evaporator coil when the RTU run in cooling mode.

Table 11: Estimated heat balance results

$T_{approach}$ (°F)	$T_{db,out}$ (°F)	$\dot{Q}_{ref-side}$ (BTU/h)	$\left(\frac{\dot{Q}_{ref-side}-\dot{Q}_{air-side}}{\dot{Q}_{air-side}}\right) \times 100\%$
2	82	94928	8.3%
	72	96366	1.1%
	65	98271	-4.2%
5	82	93456	6.6%
	72	94997	-0.3%
	65	96952	-5.5%
10	82	90957	3.8%
	72	92679	-2.8%
	65	94721	-7.7%
15	82	88390	0.8%
	72	90310	-5.3%
	65	92449	-9.9%

The differences between the estimated refrigerant side heat transfer capacities and the measured air side heat transfer capacities were less than 10% regardless of the condenser temperature approach used as parameter in the sensitivity analysis. This result suggested that the measured air side heat transfer capacities in the present work were accurate enough to be representative of the RTU performance or at the very least that they provided the true capacity of the RTU within 10% maximum error in case of worst case scenario.

CHAPTER VII

VII. RESULTS AND DISCUSSION

Total of 84 tests were conducted in the present work during the feasibility study and the gradual development of the new load-based method of test for the RTU with economizer and variable speed fan technologies. In this section, 64 tests in cooling mode and 5 tests in heating mode are presented and the results discussed. The remaining 15 tests were conducted at the very beginning of the project and they were exploratory tests to document the feasibility and limitation of the test procedures and define the test conditions. In other words, the very first 15 tests provided valuable information for developing the experimental methodology, data reduction, and determining the test conditions of table 4 but they are not reported in this thesis because of the trial and error approach of these preliminary tests.

Table 12 summarizes the experimental results of this project for the various types of tests conducted in order to develop and validate a first load-based method of testing. The effects on the RTU overall figure of merit from the economizer and variable speed fan technologies were assessed during the tests as these technologies were individually integrated and run with the RTU in the laboratory.

The modulating capacity capability of digital scroll compressor technology installed in the RTU was also tested in addition to the economizer and variable speed fan technologies. The influence of such modulating capability on unit efficiency in terms of energy consumption and return temperature control was investigated

Digital scroll compressor technology tests were not in the original scope of the project but they provided interesting results and intriguing observations for expansion and further developments of the procedures required by the new standard of the load-based method of test in future research. Furthermore, the effects of off-design load conditions was studied, that is, the RTU was tested with intentionally reduced cooling load with respect to the PNNL loads at the same outdoor temperatures. These tests were conducted to understand the impact of the set load on the output results coming from the load-based method of testing. An additional series of tests was conducted with economizer running with fan at half speed at all times. This additional series of tests focused on isolating and quantifying the effect of fan speed only on the output figures of merit that resulted from the load-based method of testing. With the modulating capacity tests, the off-design conditions tests, and the additional series of tests with economizer and fan at half speed, the total number of tests increased from the original 38 tests indicated in table 4 to a total number of 69 tests as indicated in table12.

7.1 Summary of actual tested conditions used in the present study

The 64 cooling and 5 heating tests were divided in 13 subcategories or series, which are explained in the following section. This section is very similar to section 5.4. However, tests series here described include all 69 tests performed for developing the method of test, while section 5.4 includes only the narrowed down version of the tests that are being recommended in this project when the load-based method of test is applied.

A. 2 steady state standard cooling tests- determine unit capacity in cooling mode as per ASHRAE 116-2010

Conditions for these tests were based on ANSI/AHRI 340/360 and ASHRAE116-2010 standards. The unit was operated at full load, steady state cooling and no outside air. The return air dry bulb temperature was representative of the indoor room conditions. The indoor room dry bulb temperature was set to 80°F (26.7°C) and the indoor room wet bulb temperature is set to 67°F (19.4°C). The economizer was set to the closed position. The unit static pressure was set to 0.3 inH₂O.

The objective of these two tests was to determine unit actual capacity and COP according to current standards. The unit actual capacity measured from these tests was used to scale the loads in the series B to J (i.e. load-based tests in unit cooling mode). These two tests also served to provide baseline data to characterize the unit according to the current standards.

B. 18 cooling tests with min OA & Full fan, marine climate (Salem, OR, zone 4C)

Temperatures representative for this climate zone were based on TMY3 data for Salem, OR. The total cooling loads were calculated for a small office space based on PNNL prototype simulations for Salem, OR. The unit static pressure is set to 1.0 inH₂O (~249 Pa), which is higher than the ones set in the standard ANSI/AHRI 340/360. The reason for this deviation is that field studies such as Jacobs et al 2003 reported that average static pressure drop across typical rooftop units is higher

than 0.3 inh₂O. The latent load was calculated based on ASHRAE Handbook of Fundamentals 2009 resulting on a latent load per person of 295 Btu/h. For the calculation, the office space was considered occupied from 8am to 5pm by 31 people, which were performing moderately active office work. The sensible cooling load was calculated as the difference of the total cooling load and the latent cooling load. The load was set as calculated for 12 out of the 18 tests, while the remaining 6 had “off-design” reduced load conditions. This reduced load was approximately half of the load calculated as described in the previous paragraphs. The second to last column of Table 12 indicates whether the test was performed with “Regular” load (full load) or “Reduced” load (approximately half load). From test 3 until test 8 and 15 through 20, the load setting was “Regular”, while tests 9 to 14 had their load setting “Reduced”. Two methods were used to control the temperature in the indoor room:

- Method 1: This method consisted in cycling the compressor according to the thermostatic settings already explained and was used in 10 out of the 18 tests of series “B”.
- Method 2: This method used the digital scroll compressor, which allows full modulation of the cooling capacity to control the temperature in the indoor room. This method was used in the remaining 8 tests of series “B”. The last column of Table 12 indicates which one of the methods was used on a particular test.

C. 6 cooling tests with fan control, marine climate (4C)

Outside air temperatures and loads (“Regular” load) of the tests 22, 25 and 26 were the same as in tests 4, 15, and 16 respectively. Tests 21, 23 and 24 had the same outside air temperature settings as 22, 25 and 26 but their load setting was reduced. Tests in this series introduced fan speed control (see column labeled “Variable Speed Fan” on Table 12).

D. 9 cooling tests with economizer, marine climate (4C)

These tests introduced economizer operation (see column labeled “Economizer or Min OA” on Table 12) in addition to the fan speed control. Three methods were used for this series:

- Method 1: The compressor was cycled ON and OFF, and the economizer was opened or closed according to the thermostatic settings, however, the fan speed remained constant at its low value of 66%. The reason not to modify the fan speed was to introduce one variable change at a time while progressively developing the economizer control procedure explained in the thermostatic settings for cooling tests.
- Method 2: The compressor operated based on its fully modulating capacity and the economizer was opened or closed according to the thermostatic settings, while the fan speed remained constant at 66% for the same reasons as in method 1.
- Method 3: The compressor was cycled ON and OFF, the economizer was opened or closed and the supply air fan speed was adjusted according to the thermostatic settings. Method 3 introduced all the variables and settings as indicated in chapter V. Which method was used is indicated in the last column of Table 12.

Temperature and load setting for this series are the following:

- Outside air temperatures (72°F DB) of tests 27, 28 and 29 are the same as test 16.
- Outside air temperatures (65°F DB) of tests 30, 31 and 32 are the same as test 17.
- Outside air temperatures (57°F DB) of tests 33, 34 and 35 are the same as test 19.
- Load of test 29 is set to be the same as test 16 (“Regular” load).
- Load of tests 31, 32 and 33 are set to be the same as test 17 (“Regular” load).
- Load of test 35 is set to be the same as test 19 (“Regular” load).
- Tests 27, 28, 30 and 34 have “Reduced” load.

E. 8 cooling tests with fan control and economizer, moist climate (3A) outdoor dry bulb temperature and, loads from (4C) zone

The objective of this series was to measure the impact of the outside air relative humidity on the new method of testing. The loads (the “Regular” ones) are the same as in series “D” but the wet

bulb temperatures were selected for climate zone 3A (i.e. moist climate zone). The same three methods were used as in series “D” and the last column of Table 12 indicates which method was used for a particular test.

Temperature and load setting for this series are the following:

- Outside air dry bulb temperatures (72°F DB) of tests 36 and 37 are the same as test 16.
- Outside air dry bulb temperatures (65°F DB) of tests 38, 39, 40 and 41 are the same as test 17.
- Outside air dry bulb temperatures (57°F DB) of tests 42 and 43 are the same as test 19.
- Load of test 37 is set to be the same as test 16 (“Regular” load).
- Load of tests 39 and 41 are set to be the same as test 17 (“Regular” load).
- Load of test 43 is set to be the same as test 19 (“Regular” load).
- Tests 36, 38 and 42 have “Reduced” load while test 40 has a higher load setting than desired.

Result of test 40 is presented because it was key as an intermediate step towards the development of the procedure for determining sensible heat transfer from the fans circulating air in the chamber explained in chapter V.

F. 2 repeated selected partial load tests with econ and fan (65°F OA)

Tests 44 and 45 were repetitions of test 33. The purpose of these tests was to verify repeatability of the measured performance with the new method of tests for one test condition.

G. 3 repeated previously done tests without exhaust duct to explore short cycling effect

For the experimental campaign a duct was installed at the exhaust damper (see Figure 8) in order to direct the exhaust air stream away from the economizer inlet and prevent it to bounce against surfaces in the chamber (i.e. the chamber wall) and re-enter the unit. This air recirculation effect is referred to in this document as short cycling effect. The exhaust duct was removed in order to understand the influence of the short cycling effect in unit performance. Tests 46, 47 and 48 replicated conditions of tests 33, 41 and 29 without the exhaust duct installed in the unit.

H. 7 repeating tests: three from series B, two from series C and two from series D, marine climate (4C)

Tests in this section focused on determining repeatability of results for tests with three different levels of difficulty:

- Three Series B cooling tests with min OA & full speed fan, marine climate (Salem, OR, zone 4C): tests 49, 50 and 51 were repetitions of tests 15, 7 and 17 respectively and they showed the least difficulty when setting loads in the psychrometric chamber used for the development of the method as compared to other series.
- Two Series C cooling tests with fan control, marine climate (Salem, OR, Zone 4C): tests 52 and 53 were repetitions of tests 10 and 11, which showed moderate difficulty of load setting. The moderate difficulty of these tests is due to the fact that different heater settings needed to be determined for the different fan speeds according to the procedure for fan calibration described in chapter V.
- Two Series D cooling tests with economizer, marine climate (Salem, OR, Zone 4C): tests 54 and 55 were repetitions of tests 26 and 25, which showed the highest difficulty of load setting. When the economizer opened, the fan speed was increased to a 100% to take advantage of the cold outside air, while the fan speed went back to 66% of its maximum value when the economizer closed due to either low indoor temperature or high outdoor temperature as explained in thermostatic settings in chapter V. Having two different speeds in a same test implied that the indoor room electric heaters power had to be adjusted in synchronicity with the fan speed change and economizer opening/closing actions to keep a constant load in the indoor room. The above statement is true for any series of tests involving economizer operation.

I. 2 cooling tests with fan control, marine climate (4C), with load variations (82°F OA)

The objective of tests 56 and 57 in this section was to determine the impact of fluctuations of the set load in the average load calculated and the performance figure of merit.

- One series C cooling test with fan control, marine climate (Salem, OR, Zone 4C): Test 56 was a repetition of test 10 but the load oscillated from -15% to +15% of the nominal heater setting every 20 minutes.
- One series C cooling test with fan control, marine climate (Salem, OR, Zone 4C): Test 57 was a repetition of test 10 but the load oscillated from -15% to +15% of the nominal heater setting every 10 minutes.

J. Uncertainty Estimation Tests, marine climate (4C), economizer and fan (65°F OA)

Tests 58, 59, 60, 61 and 62 were repetitions of test 33. The purpose of these tests was to verify repeatability of the load setting and associated measured performance with the new method of tests for one test condition. This helped estimating an experimental uncertainty, not only due to instrumentation but also due to the equipment arrangement and the human operator.

K. 2 Cooling steady state tests - determine unit capacity in heating mode as per ASHRAE 116-2010 with 1.0 inH₂O external resistance (unit static pressure)

Conditions for these tests were based on ANSI/AHRI 340/360 and ASHRAE116-2010 standards. The unit was operated at full load, steady state cooling and no outside air. The return air dry bulb temperature was representative of the indoor room conditions. The indoor room dry bulb temperature was set to 80°F and the indoor room wet bulb temperature was set to 67°F. The economizer was set to the closed position. The unit static pressure was set to 1.1 inH₂O as in the load-based tests instead of 0.3 inH₂O as series A. These tests measured the effect of static pressure increase only, as a deviation from standard testing.

L. 2 Heating steady state standard tests – determine unit capacity in heating mode as per ASHRAE 116-2010

Conditions for tests 65 and 66 were based on steady state heating and no outside air tests as described by ASHRAE 116-2010 and AHRI 340/360. The objective of these two tests was to determine unit actual capacity and COP according to current standards.

M. 3 heating tests with constant load

Temperatures representative for this climate zone were based on the climate zone data TMY3 for Salem, OR. The total heating loads were selected for a small office space, based on PNNL prototype simulations Salem, OR. The unit static pressure was set to 1.0 inH₂O. (~249 Pa).

Table 12: Summary of experimental results of the present work

Test No.	Test Type	Indoor		Total Load, (Btu/h)	Sensible Load, (Btu/h)	Total Latent Load, (Btu/h)	COP	COP _{SENS}	Outdoor		Static Pressure (inH2O)	Objective	Economizer or Min OA	Variable Speed Fan	Duration (minutes)	Location	Load Setting	Method
		DB, (°F)	WB, (°F)						DB, (°F)	WB, (°F)								
A: 2 steady state standard cooling tests- determine unit capacity in cooling mode as per ASHRAE 116-2010																		
1	Cooling	80.0	67.0	134760	97255	37505	2.4	1.7	95.0	----	0.47	SS Full Load (Baseline)	No OA	Full	90	----	----	1
2	Cooling	80.0	67.1	150877	104266	46611	2.9	2.0	82.0	----	0.45	SS Full Load (Baseline)	No OA	Full	90	----	----	1
B: 6 cooling tests with min OA & Full fan, marine climate (Salem, zone 4C)																		
3	Cooling	81.6	66.7	116539	96716	19824	1.7	1.4	105.0	71.1	1.05	Cooling Full Load	Min OA	Full Speed	90	Salem, OR (zone 4C)	Regular	1
4	Cooling	76.4	64.5	100536	79847	20689	1.9	1.5	95.0	67.4	1.05	Cooling Full Load	Min OA	Full Speed	90	Salem, OR (zone 4C)	Regular	1
5	Cooling	77.3	64.3	99233	80095	19138	2.0	1.6	94.9	67.6	1.15	Cooling Full Load	Min OA	Full Speed	90	Salem, OR (zone 4C)	Regular	1
6	Cooling	77.4	64.8	99914	81033	18882	2.0	1.6	95.0	67.8	1.15	Cooling Full Load	Min OA	Full Speed	90	Salem, OR (zone 4C)	Regular	2
7	Cooling	77.0	65.1	90422	70264	20157	2.4	1.9	81.9	63.5	1.15	Cooling Partial Load	Min OA	Full Speed	90	Salem, OR (zone 4C)	Regular	1
8	Cooling	77.3	65.8	90530	70235	20295	2.4	1.9	82.0	63.2	1.15	Cooling Partial Load	Min OA	Full Speed	90	Salem, OR (zone 4C)	Regular	2
9	Cooling	76.3	69.8	48036	34755	13281	2.1	1.5	82.0	66.2	1.18	Cooling Partial Load	Min OA	Full Speed	90	Salem, OR (zone 4C)	Reduced	1
10	Cooling	76.3	69.6	49219	34619	14600	1.9	1.3	82.0	66.2	1.18	Cooling Partial Load	Min OA	Full Speed	90	Salem, OR (zone 4C)	Reduced	2
11	Cooling	76.1	71.2	37275	24095	13179	2.2	1.4	72.0	60.1	1.16	Cooling Partial Load	Min OA	Full Speed	90	Salem, OR (zone 4C)	Reduced	1
12	Cooling	76.4	71.2	37335	23875	13460	1.7	1.1	72.1	60.7	1.19	Cooling Partial Load	Min OA	Full Speed	90	Salem, OR (zone 4C)	Reduced	2
13	Cooling	76.1	69.5	42477	29654	12823	2.2	1.5	72.0	59.4	1.12	Cooling Partial Load	Min OA	Full Speed	90	Salem, OR (zone 4C)	Reduced	1
14	Cooling	76.4	69.9	44405	29154	15251	1.9	1.2	72.0	59.6	1.14	Cooling Partial Load	Min OA	Full Speed	90	Salem, OR (zone 4C)	Reduced	2
15	Cooling	76.4	67.5	67435	50763	16673	2.5	1.9	72.1	59.8	1.16	Cooling Partial Load	Min OA	Full Speed	90	Salem, OR (zone 4C)	Regular	1
16	Cooling	76.4	67.9	66146	49486	16660	2.3	1.8	72.0	59.8	1.16	Cooling Partial Load	Min OA	Full Speed	90	Salem, OR (zone 4C)	Regular	2
17	Cooling	76.0	69.9	42125	28778	13346	2.6	1.8	65.0	56.0	1.06	Cooling Partial Load	Min OA	Full Speed	90	Salem, OR (zone 4C)	Regular	1
18	Cooling	76.4	69.2	43007	28507	14500	2.0	1.3	64.6	56.1	1.07	Cooling Partial Load	Min OA	Full Speed	90	Salem, OR (zone 4C)	Regular	2
19	Cooling	75.7	68.6	27143	14093	13050	2.2	1.1	57.1	51.0	1.15	Cooling Partial Load	Min OA	Full Speed	90	Salem, OR (zone 4C)	Regular	1
20	Cooling	76.3	69.2	23624	10882	12742	1.9	0.9	57.0	50.9	1.15	Cooling Partial Load	Min OA	Full Speed	90	Salem, OR (zone 4C)	Regular	2
C: 3 cooling tests with fan control, marine climate (4C)																		
21	Cooling	76.6	65.8	62658	49781	12878	2.3	1.9	95.0	71.5	0.35	Cooling Full Load	Min OA	Speed Control	120	Salem, OR (zone 4C)	Reduced	1
22	Cooling	83.2	61.9	108910	94628	14283	2.1	1.8	95.3	66.7	0.76	Cooling Full Load	Min OA	Speed Control	120	Salem, OR (zone 4C)	Regular	1
23	Cooling	76.2	68.7	45160	33439	11721	2.9	2.1	82.0	64.0	0.35	Cooling Partial Load	Min OA	Speed Control	120	Salem, OR (zone 4C)	Reduced	1
24	Cooling	76.1	70.4	37782	24950	12832	3.3	2.2	71.9	59.7	0.34	Cooling Partial Load	Min OA	Speed Control	120	Salem, OR (zone 4C)	Reduced	1
25	Cooling	77.2	62.1	89161	74304	14857	2.5	2.1	81.3	62.4	0.45	Cooling Partial Load	Min OA	Speed Control	120	Salem, OR (zone 4C)	Regular	1
26	Cooling	76.5	64.7	65270	52995	12275	3.3	2.7	71.9	59.4	0.44	Cooling Partial Load	Min OA	Speed Control	120	Salem, OR (zone 4C)	Regular	1
D: 3 cooling tests with economizer, marine climate (4C)																		
27	Cooling	76.0	65.2	37911	24105	13806	4.3	2.7	72.0	60.8	0.39	Econom + fan control	Economizer	Speed Control	120	Salem, OR (zone 4C)	Reduced	1
28	Cooling	76.4	65.0	37850	23381	14469	2.8	1.7	72.0	60.6	0.41	Econom + fan control	Economizer	Speed Control	120	Salem, OR (zone 4C)	Reduced	2
29	Cooling	76.3	64.5	66915	47760	19155	3.0	2.1	72.0	60.6	0.41	Econom + fan control	Economizer	Speed Control	120	Salem, OR (zone 4C)	Regular	3
30	Cooling	75.4	64.4	29032	14852	14180	11.3	5.8	65.2	57.0	0.45	Econom + fan control	Economizer	Speed Control	120	Salem, OR (zone 4C)	Reduced	1
31	Cooling	75.8	64.1	39097	25273	13824	7.8	5.0	64.5	56.3	0.39	Econom + fan control	Economizer	Speed Control	120	Salem, OR (zone 4C)	Regular	1
32	Cooling	76.4	64.2	37487	24061	13426	5.5	3.6	65.2	56.8	0.39	Econom + fan control	Economizer	Speed Control	120	Salem, OR (zone 4C)	Regular	2
33	Cooling	76.0	63.0	40940	27886	13054	3.8	2.6	65.0	56.7	0.41	Econom + fan control	Economizer	Speed Control	120	Salem, OR (zone 4C)	Regular	3
34	Cooling	73.6	69.7	10301	2923	7378	3.9	1.1	57.0	51.9	0.74	Econom + fan control	Economizer	Speed Control	120	Salem, OR (zone 4C)	Reduced	1
35	Cooling	75.2	63.8	30957	15023	15934	5.9	2.9	57.0	52.4	0.55	Econom + fan control	Economizer	Speed Control	120	Salem, OR (zone 4C)	Regular	3

Table 12: Summary of experimental results of the present work (continued)

Test No.	Test Type	Indoor		Total Load, (Btu/h)	Sensible Load, (Btu/h)	Total Latent Load, (Btu/h)	COP	COP _{SENS}	Outdoor		Static Pressure (inH2O)	Objective	Economizer or Min OA	Variable Speed Fan	Duration (minutes)	Location	Load Setting	Method
		DB, (°F)	WB, (°F)						DB, (°F)	WB, (°F)								
<i>F: 2 cooling tests with fan control and economizer, moist climate (3A) outdoor dry bulb temperature and, loads from (4C) zone</i>																		
36	Cooling	76.1	66.7	38514	24758	13756	4.0	2.6	71.6	62.5	0.39	Impact of OA humidity	Economizer	Speed Control	120	Memphis, TN (zone 3A)	Reduced	1
37	Cooling	76.5	64.8	69411	54832	14579	3.2	2.6	72.0	61.2	0.45	Impact of OA humidity	Economizer	Speed Control	120	Memphis, TN (zone 3A)	Regular	3
38	Cooling	75.4	64.0	29811	15257	14554	11.6	5.9	65.0	56.6	0.44	Impact of OA humidity	Economizer	Speed Control	120	Memphis, TN (zone 3A)	Reduced	1
39	Cooling	75.9	63.7	36415	22853	13562	8.7	5.5	65.0	56.2	0.39	Impact of OA humidity	Economizer	Speed Control	120	Memphis, TN (zone 3A)	Regular	1
40	Cooling	76.0	62.0	58550	46642	11907	3.7	2.9	65.0	55.5	0.42	Impact of OA humidity	Economizer	Speed Control	120	Memphis, TN (zone 3A)	High	3
41	Cooling	75.9	62.5	46221	25621	20600	4.9	2.7	65.2	55.7	0.42	Impact of OA humidity	Economizer	Speed Control	120	Memphis, TN (zone 3A)	Regular	3
42	Cooling	73.0	69.4	10717	3177	7540	4.1	1.2	57.0	50.7	0.75	Impact of OA humidity	Economizer	Speed Control	120	Memphis, TN (zone 3A)	Reduced	1
43	Cooling	75.3	62.1	40636	22191	18445	6.4	3.5	57.0	51.4	0.50	Impact of OA humidity	Economizer	Speed Control	120	Memphis, TN (zone 3A)	Regular	3
<i>F: 2 Repeat selected partial load tests with econ and fan (65 °F OA)</i>																		
44	Repeat Test 33	75.9	63.6	46709	27457	19252	4.5	2.6	64.4	56.7	0.41	Econom. + fan control	Economizer	Speed Control	120	Salem, OR (zone 4C)	Regular	3
45	Repeat Test 33	75.9	63.4	47900	27744	20156	4.4	2.6	64.7	56.6	0.41	Econom. + fan control	Economizer	Speed Control	120	Salem, OR (zone 4C)	Regular	3
<i>G: 3 tests repeat previously done tests without exhaust duct to explore short cycling effect</i>																		
46	Repeat Test 33	75.9	63.5	49308	28745	20563	5.0	2.9	64.8	56.9	0.71	Econom. + fan control	Economizer	Speed Control	120	Salem, OR (zone 4C)	Regular	3
47	Repeat Test 41	75.9	63.2	50503	30445	20058	4.8	2.9	65.0	56.5	0.72	Impact of OA humidity	Economizer	Speed Control	120	Memphis, TN (zone 3A)	Regular	3
48	Repeat Test 29	76.3	65.1	68742	50115	18627	3.1	2.2	72.0	61.5	0.72	Econom. + fan control	Economizer	Speed Control	120	Salem, OR (zone 4C)	Regular	3
<i>H: 7 repeating tests: three from series B (easy to set), two from series C (moderate to set) and two from series D (difficult to set), marine climate (4C)</i>																		
49	Repeat Test 15	76.4	67.9	65982	49197	16785	2.5	1.8	72.1	60.3	1.14	Cooling Partial Load	Min OA	Full Speed	90	Salem, OR (zone 4C)	Regular	1
50	Repeat Test 7	77.0	66.0	91409	70005	21405	2.7	2.1	82.1	65.2	1.15	Cooling Partial Load	Min OA	Full Speed	90	Salem, OR (zone 4C)	Regular	1
51	Repeat Test 17	76.1	70.3	43591	28846	14744	2.4	1.6	64.7	56.2	1.15	Cooling Partial Load	Min OA	Full Speed	90	Salem, OR (zone 4C)	Regular	1
52	Repeat Test 29	76.3	64.2	66894	47993	18901	2.9	2.1	72.0	60.4	0.42	Econom. + fan control	Economizer	Speed Control	120	Salem, OR (zone 4C)	Regular	3
53	Repeat Test 33	76.0	63.1	44635	24791	19844	4.7	2.6	65.0	56.5	0.41	Econom. + fan control	Economizer	Speed Control	120	Salem, OR (zone 4C)	Regular	3
54	Repeat Test 26	76.5	64.7	67288	53679	13609	3.4	2.7	71.9	59.0	0.44	Cooling Partial Load	Min OA	Speed Control	120	Salem, OR (zone 4C)	Regular	1
55	Repeat Test 25	77.2	62.1	90316	75157	15159	2.8	2.3	81.4	62.7	0.45	Cooling Partial Load	Min OA	Speed Control	120	Salem, OR (zone 4C)	Regular	1
<i>I: 2 cooling tests with fan control, marine climate (4C), with load variations (82 °F OA)</i>																		
56	Vary Test 25	77.1	62.1	87193	73506	13687	2.6	2.2	80.4	61.6	0.45	+/- 15% Load 20min	Min OA	Speed Control	120	Salem, OR (zone 4C)	Regular	1
57	Vary Test 25	77.1	61.9	88830	74340	14489	2.8	2.3	82.0	62.2	0.45	+/- 15% Load 10min	Min OA	Speed Control	120	Salem, OR (zone 4C)	Regular	1
<i>J: Uncertainty Estimation Tests, marine climate (4C), econ and fan (65 °F OA)</i>																		
58	Repeat Test 33	75.5	62.3	44703	25904	18799	4.7	2.7	64.4	55.5	0.42	Econom. + fan control	Economizer	Speed Control	120	Salem, OR (zone 4C)	Regular	3
59	Repeat Test 33	75.5	62.1	44978	25444	19534	4.8	2.7	64.4	55.4	0.42	Econom. + fan control	Economizer	Speed Control	121	Salem, OR (zone 4C)	Regular	3
60	Repeat Test 33	75.6	62.1	44109	25269	18840	4.7	2.7	64.5	55.4	0.42	Econom. + fan control	Economizer	Speed Control	122	Salem, OR (zone 4C)	Regular	3
61	Repeat Test 33	75.6	61.9	45275	25638	19637	4.8	2.7	64.4	55.2	0.43	Econom. + fan control	Economizer	Speed Control	123	Salem, OR (zone 4C)	Regular	3
62	Repeat Test 33	75.6	61.9	45434	25393	20042	4.8	2.7	64.4	55.2	0.42	Econom. + fan control	Economizer	Speed Control	124	Salem, OR (zone 4C)	Regular	3
<i>K: 2 tests cooling steady state - determine unit capacity in heating mode as per ASHRAE 116-2010 with 1.0 inH2O external resistance (unit static pressure)</i>																		
63	Cooling	80.0	67.0	117106	87824	29282	2.0	1.5	95.0	---	1.12	SS Full Load (Baseline)	No OA	Full	90	---	---	---
64	Cooling	80.0	67.1	126320	92207	34113	2.4	1.7	82.0	---	1.14	SS Full Load (Baseline)	No OA	Full	90	---	---	---
<i>L: 2 Heating steady state standard tests – determine unit capacity in heating mode as per ASHRAE 116-2010</i>																		
65	Heating	70.0	54.4	56526	59999	-3473	2.0	2.1	47.0	43.5	0.40	Standard (baseline)	No OA	Full	90	---	---	---
66	Heating	70.0	59.1	78057	76869	1188	2.6	2.6	62.0	55.7	0.37	Standard (baseline)	No OA	Full	90	---	---	---
<i>M: 3 heating tests with constant load</i>																		
67	Heating	76.8	55.2	47595	32904	14691	1.7	1.2	37.0	34.6	1.14	Heating Load	Min OA	Full	120	Salem, OR (zone 4C)	Regular	1
68	Heating	77.0	58.0	60589	19154	41435	3.2	1.0	47.0	44.6	1.13	Heating Load	Min OA	Full	120	Salem, OR (zone 4C)	Regular	1
69	Heating	77.1	62.7	-18719	2502	-21221	-2.0	0.3	56.9	53.5	1.14	Heating Load	Min OA	Full	120	Salem, OR (zone 4C)	Regular	1

7.2 Discussion of Results

7.2.1 Cooling load

Figures 26 and 27 in this section provide an insight in the general cooling load trends observed throughout the totality of cooling tests performed.

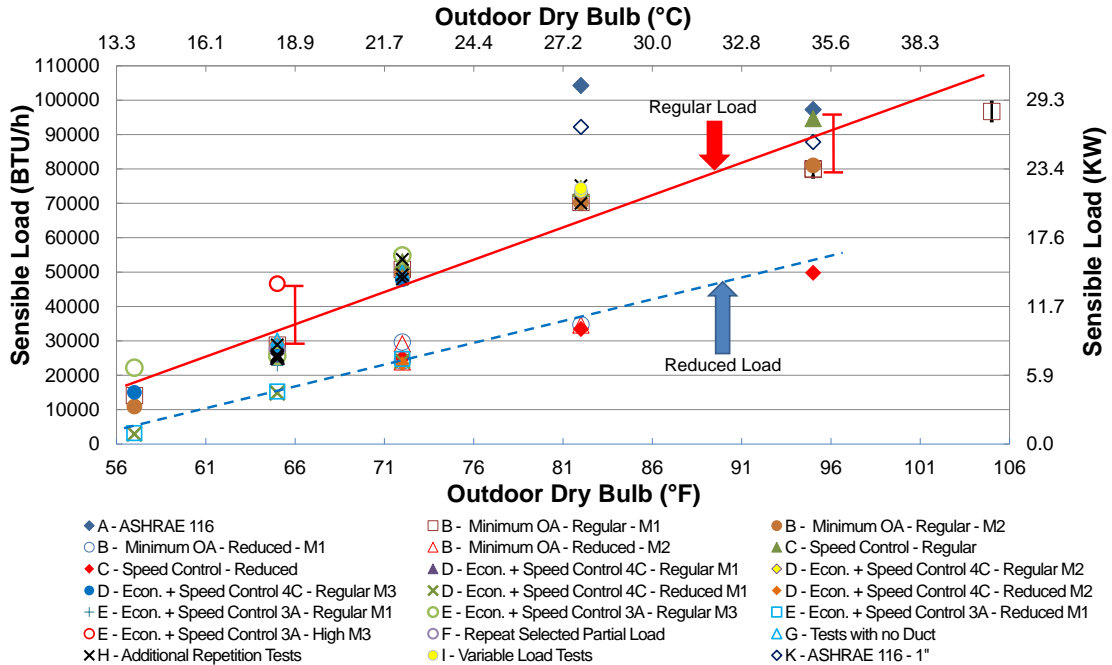


Figure 26: Sensible Load vs. Outdoor Dry Bulb Temperature in Cooling Mode

Figure 26 shows the sensible load as calculated by equation (28) with outdoor air temperatures spanning between 57°F and 105°F (13.9°C to 40.6°C). Sensible cooling loads varied from 3177 BTU/h to 96715 BTU/h (0.93KW to 28.35KW) for load-based tests. The maximum sensible load obtained was 104266 BTU/h (30.56KW) corresponding to series A of the ASHRAE 116 baseline test at 82°F (27.8°C).

Series A stands out in general for having the higher sensible loads as seen in Figure 26. It was observed in this series that the sensible load measured at the 82°F (27.8°C) outside dry bulb test was higher than 95°F (35°C) one by approximately 7000 BTU/h (2.05 KW). Since both tests had the same constant supply airflow rate, a lower supply temperature of 59.5°F (15.3°C) for the 82°F

(27.8°C) test vs 60.9°F (16.1°C) for the 95°F (35°C) test was the reason for the sensible load difference. Series K, which were the ASHRAE 116 tests but with the introduction of a different static pressure drop across the unit, show how the measured sensible capacity of the unit declines as it deviates from current standard conditions. Similarly to series A, the measured load in the series K 82°F (27.8°C) test is higher than the of the 95°F (35°C) one, for the exact same reason.

Now, moving on to the load-based tests, two main groups were observed in the figure: the ones with regular load, which follow the red solid trend-line, and the ones with reduced load following the blue dashed trend-line. Sensible loads increased as the outdoor air temperatures increased. This increasing trend is a result of the PNNL simulations applied and reflects load conditions that are closer to real building load profiles.

Test 40 of the economizer with fan speed control series E (represented by a hollow red circle mark) deviates from the regular load line. The sensible load came out to be almost 1.8 times higher than the average sensible load of the remaining 65°F (18.3°C) tests. Nonetheless, its result is presented here since it provided valuable information on how to adjust the indoor room heaters for tests where fan speed is not constant and from the iterative process to set the load even after the calibration procedure explained in 5.5.1.2. A similar result is observed in the 95°F (35°C) speed control series C test, but in this case, the sensible load is increased by a factor of 1.25 only.

All the points at the same temperature following each one of the trend-lines should collapse on top of each other. This is because one of the intentions of this method of testing is to see how the use of different technologies handle the same temperature and load conditions. In general, the measured sensible loads were within ± 1.5 KW (± 5118 BTU/h) of each other for a particular temperature and load condition. The reason for this tolerance is that the sensible load provided by the electric heaters increased discretely in factors of 2 KW (6824 BTU/h). That is, on top of the fan power, the sensible load in the indoor room could be increased by 2, 4, 6 KW, etc. by using the heaters. Tests outside the ± 1.5 KW (± 5118 BTU/h) tolerance were considered outliers and are indicated as such in the results.

On the other hand, tests with 57 °F outside dry bulb in general were subject to a greater difficulty regarding sensible load setting. Loads associated with this temperature were lower than the ones provided by the fans in the indoor room and the cooling coil balancing method had to be applied. This method, used to counteract the sensible heat set in the room by the fans required more iterations even after the procedure to determine sensible cooling removed from the air by the coils was applied.

Despite the difficulties for setting the desired load under different operational conditions, the ability to repeat a particular test with the exact same load, temperature and technology used was much better than the allowed tolerance. Series H repetition tests addressed this issue; also an experimental uncertainty analysis indicates the sensible load measurements have an accuracy of $\pm 2.9\%$ of the measured sensible load. This accuracy was smaller than the size of the symbols used in Figure 26.

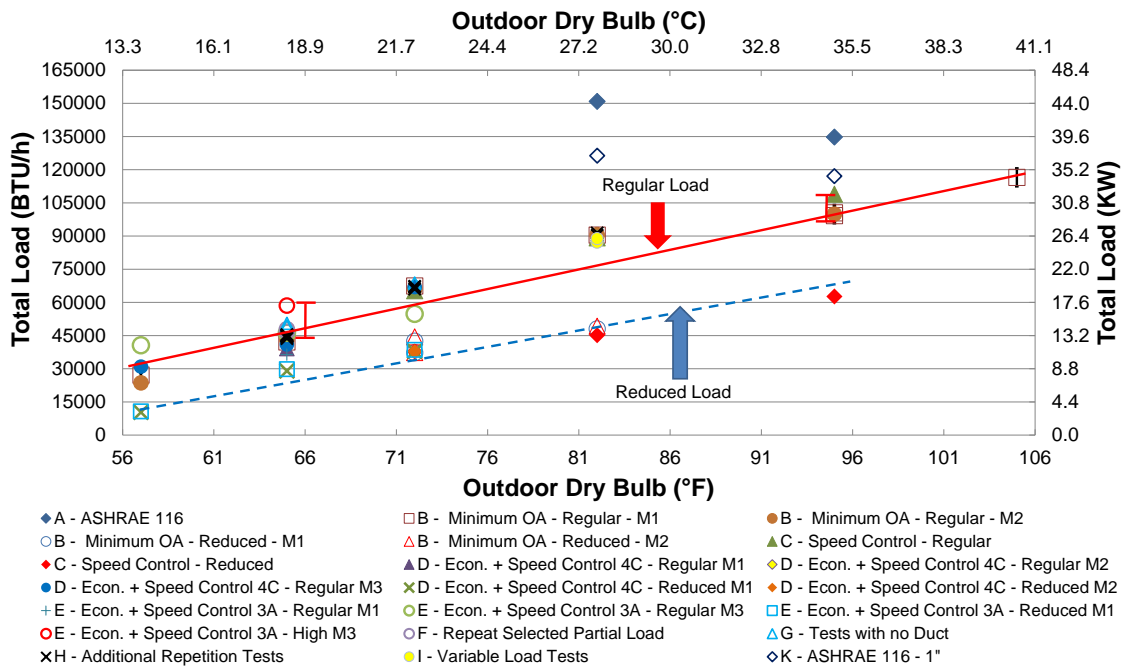


Figure 27: Total Load vs. Outdoor Dry Bulb Temperature in Cooling Mode

Figure 27 shows the total cooling load as calculated by equation (29) with outdoor air temperatures spanning between 57°F and 105°F (13.9°C to 40.6°C). Total cooling loads varied from 10717

BTU/h to 116539 BTU/h (3.14KW to 34.16KW) for load-based tests. The maximum cooling load obtained was 150877 BTU/h (44.22KW) corresponding to series A of the ASHRAE 116 baseline test at 82°F (27.8°C).

Overall, total cooling load measurements followed an analogous trend to the ones described for the sensible load. The higher total cooling loads were measured in Series A. The 82°F (27.8°C) outside dry bulb test load value was higher than the one at 95°F (35°C) one by approximately 16000 BTU/h (4.69 KW). Since both tests had the same constant supply airflow rate, a lower supply air enthalpy of the 82°F (27.8°C) test compared to the 95°F (35°C) one, produced this load difference. Series K shows how the total cooling capacity of the unit declined as it deviated from current standard conditions. Similarly to series A, the measured load in the series K 82°F (27.8°C) test was higher than the of the 95°F (35°C) one, for the exact same reason.

Two main groups are observed in the figure: the ones with regular load, which follow the solid red trend-line and the ones with reduced load following the blue dashed trend-line. Test 40 of the economizer with speed control series E was an outlier in the regular load line. The reason being the already mentioned sensible load difference in Figure 26 discussion. The 95°F (35°C) speed control series C test was also an outlier as explained in the sensible load discussion; however, the total load is increased 11% while the sensible load is increased by 25% with respect to the other 95°F (35°C) tests. The reason for this is that the latent load of the speed control series C test is 35% lower than the latent load of the corresponding full speed 95°F (35°C) test.

This observation is applicable for any tests that use fan speed control, since the airflow fluctuates between low and high fan speed values. A different airflow rate than at full fan speed tests changed the amount of humidity being introduced to the indoor room. Additionally, a different amount of air circulating back to the evaporator meant a different amount of dehumidification. The combination of these two effects, modified the humidity balance between indoor and outdoor rooms, therefore the latent load did not necessarily have to be the same as in full fan speed tests.

More specifically, tests in the speed control series C, with low fan speed and damper at minimum outside air position, resulted in lower latent loads than the corresponding full speed tests under the same conditions. On the other hand, economizer with speed control tests (series D and E) have low fan speed with damper in minimum outside air when the indoor return temperature was below thermostatic settings or when the outdoor air was above economizer high limit, just like series C tests. However, when the indoor temperature was above the minimum thermostatic limit of 75°F (23.9°C) and the outdoor air was below the high limit the fan operated at full speed with economizer damper at fully open position. This introduced a greater amount of outdoor air into the indoor room, therefore increasing the latent load.

Different latent load values for different types of tests under same outdoor temperatures and sensible load conditions translated into different total cooling loads. Hence, points in Figure 27 did not collapse on top of each other when comparing the different technologies being tested. In other words, a speed control test or an economizer with speed control test did not necessarily have the same total cooling loads as the corresponding full fan speed test.

To sum up, for every test, the sensible load was set as close as possible to the desired condition, regardless of the technology used. Whereas the latent load, was a combination of the constant space load set by the steam wand and the humidity that entered the room through the economizer damper and is therefore inherent to the technology being tested. Later on, the effects of that additional latent load introduced by the additional outside airflow in unit performance will be discussed in more detail.

Furthermore, the accuracy of total load measurements was estimated to be $\pm 3.5\%$ of the measured load. This accuracy is approximately the same size of the symbols used in Figure 27.

7.2.2 Cooling COP

Figures 28 and 29 in this section provide an insight of the general COP efficiency trends observed throughout the totality of cooling tests performed.

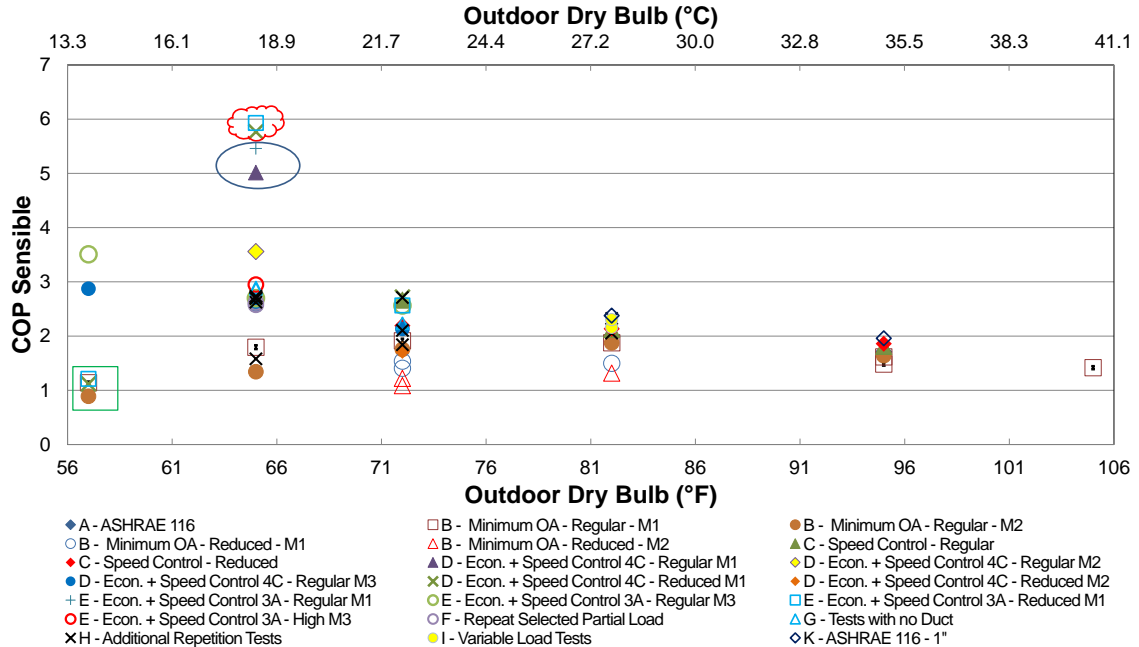


Figure 28: COP Sensible vs Outdoor Dry Bulb Temperature in Cooling Mode

Figure 28 shows how the sensible COP efficiency varied as a function of outdoor air temperatures and technologies used. The estimated uncertainty for the sensible COP was about 2%, and the error bars used to represent it are smaller than the symbols used in Figure 28.

Starting from 57°F and ending at 105°F (13.9°C to 40.6°C) the main trend observed is decreasing COP as temperature increases. As outdoor air temperature increased so did the sensible load. Therefore, in general, the lower the sensible load, the lower the power the unit needed to invest in balancing the load to control the indoor temperature to a desired value. However, three groups of outliers are identified in the figure.

Data points inside the red cloud had a reduced load setting and the supply air fan operated at constant low speed, even when the economizer damper was open. The combination of these two off-design conditions resulted in increased COPs.

Like data points in the red cloud, data points inside the blue ellipse kept a low supply air fan speed at all times even when the economizer was being used. However, these tests had the appropriate or “regular” load setting. Interestingly enough, an off-design operation of the unit turned out to be more efficient than when the proper operation was taking place. This indicates that this particular load could be balanced with a lower air supply to the indoor room.

Furthermore, data points in the green square at the lower left side of the figure did not follow the trend of increasing COP when the load decreased. Inside this square, there are two types of tests: economizer with speed control tests and full speed tests. The economizer with speed control tests had their load reduced; which is an off-design condition, while for the full speed tests the desired load was set. However, the reason for their reduced COP efficiency is the same; load values are so low that the unit approaches its minimum power consumption. Power consumption reached its lower limit when only the supply air fan was running, thus, no further COP improvement occurred at very low loads. Instead, the efficiency decreased because the ratio of power consumed to cooling load was high in contrast with the other temperatures (above 65°F) and loads tested.

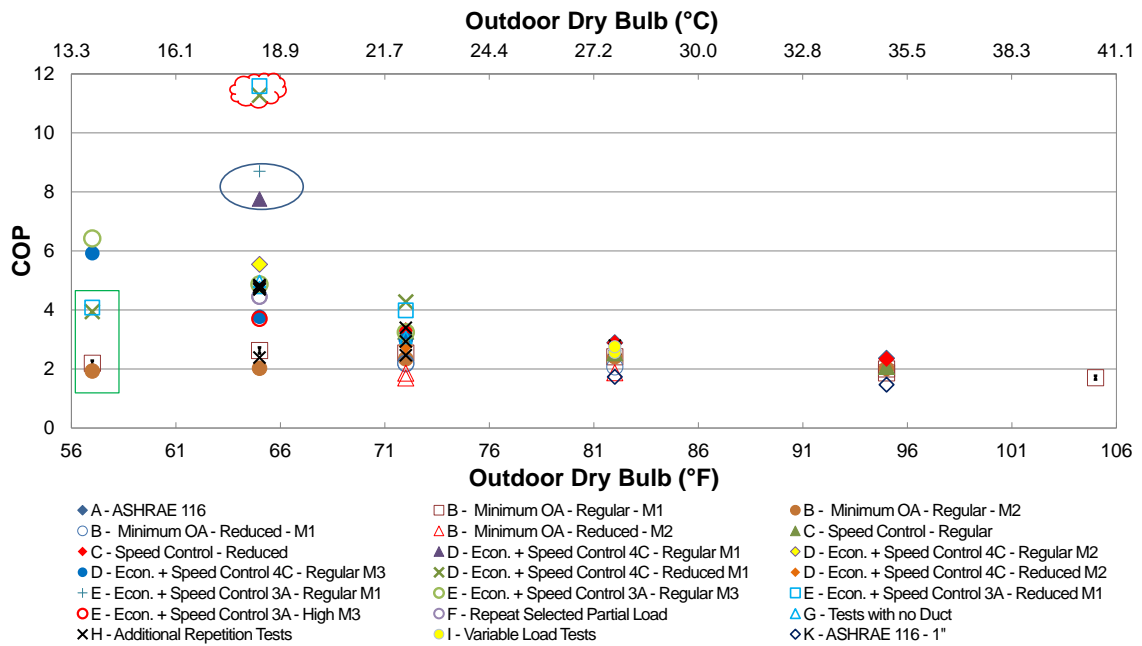


Figure 29: COP vs. Outdoor Dry Bulb Temperature in Cooling Mode

Figure 29 shows how the COP efficiency varied as a function of outdoor air temperatures and technologies used. The estimated uncertainty for the total COP was 4% and is represented by error bars smaller in size than the symbols used in Figure 29.

Starting from 57°F and ending at 105°F (13.9°C to 40.6°C) the main trend observed was decreasing COP as temperature increased. As outdoor air temperature increased so did the total cooling load. Therefore, like in figure 28, the lower loads resulted in lower unit power consumption. The same three groups of outliers as in figure 28 are observed in figure 29.

Data points inside the red cloud had a reduced load setting and the supply air fan operated at constant low speed, even when the economizer damper was open. The combination of these two off-design conditions resulted in increased COPs.

Data points inside the blue ellipse kept a low supply air fan speed at all times even when the economizer was being used. However, these tests had the appropriate or “regular” load setting. Since the total load of the data points inside the ellipse was higher than the ones in the cloud, power consumption was also higher. This produced lower efficiencies than the ones calculated for reduced load data points in the cloud. As noted when analyzing the COP sensible figure, it is interesting to see that an off-design operation resulted in an increased efficiency in comparison to the economizer tests where the fan speed was adjusted according to damper opening. This again, indicates that a lower supply airflow was enough to balance the indoor room load more efficiently.

Moreover, data points in the green square at the lower left side of the figure had a similar behavior than in the sensible COP figure. Nonetheless, differences between the economizer (whit low fan speed and reduced load) tests and the full speed (regular load) tests become more apparent. In this case, the additional power was a dominant effect that pulled the COP efficiency further down for the full fan speed tests.

Analyzing the results of figures 28 and 29 shows that somewhere in between the loads of 57°F (13.9°C) and 65°F (18.3°C) the COP reached a local maximum peak and then COP started to decline. Now this leads to two observations: the importance of proper unit sizing and the advantages

of fan speed controls and economizer technologies when the appropriate load and outside air temperature conditions are present. This is evident when one looks at series D and E 57°F (13.9°C) tests results. These tests, which had appropriate speed control operation and regular load settings, result in significantly better efficiencies than the points inside the green square.

7.2.3 Uncertainty analysis

Although the values of uncertainty have already been reported, this section illustrates how the reported uncertainty was estimated. Taylor series expansions were applied to understand the effect of the accuracy of measured variables in the uncertainty of the calculated sensible load, total load, sensible COP and total COP. These calculations were made using the uncertainty propagation theory already implemented in the software tool Engineering Equation Solver (EES) uncertainty propagation function. Table 13 summarizes these effects.

Table 13: Sensitivity analysis towards uncertainty propagation

Measured Variable	Sensible	Total	COP	COP
	Load	Load	Sensible	Total
Static pressure across flow nozzles	5.8%	1.3%	5.7%	1.3%
Indoor dry-bulb	46.6%	0.0%	45.7%	0.0%
Indoor wet-bulb	0.5%	54.6%	0.5%	54.4%
Supply air dry-bulb	46.8%	0.0%	45.8%	0.0%
Supply air wet-bulb	0.3%	44.1%	0.3%	43.9%
Unit Power	0.0%	0.0%	2.0%	0.5%

It is evident from Table 13 that the major contributions to the experimental uncertainty were the measured supply and return wet bulb temperatures, which combined accounted for more than 98% of the error propagation in the total load and COP calculations. The Taylor expansion method provided a good insight on where the uncertainties mostly came from but due to the transient nature of the tests performed, an alternative approach for further estimating the uncertainty was used. Based on statistical theory of Gaussian distribution, the true value of a measurement repeated a certain number of times is the average of such values and the uncertainty of such measurements is

characterized by its standard deviation. One standard deviation guarantees 68% of the data will be within the reported uncertainty, two standard deviations 95.4% and three standard deviations guarantees 99.7% of the data will be within the average value \pm three standard deviations (Taylor 1982). To find this value, a 65°F (18.3°C) economizer with speed control test was repeated five times. This test was chosen because this value of load was repeated in the full speed and economizer tests. It is also known that the economizer with speed control tests were the ones of higher complexity to set and execute. Therefore, a combination of a low load, plus some experimental complexity in setting up the test should provide a number for the experimental uncertainty that well represents the experimental error in the data, due to instrumentation accuracy, equipment arrangement, test procedures and human operator.

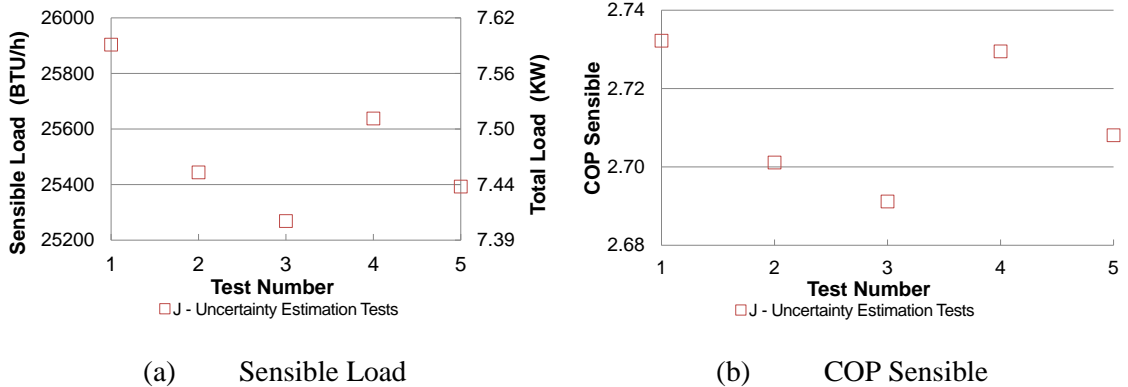


Figure 30: Sensible Load and Sensible COP uncertainties in Cooling Mode

Figures 30 (a) and (b) show the calculated sensible load and sensible COP. From figure 30 (a), the average sensible load was 25529 BTU/h (7.48 KW) with a standard deviation of 272.3 BTU/h (0.08 KW) which represents 0.97% of the average load. From figure 30 (b), the average sensible COP was 2.71 with a standard deviation of 0.02 which represents 0.66% of the average sensible COP.

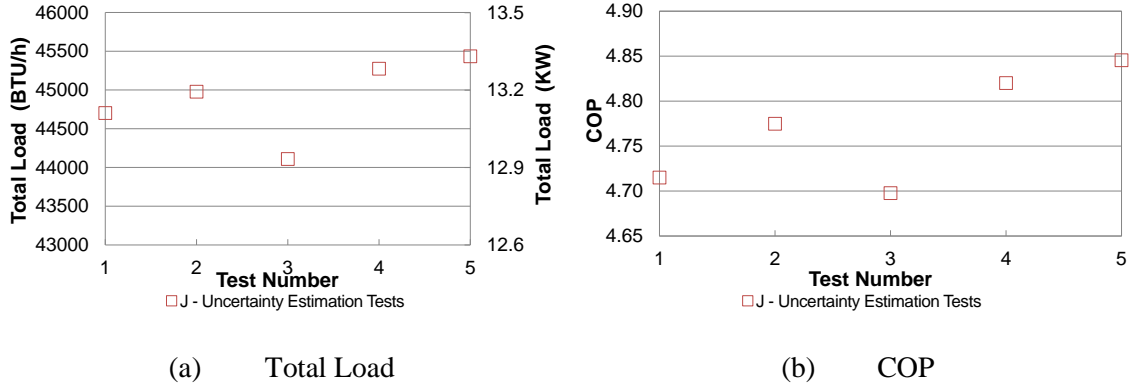


Figure 31: Total load and COP uncertainties in Cooling Mode

Figures 31 (a) and (b) show the calculated total cooling load and total COP. From figure 31 (a), the average sensible load was 44900 BTU/h (13.16 KW) with a standard deviation of 496.4 BTU/h (0.15 KW) which represents 1.17% of the average load. From figure 31 (b), the average COP was 4.77 with a standard deviation of 0.06 which represents 1.35% of the average COP.

Gaussian distribution theory indicates that 99.7% of the experiments performed using the same equipment and under similar conditions will lie within an uncertainty of three standard deviations. The uncertainty values are reported in table 14.

Table 14: Uncertainty

Calculated Variable	Uncertainty
Sensible Load	$\pm 2.91\%$
COP Sensible	$\pm 1.98\%$
Total Load	$\pm 3.50\%$
COP	$\pm 4.04\%$

Although not specifically presented in here, the same procedure was used to calculate the uncertainty of latent load resulting in $\pm 8.33\%$. This result agrees with the influence of wet bulb measurements in the total COP and total cooling loads previously determined with the Taylor series expansion method.

7.2.4 Repetition Tests

Having established the uncertainty, figures 32, 33 and 34 in this section examine 7 tests that were repeated to determine how well results could be reproduced under the same testing conditions using the load-based method in the OSU psychrometric chamber. Three tests were from series B: full fan speed with minimum outside air (considered easy to set), two from series C: fan speed control with minimum outside air (considered moderate to set) and two from series D: economizer with fan speed control for climate zone 4C (considered difficult to set).

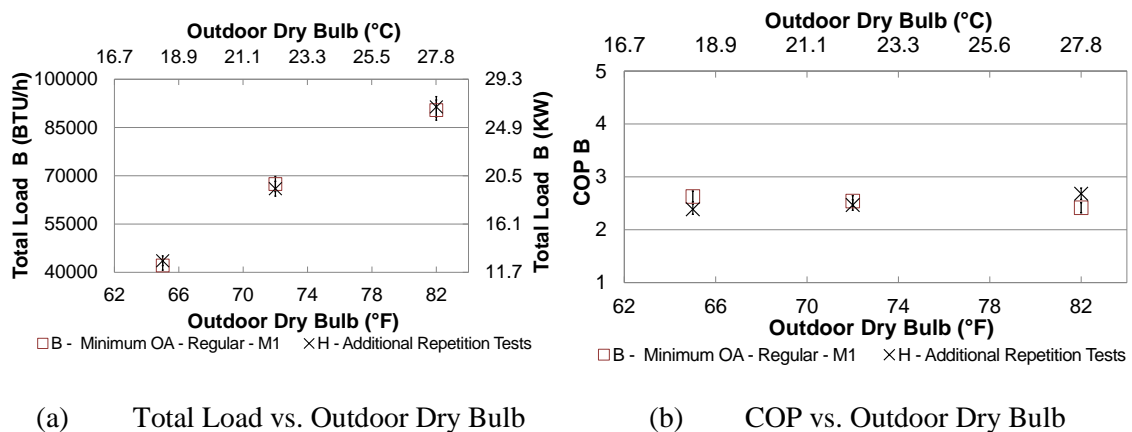
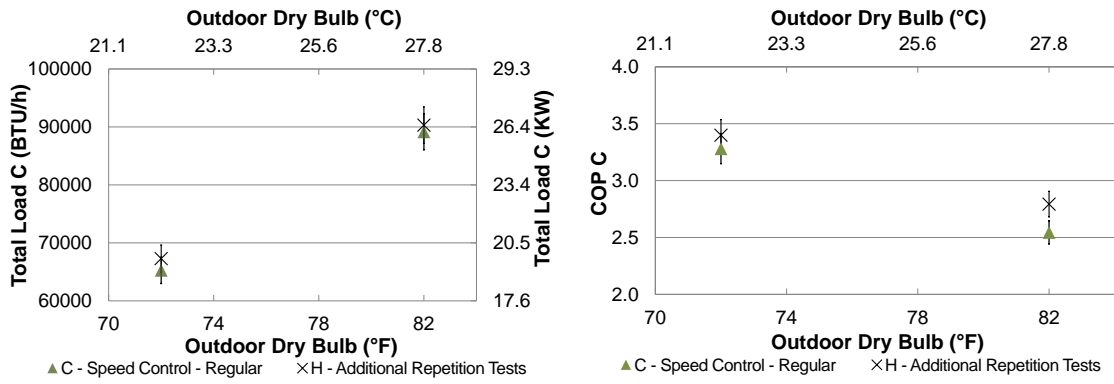


Figure 32: Total Load and COP for Series B repetition tests (easy tests to set up and execute in cooling mode)

Figure 32 (a) shows series B measured loads at 65°F (18.3°C), 72°F (22.2°C) and 82°F (27.8°C) compared to each one of their respective Series H repetitions. Results for all three repeat tests agreed with the original ones within a $\pm 3.5\%$ uncertainty error bar.

Figure 32 (b) shows series B calculated COPs compared to their respective series H repetition test results. The 65°F (18.3°C) repeat test was within $\pm 4.59\%$ of the original one. The 72°F (22.2°C) repeat test result was within the $\pm 4.04\%$ uncertainty error bar. The 82°F (27.8°C) repeat test was within $\pm 4.95\%$ of the original one.



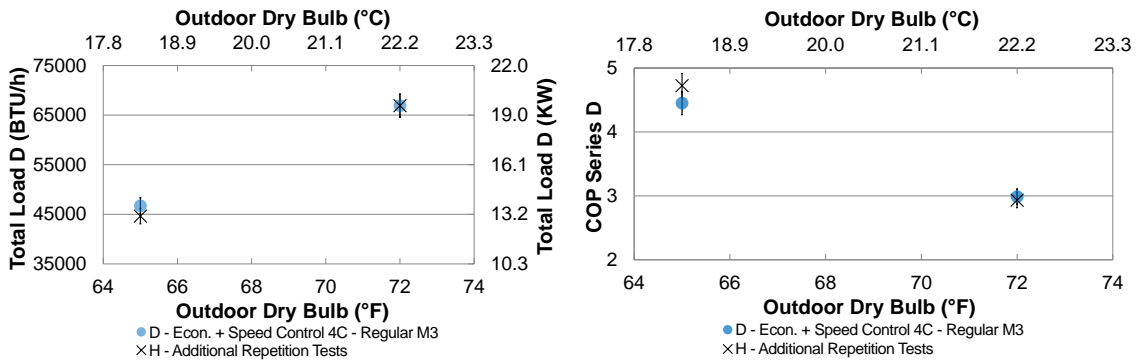
(a) Total Load vs. Outdoor Dry Bulb

(b) COP vs. Outdoor Dry Bulb

Figure 33: Total Load and COP for Series C repetition tests (moderate tests to set up and execute in cooling mode)

Figure 33 (a) shows measured loads for series C 72°F (22.2°C) and 82°F (27.8°C) tests compared to their respective Series H repetitions. Both 72°F (22.2°C) and 82°F (27.8°C) tests agreed with the original ones within the $\pm 3.5\%$ uncertainty error bar.

Figure 33 (b) shows series C calculated COPs compared to their respective series H repetitions. The 72°F (22.2°C) repeat test was within the $\pm 4.04\%$ uncertainty error bar, while the 82°F (27.8°C) test was within $\pm 4.46\%$ of the original one.



(a) Total Load vs. Outdoor Dry Bulb

(b) COP vs. Outdoor Dry Bulb

Figure 34: Total Load and COP for Series D repetition tests (difficult tests to set up and execute in cooling mode)

Figure 34 (a) shows series D 65°F (18.3°C) and 72°F (22.2°C) measured loads compared to their respective Series H repetitions. Both repetitions tests were within the $\pm 3.5\%$ uncertainty error bar.

Figure 34 (b) shows series D calculated COPs compared to their respective series H repetitions. Both 65°F (18.3°C) and 72°F (22.2°C) tests resulted in COPs within $\pm 4.04\%$ of the originally calculated ones.

7.2.5 Repeated tests without exhaust duct to explore short cycling effect

In this section, the results of repeating three economizer with speed control tests without an economizer exhaust duct are presented. The purpose of these tests was to explore the effects of exhaust air circulating back to the unit outside air inlet, due to proximity with surfaces inside the psychrometric chamber.

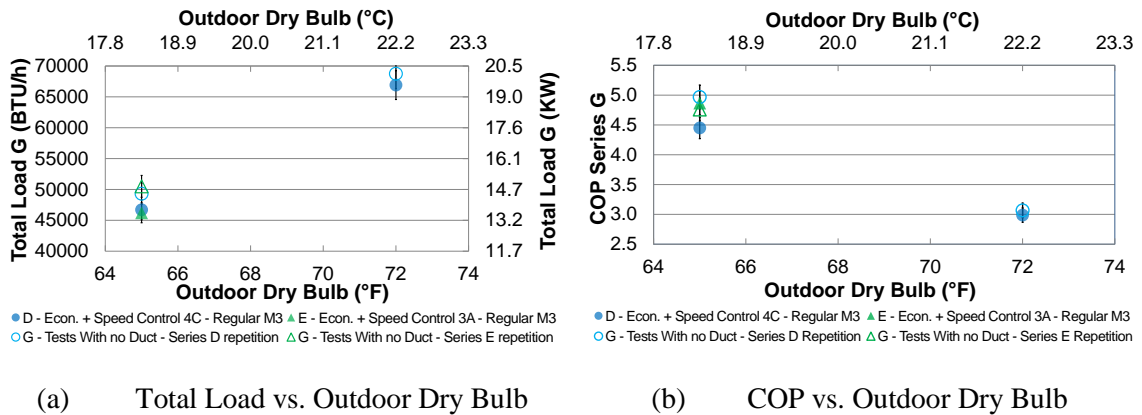


Figure 35: Total Load and COP for Series G: Tests for studying short-cycling effect (RTU in cooling mode operation)

Figure 35 (a) shows two series D (65°F (18.3°C) and 72°F (22.2°C)) tests and one series E test (65°F (18.3°C)). Difference between the two 65°F (18.3°C) tests was the outdoor wet bulb temperature. Measured wet bulb temperatures were 56.7°F for series D and 55.8°F for Series E. The difference in wet bulb temperature was due to the different climate zones conditions each test replicated. All three tests were compared to their respective ductless counterparts. Ductless tests

measured loads were within $\pm 3.5\%$ of the original series D ones. On the other hand, series E ductless test was within a $\pm 4.24\%$ of the corresponding original test.

Figure 35 (b) shows calculated COPs for the three Series D and E aforementioned tests. Ductless 65°F (18.3°C) test corresponding to series D was within a $\pm 5.22\%$ of the original test. The remaining two ductless tests agreed within $\pm 4.04\%$ of the original ones. It can be stated that the short-cycling effect did not significantly impact the loads and COP results beyond typical reported uncertainties.

7.2.6 Variable load tests

In this section, the results of introducing periodical load variations during a load-based test will be discussed. The 82°F (27.8°C) test from series C was chosen as a baseline for comparison. For test number 57, the load was set to 115% of the nominal value for a period of 20 minutes, then, for the subsequent 20 minutes, the load was set to 85% of the nominal value. This load cycling procedure was repeated for a total testing time of three hours. In a similar fashion, for test number 58, the load was set to 115% of the nominal value for 10 minutes, and 85% of the nominal load for the following 10 minutes until three hours are completed.

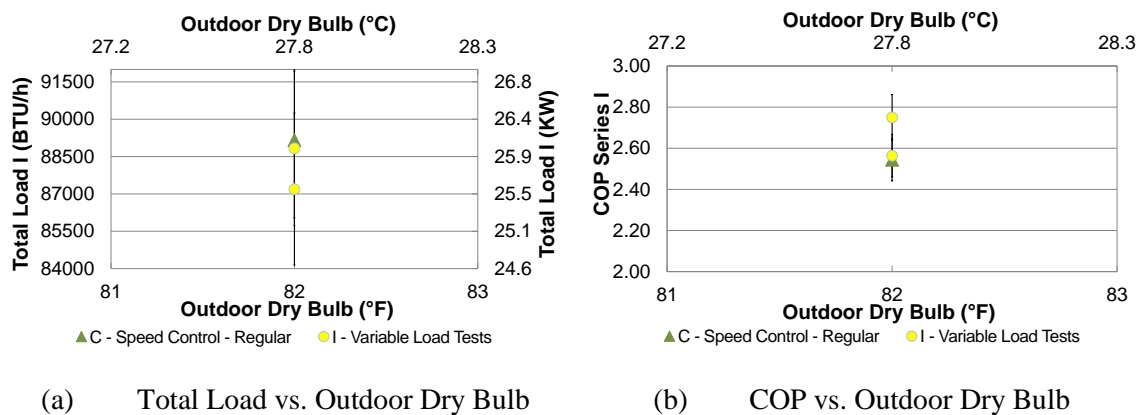


Figure 36: Total Load and COP for Series D repetition tests (RTU running in cooling mode)

Figure 36 (a) shows the measure loads for the two 82°F (27.8°C) variable load tests compared to the original series C test. Both variable tests average measured loads were within a $\pm 3.5\%$ uncertainty error bar.

Figure 36 (b) shows the calculated COPs for the two variable load tests compared to the constant load test. Calculated COPs were within a $\pm 4.04\%$ uncertainty error bar.

Results from the variable tests suggest that when $\pm 15\%$ of load fluctuations were present during a test the final average calculated COPs were still representative of the COP of the unit under constant load. The error in estimating the COPs from averages during tests with some load perturbations by as a much as $\pm 15\%$ can be up to $\pm 4\%$ with respect to COP with constant loads.

7.2.7 Averaging approach for COP calculation

7.2.7.1 ON-OFF cycling tests

In this section, the results of four tests are presented to understand how time and cycle based averaging approaches affect the results of the COP of the unit.

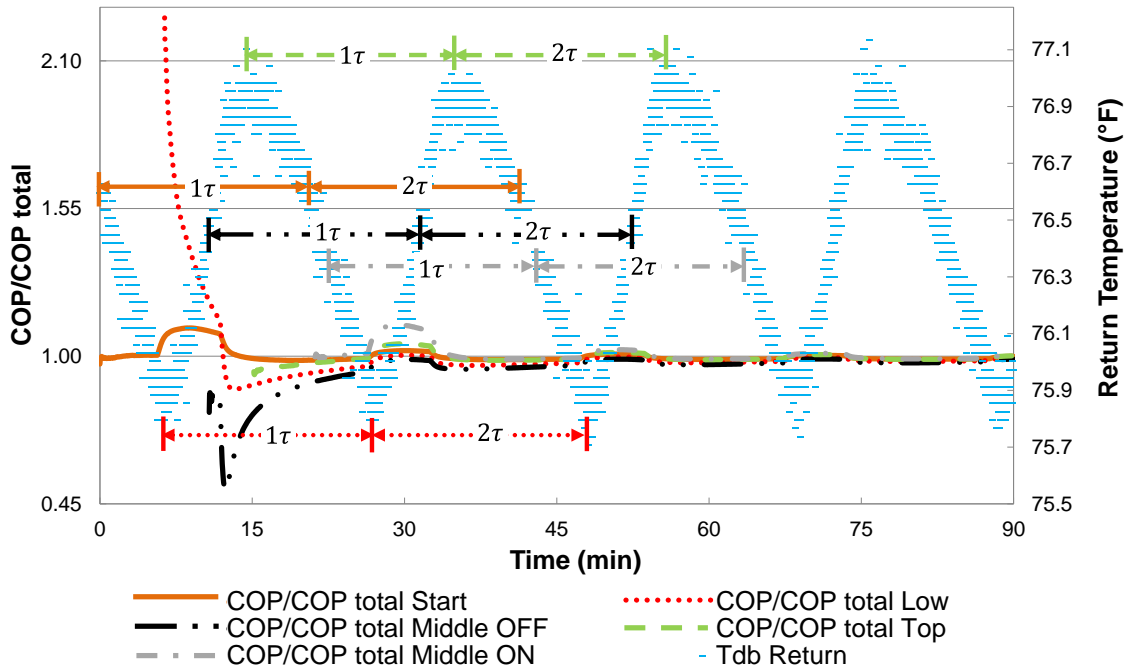


Figure 37: Normalized COP vs Time - Series B: 72°F (22.2°C) Full Fan Speed Test

Figure 37 shows the normalized COP as a function of time for Series B: 72°F (22.2°C) full speed fan test. The horizontal blue dashes show the cycling temperature profile for the test. From left to right, temperature decreasing indicates mechanical cooling is ON, while temperature increasing indicates mechanical cooling is OFF. The cycling of cooling stages was done according to the thermostatic settings. Five different starting points for COP calculation are presented. The first COP calculating starting point is the beginning of the test itself, represented in the figure by a solid dark orange line. The second starting point is the first temperature valley, which occurs between the end of the cooling ON cycle and the beginning of the cooling OFF cycle and is represented in the figure by the dotted red line. The third starting point is in the middle of the cooling OFF cycle and is represented by the dash-double dotted black line. The fourth starting point is at the first temperature peak, which occurs between the end of the cooling OFF cycle and the beginning of the cooling ON cycle and is represented by the dashed green line. The fifth starting point is in the middle of the first complete ON cycle and is represented by the dashed-single dotted gray line. In order to compare the five ways of calculating COP, they have all been normalized to the total COP calculated from the beginning to the end of the 90 minutes test. Each point at a particular time in the COP lines represents the integrated value of COP calculated from the starting point in time until that particular time on the x-axis. For example, at minute 30, the dash-double dotted black line shows the COP integrated (or averaged) from the middle of the first off cycle until the time of 30 minutes. The dimensioning arrows in the figure show the span of the first two cycles for each one of the averaging approaches. The symbol τ is the average duration of the cycles during the test and is a value to be reported according Table 8. For this particular test, the average cycle duration is $\tau = 21$ minutes and 4.3 cycles took place. Mechanical cooling was ON for an overall time of 63 minutes, which represents 70% of the test duration.

Due to the additive nature of the COP calculation, it is observed that regardless of the starting point, all averaging approaches show large peaks or valleys particularly within the first and second cycles of calculation. A good example of this is the red dotted line representing the bottom of cycle starting

point approach. In the first cycle of this calculating approach, since mechanical cooling is not operating, unit power consumption is significantly lower than it would be in the ON cycle. This results in a very high initial value of COP (2.25 times the total value of the COP). As the cycle progresses the fan energy starts to become more dominant in the equation and the COP value starts decreasing finding its minimum shortly after the compressor starts operating. This behavior continues throughout the cycles but the peaks and valleys start to be less prominent as contributions of each cycle provide balance to the COP equation. Nonetheless, as figure 38 shows, this value will keep varying through the ON/OFF cycle.

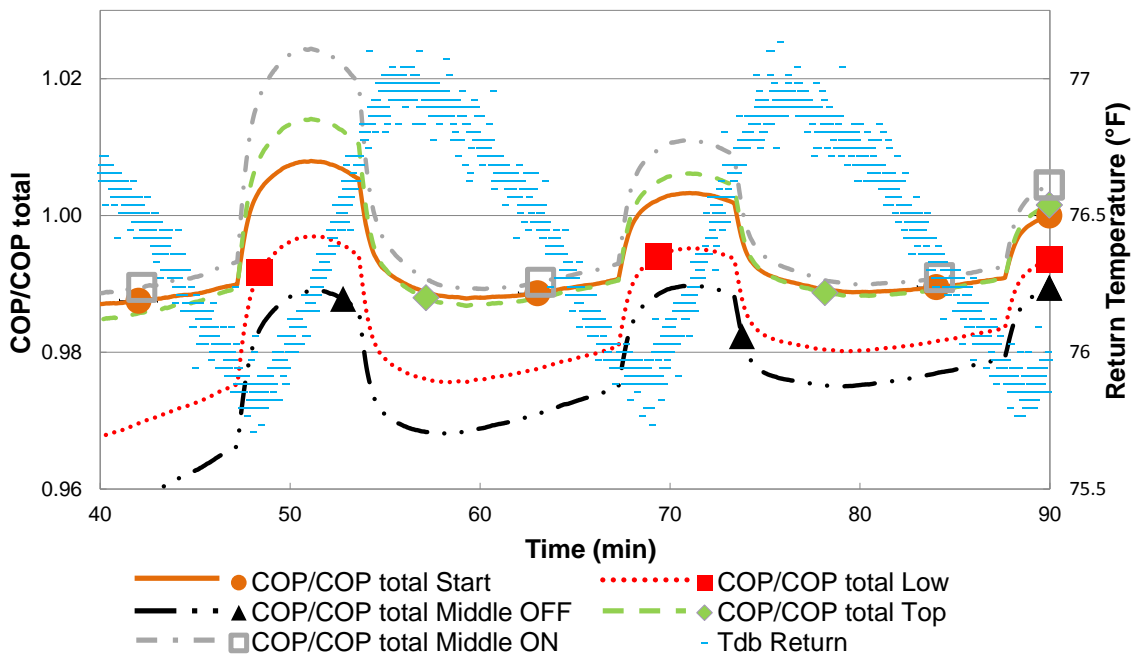


Figure 38: Normalized COP vs Time - Series B: 72°F (22.2°C) Full Fan Speed Test – After two cycles

Figure 38 shows the normalized COP as a function of time for Series B: 72°F (22.2°C) full speed fan test after two complete cycles have occurred since the beginning of the test. The absence of the initial peaks and valleys facilitate the analysis of the evolution of the COP calculation after the first two cycles have passed. In figure 38, the same legend line types as in figure 37 are used. Besides

the line types, symbols have been added to indicate when a cycle is completed. From left to right in the figure: the dark orange circle indicates when the first two cycles from the beginning of the test have been completed. The red square indicates two cycles after the first low temperature value. The first black triangle indicates two cycles after the middle point of the first OFF cycle. The first green diamond marks two cycles after the first temperature peak value and the first empty grey square indicates two cycles after the middle point of the first ON cycle.

The symbols, which represent a cycle based approach, indicate that after two cycles and regardless of the starting point, all COP values are between 98 and 99% of the COP of the full length test. For the time based approach, the analysis is done by looking at the different line types in the figure. Each line type represents a different starting point in time for COP calculation. Standing at a particular time in x-axis (for example let us take the 50th minute) and comparing the different line types it is observed that the COP can vary from 99% to 102% of the full length test COP. Hence, the starting time has a bigger effect on COP calculation when a time based approach is used than when a cycle based approach is used. More specifically, at any given time, the COP calculated starting from the middle of an ON cycle is larger than the remaining others, while the one calculated starting at the middle of an OFF cycle consistently shows the lower values. In between, lie the peak and valley approaches. The peak based value is much larger than the valley value. During the peak based cycles, the compressor is ON at the beginning, which is also the case of the middle-ON cycle, therefore, their similar behavior. Conversely, during the valley-based cycles the compressor is OFF at the beginning, therefore having a similar behavior to the middle-OFF cycle. The solid dark orange line, representing the COP since the beginning of the test, remains very close to the peak temperature line. The reason for this is that the test began shortly after a temperature peak as shown in figure 37.

Figures 39 through 42 present a similar analysis for two more types of tests.

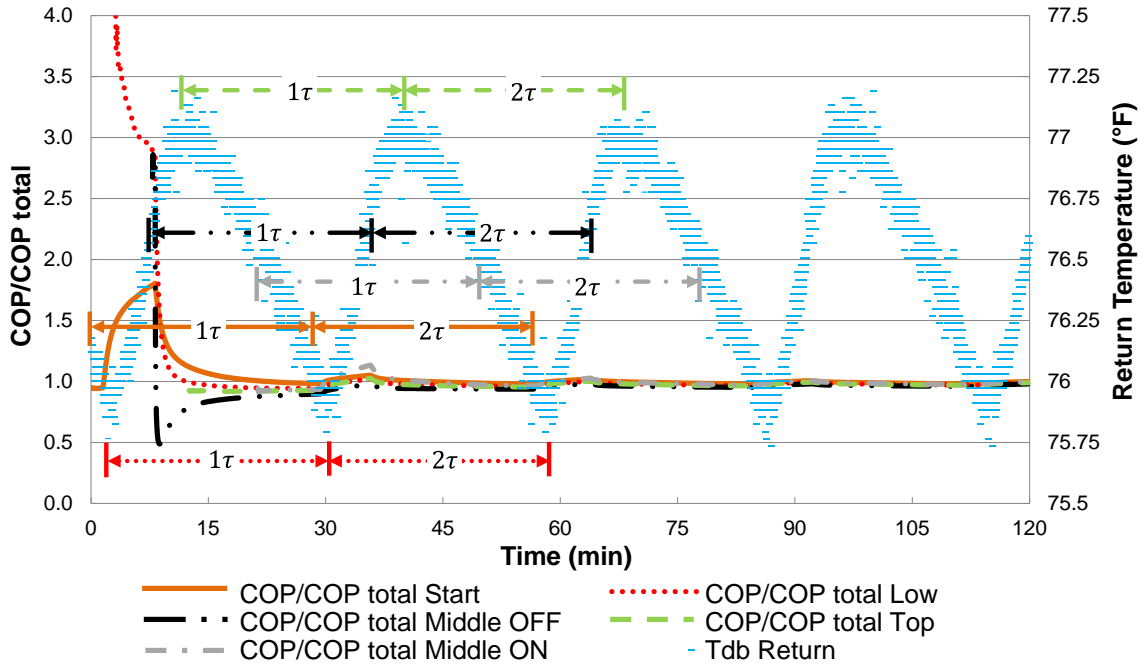
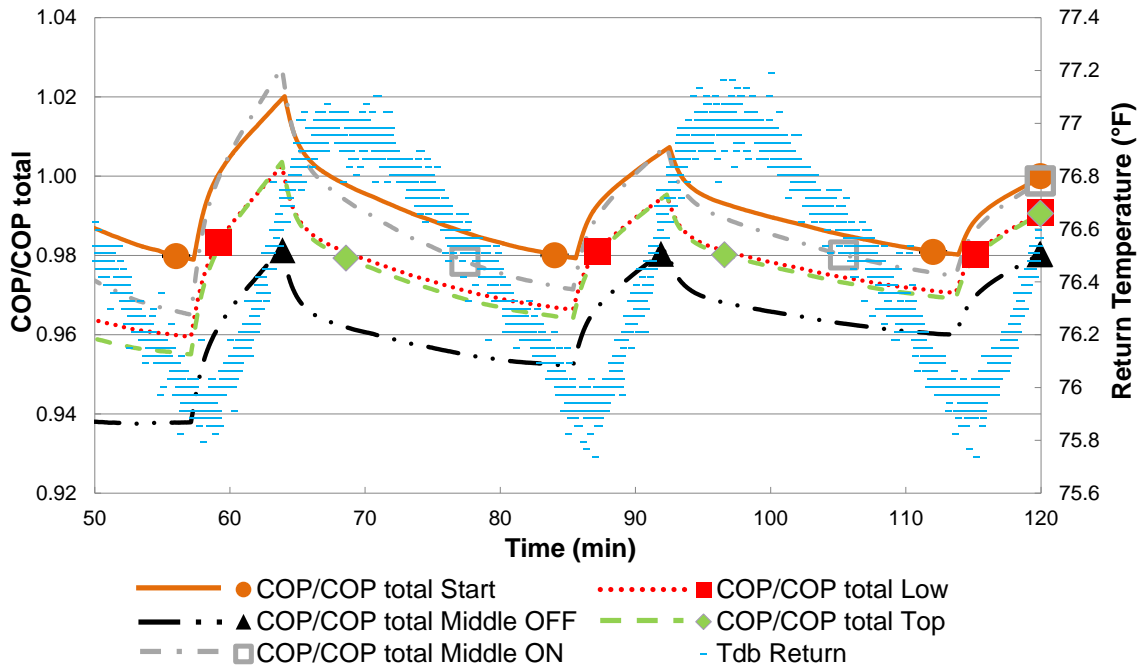


Figure 39: Normalized COP vs Time - Series C: 72°F (22.2°C) Fan Speed Control Test

Figure 39 shows the normalized COP as a function of time for Series C: 72°F (22.2°C) fan speed control test. The same legend symbols and the same average starting points of the full speed case are used. For this test, the average cycle duration is $\tau = 28$ minutes and 4.3 cycles took place. Mechanical cooling was ON for an overall time of 87 minutes, which represents 73% of the test duration. Compressor ON time is longer and has larger cycles compared to the full speed case to provide lower supply air temperatures, therefore, achieving the required cooling capacity.

Like in the full speed case, all averaging approaches show large peaks or valleys within the first and second cycles. Once more, the bottom of cycle starting point approach shows the largest starting COP value, which, on this occasion is 4 times the value of the full length test COP. Since again, peaks and valleys are less prominent as the cycles go on, a closer view of this test is presented in figure 40.



**Figure 40: Normalized COP vs Time - Series C: 72°F (22.2°C) Fan Speed Control Test -
After two cycles**

Figure 40 shows the normalized COP as a function of time for Series B: 72°F (22.2°C) fan speed control test after two complete cycles have occurred since the beginning of the test. The absence of the initial peaks and valleys facilitate the analysis of the evolution of the COP calculation after the first two cycles have passed. The same legend line types as in figure 39 are used and the symbols have been added to indicate when a cycle is completed.

The symbols, which represent a cycle-based approach, indicate that after two cycles and regardless of the starting point, all COP values are around 98% of the COP of the full-length test. As in the full speed test results, the analysis for the time-based approach is done by looking at the different line types in the figure. Each line type represents a different starting point in time for COP calculation. Standing at a particular time in x-axis (for example the 65th minute) and comparing the different line types it is observed that the COP can range from 98% to 102% of the full-length test COP. Hence, the starting time has a bigger effect on COP calculation when a time-based approach

is used than when a cycle-based approach is used. More specifically, the COP calculated starting from the middle of an ON cycle is larger than the remaining others, crossing only with the COP calculated from the beginning of the test. The reason for this is that this test started not shortly after the middle of an ON cycle took place. The COP calculated starting at the middle of an OFF cycle shows again the lower values at all times during the test. The peak and valley approaches overlap each other with slightly larger values to the COP calculated starting from the low temperature point.

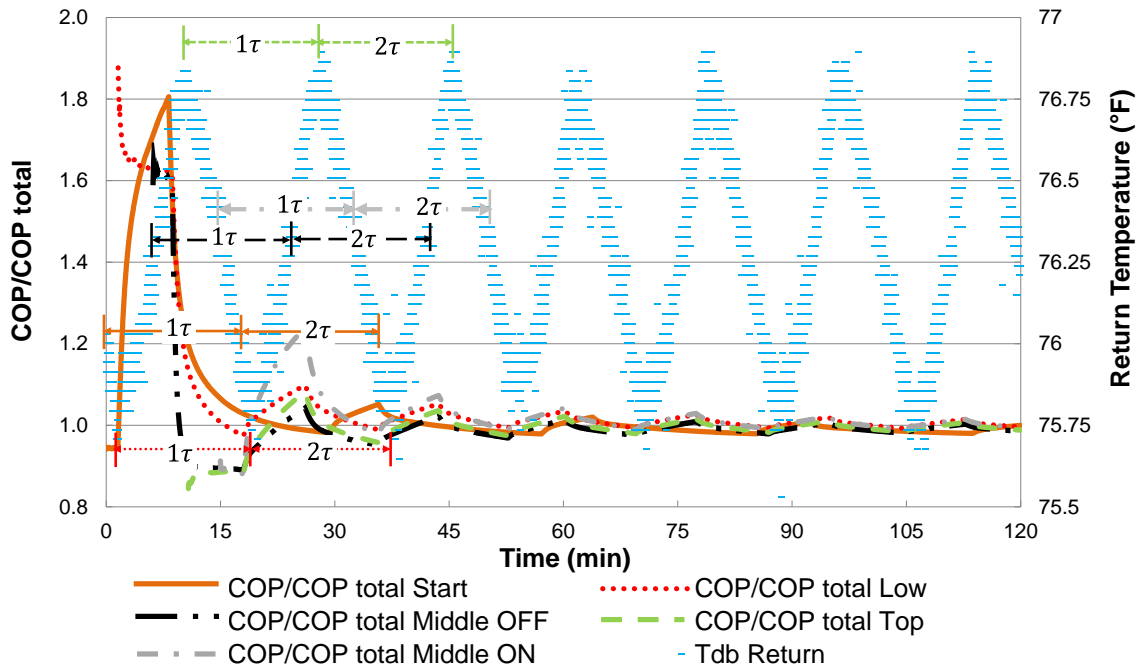


Figure 41: Normalized COP vs Time - Series D: 72°F (22.2°C) Economizer with Fan Speed Control (4C) Test

Figure 41 shows the normalized COP as a function of time for Series D: 72°F (22.2°C) marine climate (4C) economizer with fan speed control test. The same legend symbols and the same average starting points of the full speed and speed control tests are used. For this test, the average cycle duration is $\tau = 17$ minutes and nearly 7 cycles took place. Mechanical cooling was ON for an overall time of 65 minutes, which represents 54% of the test duration. Compressor ON time is less

and the cycles are shorter compared to the full speed and speed control cases because of the outside air contribution to the cooling capacity.

Like in the full speed case, all averaging approaches show large peaks or valleys within the first cycles. However, in this case, the peak and valley attenuation occurs a little bit later, between the end of the second and beginning of third cycles. In comparison, this attenuation occurs between the end of the first cycle and the middle of the second cycle in full speed and speed control cases. As with previous tests, the bottom of cycle starting point approach shows the largest starting COP value, which, on this occasion is 1.9 times the value of the full length test COP. Figure 42, shows a zoomed view of the large peaks and valleys free area to get a better understanding of what happens after two cycles.

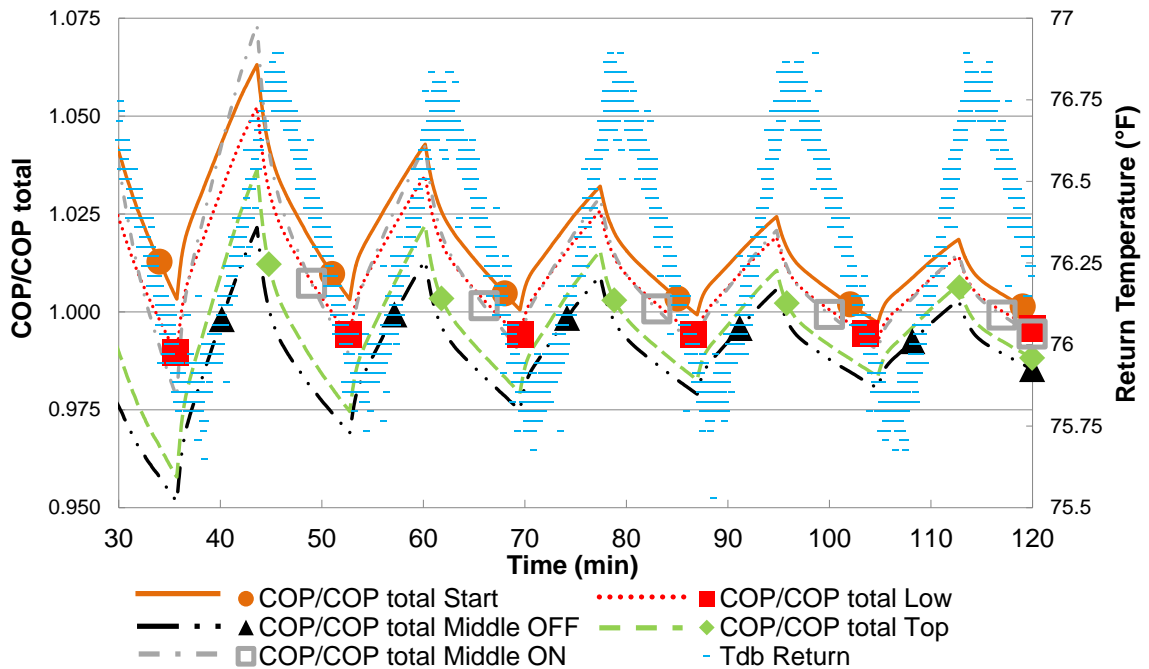


Figure 42: Normalized COP vs Time - Series C: 72°F (22.2°C) Economizer with Fan Speed Control Test - After two cycles

Figure 42 shows the normalized COP as a function of time for Series D: 72°F (22.2°C) marine climate (4C) economizer with fan speed control test. The absence of the initial peaks and valleys

facilitate the analysis of the evolution of the COP calculation after the first two cycles have passed. The same legend line types as in figure 41 are used and the symbols have been added to indicate when a cycle is completed.

The symbols, which represent a cycle-based approach, indicate that after two cycles and regardless of the starting point, results in COP values within 99% to 101% of the COP of the full length test. The different COP lines show very different values at a particular minute in the x-axis. Looking for example at the peaks that occur around the 44th minute. When the COP calculation starts from the middle of the ON cycle and finishes at minute 44, the COP results 7% higher than the full-length test. In addition, when the calculation starts from the beginning of the test and finishes at minute 44, the COP results 6% higher than the full-length test COP. This means that calculations starting at the beginning of test and at the middle-ON cycle yield higher COP values, while, as in previously analyzed tests, the middle-OFF cycle yields the lowest COP values throughout the entire test. Peak and valley based approaches give intermediate values of COPs with higher values resulting again from the low temperature approach.

Up to this point, tests where several cycles occur have been discussed, but cases where a single cycle or part of a cycle has occurred were also encountered in the experimental campaign of this project. A test with those characteristics is presented in figure 43.

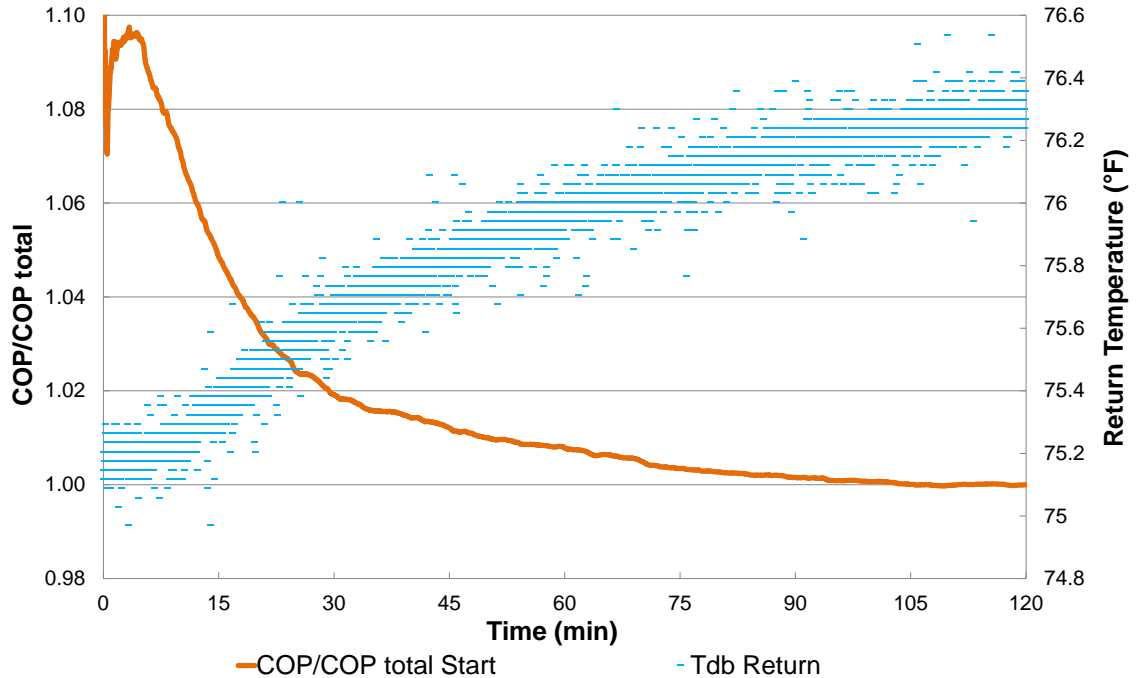


Figure 43: Normalized COP vs Time for a test in which cycling did not occur- Series E:

65°F (18.3°C) Economizer with Fan Speed Control (3A) Test

Figure 43 shows the normalized COP as a function of time for Series E: 65°F (18.3°C) economizer with fan speed control for moist climate (3A) test. The horizontal blue dashes represent the indoor room return temperature and the solid dark orange line the normalized COP calculated from the beginning of the test. During the 120 recorded minutes, no cycling occurred since the indoor return temperature remained below the 76.5°F (24.7°C) limit where mechanical cooling is activated and above the 75°F (23.9°C) limit where the economizer goes from the open to the minimum outside air position.

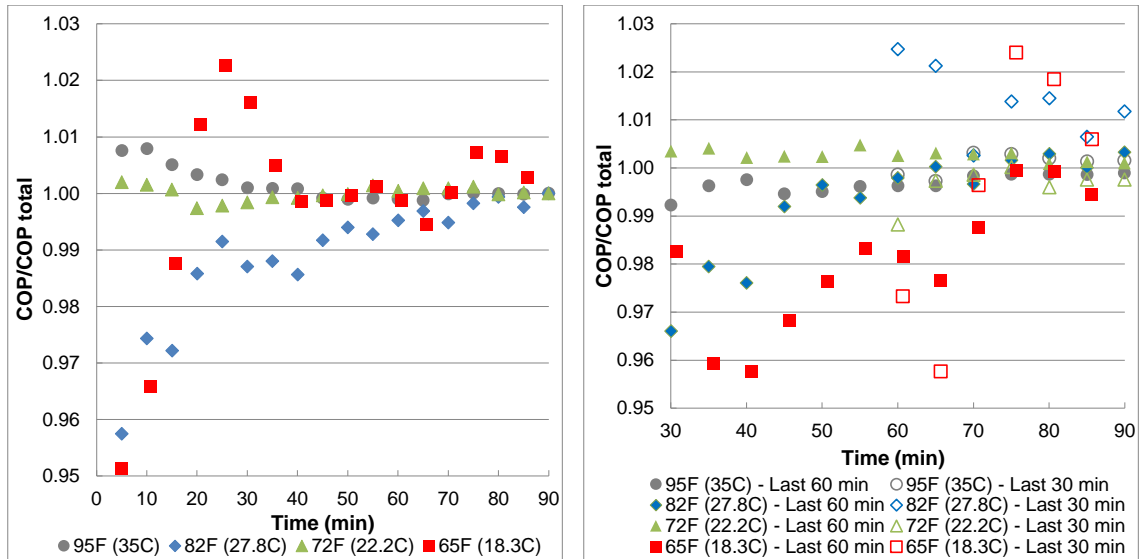
Like in the cycling cases, a peak is observed at the beginning of the test until the fan power starts to influence more the COP equation bringing the values down to within 2% of the full-length test value after approximately 30 minutes. However, had the recording continued for a few more minutes, the temperature-increasing trend would have led to mechanical cooling requirement. From previously presented tests, the additional power provided by the compressor has the effect of

decreasing the COP further, beginning a set of fluctuations that stabilize somewhere around two to three compressor cycles.

This result, along with the three previously analyzed tests, indicate that time based approach can significantly overestimate or underestimate the COP value if the end test time is not chosen appropriately. Nonetheless, after a significant number of cycles have passed (which are recommended to be two at the minimum) the time based approach error can be minimized. Figures 37 to 42 show how a cycling based approach consistently provides results that better capture long term average unit efficiency, with values ranging from 98% to 101% of the full length tests. Additionally, a calculation beginning at the middle of the OFF cycle regularly results in more conservative values of COP which can be better used for simulation and designs purposes. For all these reasons, as a result of this thesis, the recommendation for COP calculation is to average the load divided by the average unit power for the duration of at least two cycles beginning at the middle of the first OFF cycle or during the recording time prescribed in table 4, whichever one is longer.

7.2.7.2 Technologies that maintain indoor temperature within narrow temperature ranges

Some technologies, such as digital scroll compressors with fully modulating capacity apply short cycles that control indoor return temperature within smaller ranges than the ones achieved by ON-OFF cycling compressors. Having more constant temperatures resulted in more constant values of COP as well. Figure 44 shows the results of four tests where the digital scroll modulating capabilities was used to understand the impacts of three different time averaging approaches.



(a) Beginning of Test

(b) Last 60 min, Last 30 min

Figure 44: Normalized COP vs Time for digital scroll full modulation tests

Figure 44 (a) shows the normalized COP as a function of time of four series B: full fan speed with minimum outside air tests. For the 95°F (35°C), 82°F (27.8°C), 72°F (22.2°C) and 65°F (18.3°C) tests digital scroll compressors modulating technology was used. Indoor return temperature was controlled within a 72.4°F (22.4°C) to 72.6°F (22.6°C) range. The COP was calculated from the beginning of the tests. As seen in figure 44 (a) the COP values converged to $\pm 1\%$ of the COP of the full length test approximately after 45 minutes and remained within that range until the end of the test.

Figure 44 (b) shows the normalized COP as a function of time with two additional averaging approaches. The full legend symbols show the COP calculated starting at the 30th minute of the test, while the hollow symbols show the COP calculated starting at the 60th minute of the test. The COP calculated starting at the 30th minute of the test captures the last 60 minutes of the 90 minute recording. Approximately at the 75th minute, the COP calculated with this approach converged to $\pm 1\%$ of the COP of the full length test. This result is consistent with the beginning of test approach shown in figure 44, where 45 minutes were required to obtain the same calculated COPs as the full-

length test. It is also observed that using the last 30 minutes calculating approach the COP values were more scattered and within $\pm 5\%$ of the full length test COP.

Altogether, these results indicate that when technologies that control return temperature within narrow margins are used, testing time can be reduced to approximately half while still providing fairly accurate COP results.

7.2.8 Example unit profile with load-based testing

Figures 45 through 47 in this section show examples of calculated COPs for a 15-ton rooftop unit tested with the load-based method presented in this document. These results characterize the unit for the different outside air and load conditions described in table 4 providing a comparison of four different technologies tested. The four technologies were full fan speed with economizer damper at minimum outside air position (B), fan speed control (C), economizer with fan speed control (D) and digital scroll compressor modulation.

7.2.8.1 Full fan speed with minimum outside air vs. Fan speed control vs. Economizer with fan speed control

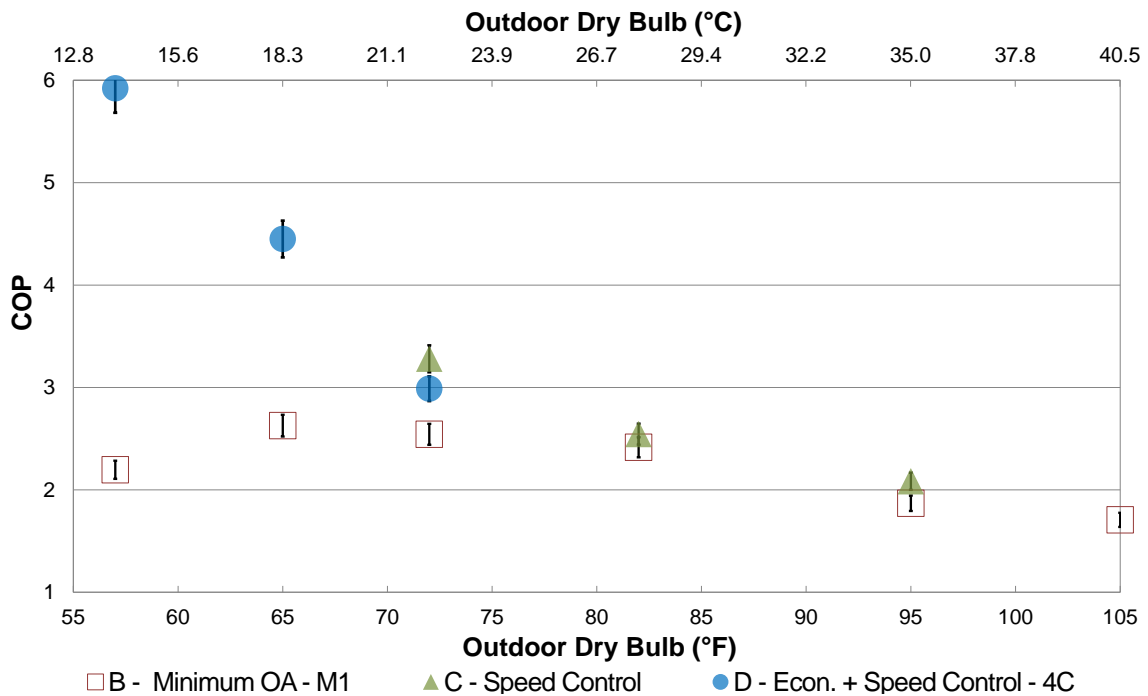


Figure 45: COP vs Outdoor Dry Bulb temperature for Series B, C and D (RTU run in Cooling Mode)

Figure 45 shows the resulting COPs for series B: full fan speed with minimum outside air, series C: fan speed control and series D: economizer with speed control tests.

COP values for series B full fan speed tests span between 1.71 for the 105°F (40.6°C) test to 2.63 for the 65°F (18.3°C) test. Also, a decreasing COP trend is observed as outdoor air temperature and load increased from the 65°F (18.3°C) to the 105°F (40.6°C) tests. The 57°F (13.9°C) result did not follow the decreasing trend due to low load values, which decrease the COP as unit power approaches its minimum operating values. Additionally, the 116539 BTU/h (34.2 KW) load associated with the 105°F (40.6°C) outdoor air temperature test resulted in an indoor return air temperature of 81.6°F (27.6°C) which is outside the desired thermostatic settings of 75°F to 77.5°F (23.9°C to 25. 3°C).

Series C fan speed control tests resulted in better efficiencies than the corresponding full fan speed 72°F (22.2°C), 82°F (27.8°C) and 95°F (35°C) tests. The major energy savings were observed at the 72°F (22.2°C) test with a COP 29% higher than the corresponding full fan speed test. Although efficiencies were higher, the unit was not able to provide enough cooling capacity at the 95°F (35°C) speed control test to meet indoor temperature requirements because of the lower supply airflow rate. The return temperature for the 95°F (35°C) test averaged 83.2°F (28.4°C).

Series D economizer with speed control tests for marine climate (4C) showed significant efficiency improvements with respect to corresponding full speed tests. At the 72°F (22.2°C), the COP was increased by a factor of 1.18 with respect to the full speed test. The COP at 65°F (18.3°C) is 1.69 times larger than the full speed test. At 57°F (13.9°C), the effect of cold outside air was even more noticeable with a COP 2.29 times larger than the full speed case. It is also noted, that at 72°F (22.2°C) the efficiency improvement of using the economizer was 11% less than the one obtained by reducing the fan speed at the speed control test. This result indicates that the cooling gained with the 72°F (22.2°C) outdoor airflow was outweighed by the additional power required when the fan ran at full speed with a fully open economizer.

7.2.8.2 Economizer with fan speed control: marine climate (Salem, OR 4C) vs. moist climate (Memphis, TN 3A)

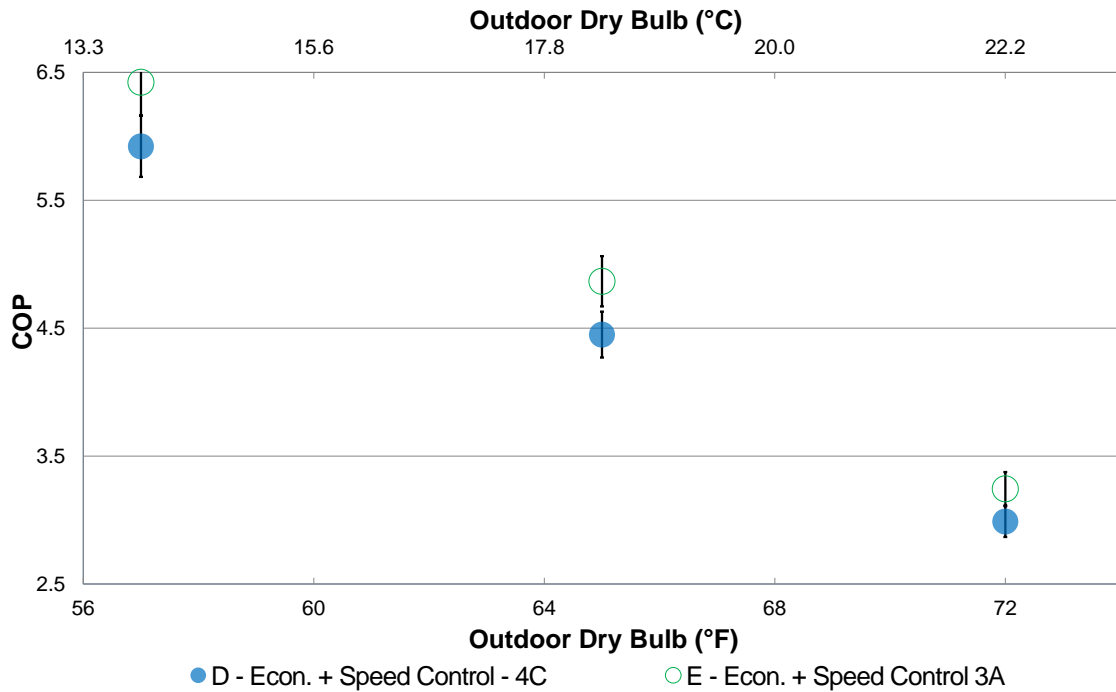


Figure 46: COP vs Outdoor Dry Bulb temperature for Series D and E (RTU run in Cooling Mode)

Figure 46 shows economizer with fan speed control tests COPs for two different climate zones. Outdoor dry bulb temperatures were 57°F (13.9°C), 65°F (18.3°C) and 72°F (22.2°C) for both climate zones. Following the same order, wet bulb temperatures were 52°F (11.1°C), 56°F (13.3°C) and 60°F (15.6°C) for the marine climate zone (Salem, OR 4C) and 49°F (9.4°C), 54°F (12.2°C) and 62°F (16.7°C) for the moist climate zone (Memphis, TN 3A).

Series E had lower wet bulb temperatures for the 57°F (13.9°C) and 65°F (18.3°C) tests, which reduced the humidity going through the coil, therefore reducing the latent load and increasing the COP with respect to series D tests. On the other hand, the 72°F (22.2°C) series E test had a higher outdoor wet bulb setting, but the economizer high limit was set a 72°F (22.2°C) instead of 65°F (18.3°C) as series E. This result concurs with the findings described after figure45, where using

speed control alone resulted in higher COPs than the 72°F (22.2°C) economizer with speed control tests.

7.2.8.9 Technology comparison: ON-OFF cycling compressor (M1) vs. digital scroll modulating compressor (M2)

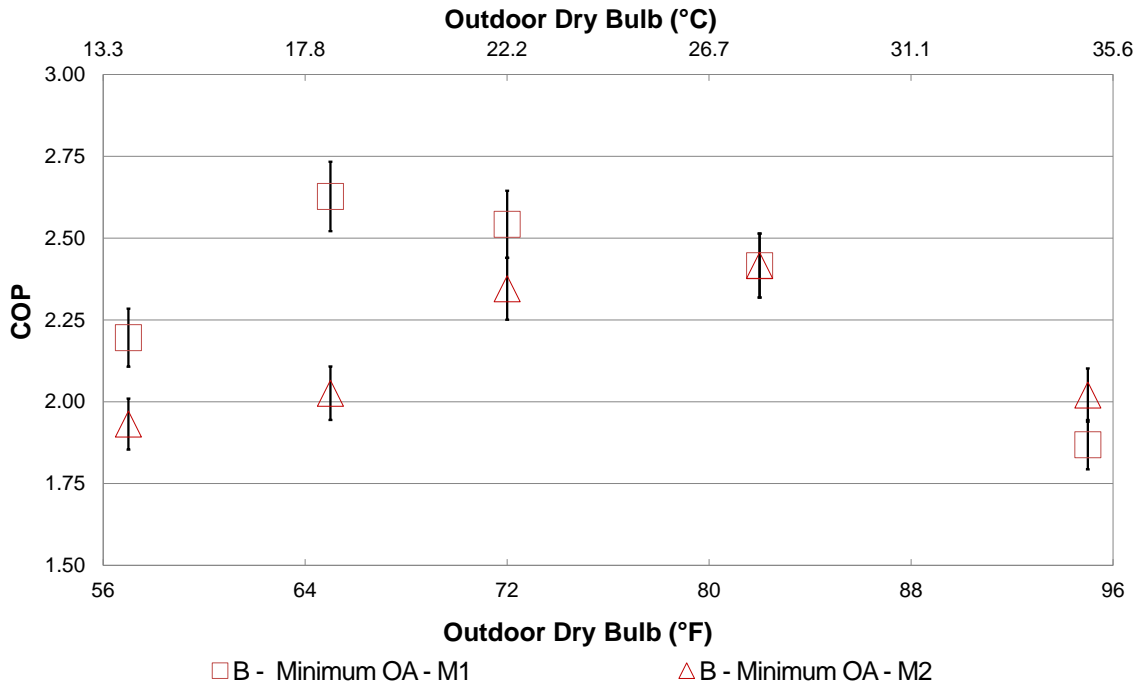


Figure 47: COP vs Outdoor Dry Bulb temperature for Series B: full fan speed tests with ON-OFF (M1) and digital scroll modulating compressors (M2)

Figure 47 shows five series B full fan speed tests performed with ON-OFF compressor cycling contrasted with five tests that used compressor modulation under same outdoor air temperatures and load conditions. Outside air temperatures ranged from 57°F (13.9°C) to 95°F (35°C). The digital scroll compressor technology was lower in efficiency in all the tests ranging from 57°F (13.9°C) to 65°F (18.3°C). At 72°F (22.2°C) compressor modulating efficiencies approach the ON-OFF COP, while at 82°F (27.8°C) are almost equal. Mild improvements were found at 95°F (35°C). Even though compressor modulation provided much more stable indoor temperatures, the savings in energy are not observed unless high cooling loads are set. At higher temperatures, using the

digital scroll short cycles allowed to save some energy by disengaging the motor from the compressor itself. Conversely, at lower loads of the low temperature range, having an unengaged motor running consumed more power than a compressor cycling in ON and OFF mode. Additionally, ON-OFF compressor cycling often comes together with condenser fan cycling, while the investigated modulating compressor technology was only in the compressor, i.e., the condensing fan of the unit was set at 100% at all times.

To highlight the effects of the parasitic power of the RTU on the COP resulting from the load-based method of test, a COP was calculated by removing the power usage of the condenser fan in the COP equation, and it is referred as to $COP_{no, fan, power}$. Figure 48 shows the COP of the RTU with the ON/OFF compressor control technology (M1) and with the digital compressor capacity modulating technology (M2) were used but the condenser fan power were not include in the COPs. The $COP_{no, fan, power}$ were similar for the range of outdoor temperature investigated in the present work. At the minimum temperature of 57°F, cycling the compressor ON/OFF resulted in slightly lower, $COP_{no, fan, power}$ with respect to the digital compressor capacity modulating technology. At outdoor temperature of 65°F, cycling the compressor ON/OFF provided slightly better $COP_{no, fan, power}$ with respect to the digital capacity modulating compressor technology. Above 65°F, the two technologies had very similar $COP_{no, fan, power}$. It should be emphasized in here that (i) the digital compressor modulating technology in the RTU was not optimized for the particular series of tests presented in the present thesis and (ii) the supply air temperature and the return air temperature for the tests conducted with the M2 technology were more stable and had less fluctuations than that of the tests conducted with the M1 technology. Figure 47 and Figure 48 confirm that the characteristic of improved stability of the air temperatures delivered to the indoor environmental (occupied) space of a building were not captured by the figure of merits defined by the COP nor by the $COP_{no, fan, power}$ of the RTU.

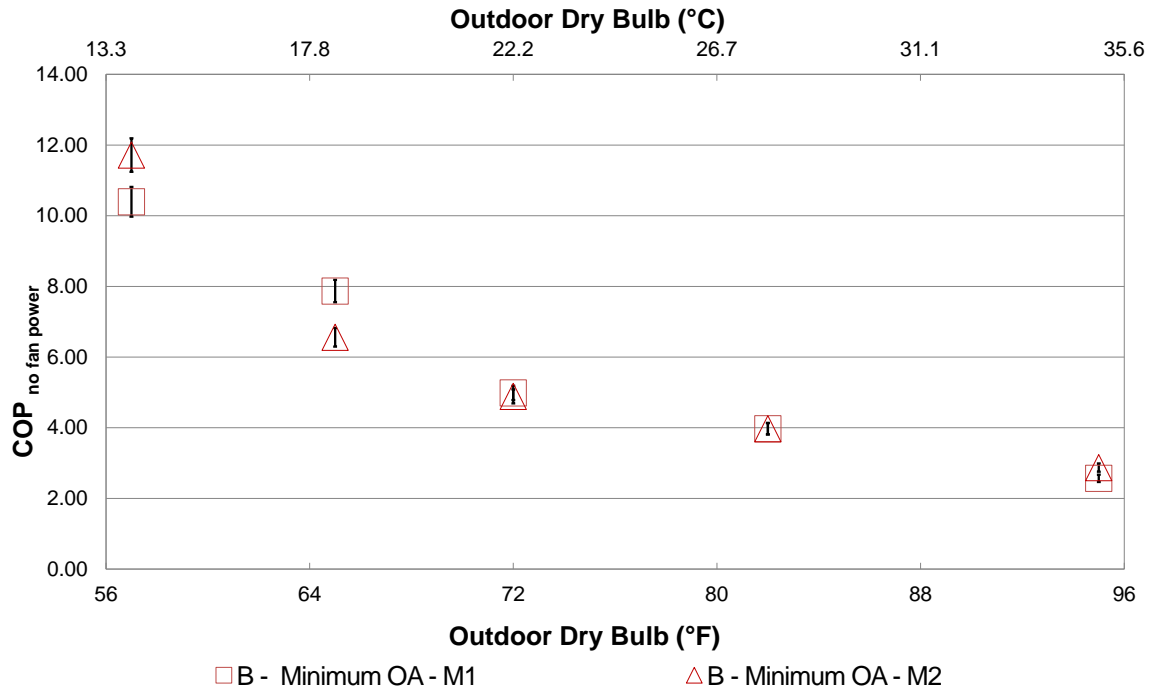


Figure 48 COP_{no fan power} vs Outdoor Dry Bulb temperature for Series B: full fan speed tests with ON-OFF (M1) and digital scroll modulating compressors (M2)

7.2.9 Effect of outside ventilation air on the reported total load and COP of the unit

The total load applied in the indoor room of the chamber was a combination of the sensible load from the conditioning fans and heaters, the latent load from the humidifier, and the latent load produced by the humidity that entered the indoor room through the economizer damper. It is interesting to show the effect that ventilation air had on the total load and on unit performance figure of merit. In order to do that, the following three quantities are introduced:

$$\dot{Q}_{total,average}' = \dot{Q}_{sens,average} + \dot{Q}_{lat,humidifier} \quad (38)$$

$$\dot{Q}_{lat,humidifier} = \dot{m}_{steam} h_{fg,steam} \quad (39)$$

$$COP' = \dot{Q}_{total,average}' / \dot{W}_{unit,average} \quad (40)$$

Where:

$\dot{Q}_{total,average}'$: Average indoor total load without ventilation effects, BTU/h (kW)

$\dot{Q}_{sens,average}$: Unit sensible cooling capacity or indoor room total cooling load averaged throughout the entire length of the test, BTU/h (kW)

$\dot{Q}_{lat,humidifier}$: Latent load set by the steam wand in the indoor room, BTU/h (kW)

\dot{m}_{steam} : Mass flow rate of steam generated by the humidifier, lbm/h (kg/s)

$h_{fg,steam}$: Steam enthalpy of vaporization BTU/lbm (kJ/kg)

$\dot{W}_{unit,average}$: Unit power consumption averaged throughout the entire length of the test, BTU/h (kW)

COP' : Load-based coefficient of performance without ventilation effects, dimensionless

The apostrophe notation (symbol ') indicates that the load and the COP were calculated without considering the sensible and latent load contributions from the ventilation air, and as summarized by the equations (25) to (27).

For this project, simulation data was used to estimate the internal latent load from 31 people occupying a prototype small office building. Equation (38) calculates the total average load taking

into account only the latent load provided by the humidifier, which simulates the people internal latent heat gain.

The latent load from the humidifier was calculated by multiplying the mass flow rate of the steam generated by the humidifier, times the enthalpy of vaporization at atmospheric pressure. Thus, applying equation (39) yields:

$$\dot{m}_{steam} = 8 \text{ lbm/h (0.001 kg/s)}$$

$$h_{fg,steam} = 970.2 \text{ BTU/h [} 2275 \times 10^6 \text{ J/kg]}$$

$$\dot{Q}_{lat,humidifier} = \dot{m}_{steam} h_{fg,steam} = 8 \text{ lbm/h} \times 970.2 \text{ BTU/lbm} = 7762 \text{ BTU/h (2275 W)}$$

Equations (38) through (40) were used to calculate the total load $\dot{Q}_{total,average}'$ and COP' without the effects of outside air ventilation for the tests described in the example unit profile presented in figure 45. Figures 49 and 50 show the comparison between the total load and COP with and without ventilation.

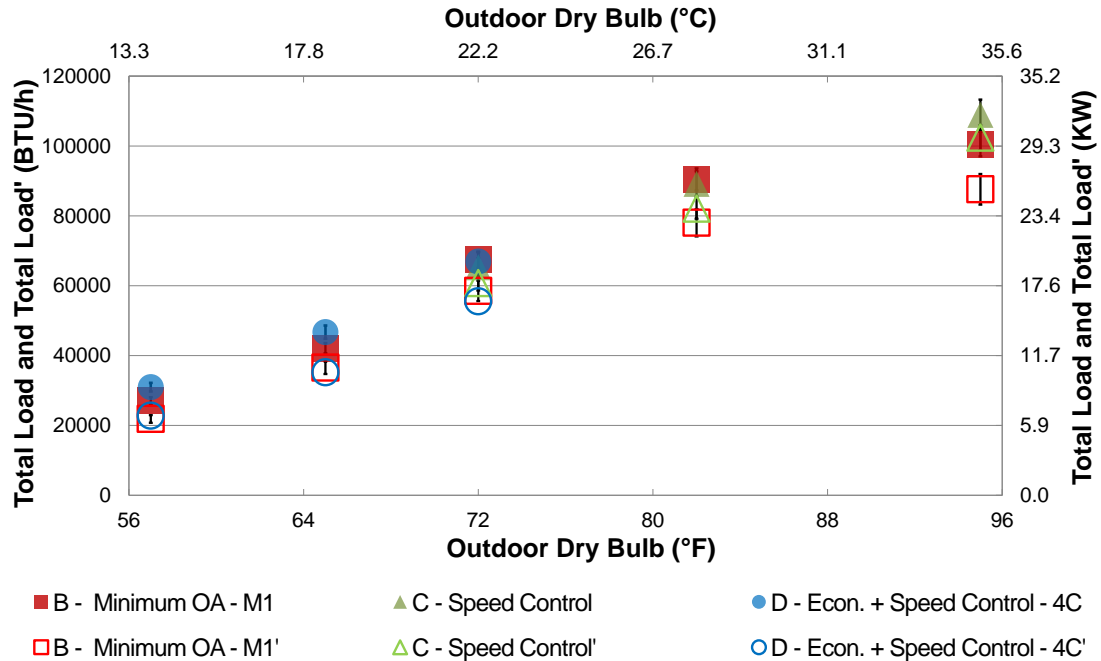


Figure 49: Comparison of total load with and without ventilation contribution for series B, C and D (The apostrophe notation (symbol ') in the legend indicates that the loads were calculated without considering the sensible and latent load contributions from the ventilation air, and as summarized by the equations (38) and (39)).

Figure 49 shows the total load $\dot{Q}_{total,average}$ compared to the total load without ventilation $\dot{Q}_{total,average}'$ for series B: full fan speed with minimum outside air, series C: fan speed control and series D: economizer with speed control tests. The full symbols represent the total load, while the hollow symbols represent the total load without ventilation effects. The total load with ventilation was always higher than the one that only included the internal latent heat gains. For Series B, the total load without ventilation was 10% to 19% lower than the total load with ventilation. Where 10% is the difference for the higher load at 105°F (40.6°C) and 19% is the difference for the lower load at 57°F (13.9°C). For Series C, the total load without ventilation was 6% to 8% lower than the total load with ventilation. For series D, the total load without ventilation was 17% to 26% lower than the total load with ventilation. Where 17% is the difference for the

higher load at 72°F (22.2°C) and 26% is the difference for both lower loads at 57°F (13.9°C) and 65°F (18.3°C). The largest difference was observed in the series D economizer with speed control tests. The reason for this difference was the higher outside airflow entering through the economizer damper, which significantly increased the humidity being introduced to the indoor room.

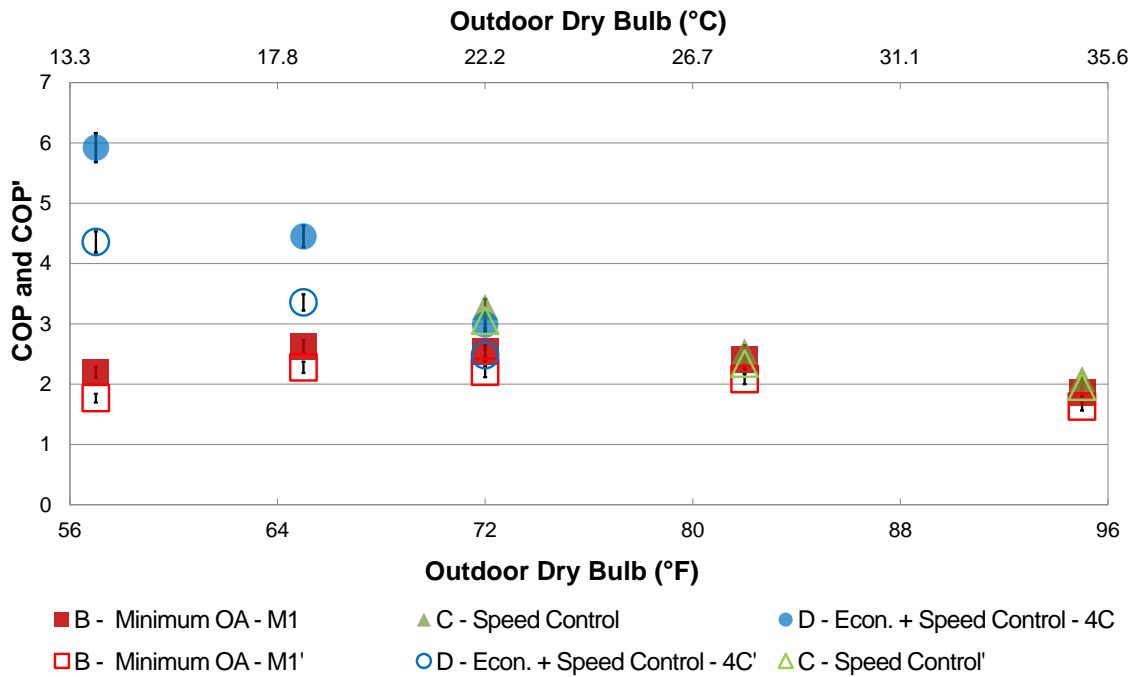


Figure 50: Comparison of COP with and without ventilation for series B, C and D (The apostrophe notation (symbol ') in the legend indicates that the COPs were calculated without considering the sensible and latent load contributions from the ventilation air, and as summarized by the equations (38) to (40)).

Figure 50 shows the total COP compared to the total COP' without ventilation for series B: full fan speed with minimum outside air, series C: fan speed control and series D: economizer with speed control tests. The full symbols represent the total COP while the hollow symbols represent the COP' without ventilation effects. The total COP with ventilation was always higher than COP' which only accounted the internal latent heat gains. For Series B, the COP' was 10% to 19% lower than the total COP_{LB} with ventilation. Where 10% is the difference for the higher load at 105°F

(40.6°C) and 19% is the difference for the lower load at 57°F (13.9°C). For Series C, the COP' without ventilation was 6% to 8% lower than the total COP with ventilation. For series D, the COP' without ventilation was 17% to 26% lower than the total COP with ventilation. Where 17% is the difference for the higher load at 72°F (22.2°C) and 26% is the difference for both lower loads at 57°F (13.9°C) and 65°F (18.3°C). The larger difference between COP' and COP was observed in the series D economizer with speed control tests. This larger difference occurred because of the additional humidity introduced by the outside airflow entering through the economizer damper. In summary, the total loads without ventilation $\dot{Q}_{total,average}'$ were lower than the total loads with ventilation $\dot{Q}_{total,average}$ for the economizer tests. This resulted in the largest differences between COP' (that is, COP calculated with no ventilation contributions) and COP , that is COP calculated in which the ventilation contribution were accounted for.

7.2.10 Heating Load

Figure 51 in this section provides an insight in the general heating load trends observed throughout the totality of heating tests performed.

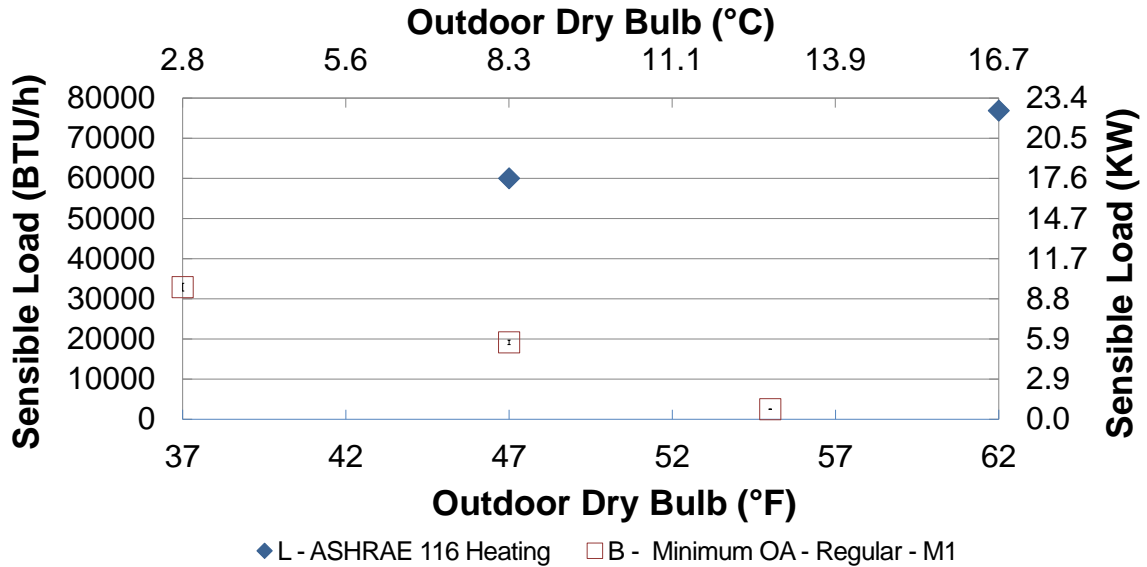


Figure 51: Sensible Heating Load vs. Outdoor Dry Bulb Temperature

Figure 51 shows the sensible load as calculated by equation (31) with outdoor air temperatures spanning between 37°F and 62°F (2.8°C to 16.7°C). Sensible heating loads vary from 2502 BTU/h to 32094 BTU/h (0.73 KW to 9.41 KW) for load-based tests. The maximum sensible load obtained was 59999 BTU/h (17.58 KW) corresponding to series L of the ASHRAE 116 baseline test at 47°F (8.3°C).

Series L stands out in general for having the higher sensible loads as seen in Figure 51. It is observed in this series that the sensible load measured at the 47°F (8.3°C) outside dry bulb test was lower than the 62°F (16.7°C) one by approximately 7000 BTU/h (2.05 KW). Since both tests have the same constant supply airflow rate, a lower supply air temperature of 82.9°F (28.3 °C) for the 47°F (8.3°C) test vs 86.5°F (°C) for the 62°F (16.7°C) test is the reason for the sensible load difference. Regarding load-based tests, sensible loads decreased as the outdoor air temperatures increased. This decreasing trend is a result of the applied PNNL simulations load profiles and reflects load

conditions that are closer to real building load profiles. Sensible load measurements had an accuracy of $\pm 2.9\%$ of the measured sensible load. This accuracy is smaller than the size of the symbols used in figure 51.

7.2.11 Heating COP

Figure 52 in this section provided an insight of the general COP efficiency trends observed throughout the totality of heating tests performed.

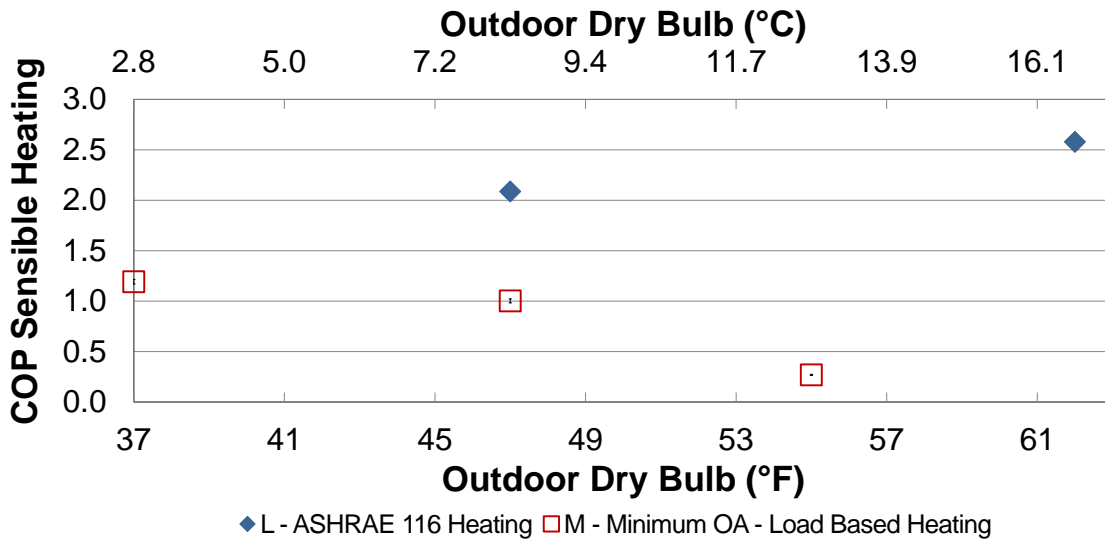


Figure 52: COP Sensible vs Outdoor Dry Bulb Temperature

Figure 52 shows how the sensible COP efficiency varied as a function of outdoor air temperatures. The estimated uncertainty for the sensible COP was about 2%, and the error bars used to represent it were smaller than the symbols used in the figure.

The ASHRAE baseline tests showed an increasing trend in COP as the outdoor temperature and load increased. For the load-based tests, starting from 37°F and ending at 55°F (2.8°C to 12.8°C) the main trend observed was a COP decreasing if the temperature increased and load decreased. Both temperature and load-based heating tests show opposite trends to the majority of the cooling load-based tests, for which the COP decreased as load increased. Even though only sensible loads and COP values were presented, (as it is typical with heating tests because no dehumidification

occurs in the coil), it is important to look at the latent loads because of the influence of the outdoor air. The 37°F (2.8°C) and 47°F (8.3°C) outdoor air temperature tests had positive latent loads. That is, the outdoor air humidity was higher than the indoor one, which resulted in an increase on the total heating load provided by the unit. This is not the case of the 55°F (12.8°C) test, which had a negative latent load. This means the outdoor air was less humid than the indoor, and even if the sensible load provided by the unit was positive (the unit provides sensible heating), the lower humidity in the outdoor provided a “latent cooling” or dehumidification to the indoor room. This is obviously a counterproductive effect and indicates that perhaps the supply air fan should operate at low speed during this type of situation (this was not the case for the load-based heating tests, for which the supply air fan was set at full speed). Another aspect about the 55°F (12.8°C) test is that the indoor temperature setting was reached only with air circulation (no mechanical heating) during the 120 minutes the test lasted (and the transitory 60 minutes period before). That is, mechanical heating was not required. Indoor temperature showed a slight decrease during the 3-hour period but first stage heating was never required for this test. Even though the COP here presented is only sensible, it is possible that the undesired “latent cooling” and the fact that the compressor did not operate during the test are the causes of the less than 1 COP shown in the figure, because the observed net effect was the unit providing cooling, rather than heating. In other words, the unit provided a sensible heating of 2502 BTU/h because of the slightly higher average supply air temperature with respect to the average indoor return temperature.

Relevant data of this test were as follows:

$$T_{db, supply} = 77.68^{\circ}\text{F}, T_{wb, supply} = 61.57^{\circ}\text{F}, h_{supply} = 27.8 \text{ BTU/lbm}$$

$$T_{db, return} = 77.07^{\circ}\text{F}, T_{wb, return} = 62.70^{\circ}\text{F}, h_{return} = 28.7 \text{ BTU/lbm}$$

$$T_{db, outdoor} = 56.93^{\circ}\text{F}, T_{wb, outdoor} = 53.48^{\circ}\text{F}$$

$$\text{Load in the room: } Q_{sens, heating} = 2502 \text{ BTU/h}$$

$$W_{unit} = 2728 \text{ BTU/h}$$

$$\text{Balance} = W_{unit} - Q = 228 \text{ BTU/h}$$

$$Q_{\text{total,cooling}} = 18719 \text{ BTU/h (-)}$$

$$Q_{\text{latent,cooling}} = 21221 \text{ BTU/h (-)}$$

$$V_{\text{supply}} = 5037 \text{ cfm}$$

$$V_{\text{outdoor}} = 364 \text{ cfm}$$

Supply air fan speed: 82% (full speed)

Figure 53 shows the psychrometric process of the 55°F load-based test. This result indicates that first: the small percentage of outside air made the mixed air temperature (state 4) closer to the indoor return air conditions (state 2). Second: it is assumed that mechanical dehumidification occurred at the filter and at the surface temperature of the evaporator coil (this is observed between states 4 and 4' and it is the undesired "latent cooling" that was previously mentioned). The evaporator was cold because the compressor was not running and the room was at 56.9°F (the average outdoor temperature of the nominal 55°F test was 56.9°F). The sensible load in the room was balanced by the RTU indoor fan (blower) which increased the mixed air temperature by approximately 1.5°F. This is observed between states 4' and 1.

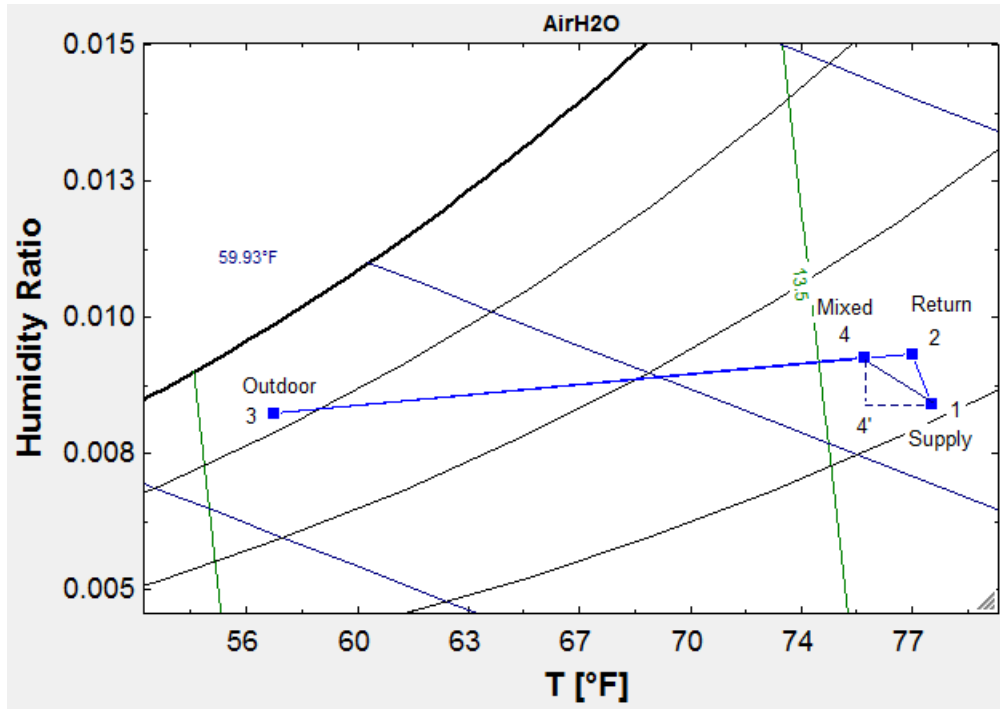


Figure 53: Psychrometric process of the 55F load-based heating test

A schematic of the RTU air side is shown in figure 54 to better understand the states in Figure 53.

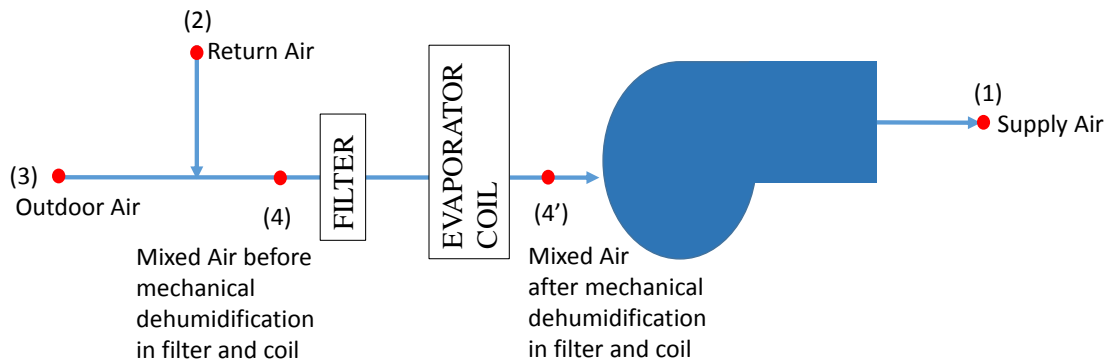


Figure 54: Representation of the air side psychrometric states of RTU for the 55°F load-based test with the RTU in heating mode.

CHAPTER VIII

VIII. CONCLUSIONS AND RECOMMENDATIONS FOR FUTURE WORK

8.1 Conclusions

The feasibility of a load-based method of test was studied by performing 84 tests that allowed investigating the instrumentation required in the new method of test. The 84 tests consisted of 64 test in cooling mode, 5 test in heating mode heating and 15 initial exploratory and preliminary tests in cooling mode to understand the behavior of the unit and facility during load-based test. Protocols of preparing the testing units inside the lab, procedures for setting up the load conditions, and data recording and data reduction procedures were set for the experiments and they were reviewed and gradually modified as the results from the tests were obtained and analyzed during the work of the present thesis. Only the final successful versions of the test protocol and data reduction procedures were reported in details this thesis.

The uncertainty, repeatability and degree of confidence of the load-based tests results were studied by conducting 5 uncertainty estimation tests, 7 repeatability tests and 2 load perturbation tests. The uncertainty was estimated at 3.5% for the total load and 4% for the COP. This was also validated with repetition tests, which yielded total loads within 3.5% (or less) than the original tests and total COPs within 4 to 5.2% of the original tests.

The conditions derived from the available simulations and climate data were done in such a way that they would be broad enough to be realistic for representing RTUs integrated with light commercial buildings but also doable in a conventional psychrometric chambers. It was also important that the conditions allowed the unit to be tested under part-load operation for a broad range of outdoor temperatures.

One limitation of the method of test is that it required a high understanding of the RTU control sequence prior to testing it. The thermal inertia of the unit, chamber and associated ducted flow to the flow nozzle had to be characterized prior to commence the load-based tests. In this project, the thermostat setting sequence was simulated and controlled using laboratory equipment. It was found for example, that different indoor fan (or blower) speeds and economizer openings had an influence in the air side measured load. This was due to the different pressure drop induced across the conditioning loop fans by the different airflow rate provided by the supply air fan when its speed was modified. Since the idea of the method is to set a constant load in the indoor room, the change of load in the indoor room with fan speed could be challenging when testing a unit with its own independent set of controls.

Different data analysis approaches were studied in order to understand and recommend which one better captured unit performance in long periods of time. Time based and cycle based averaging approaches were presented, as well as, the influence of the starting and finishing times for the analysis. A cycle-based approach where a minimum of two cycles occurs was recommended, although it was found that for long periods of time if more than two cycles had occurred, time based approach was also valid. On the other hand, when technologies that kept fairly constant indoor room temperatures were used, a time based approach was sufficient and table 4 test duration could be reduced to half of the recommended values if desired. The thermal inertia was the basis to select the duration of the startup time, the duration of the transition from temperature based to load-based operation, and the minimum recording time of the test. In the present project, the startup time was

30 min, the transition time from temperature based to load-based was 60 minutes and the minimum recording time was 2 cycles after the first cycle, which was approximately 45 minutes.

Besides the procedures for load setting, thermostatic setting sequence and data analysis, a series of results for the studied rooftop unit were presented. These results, provided a comprehensive example of how a rooftop unit can be characterized using the load-based method described in this thesis. Technologies such as fan speed control provided efficiency improvements at the mid-range temperatures but fell short to meet the require load at the higher ones. The economizer provided significant savings compared to the full speed and speed control cases, except at 72°F (22.2°C) where the contribution of outside air increased the mixed air humidity, which in consequence increased the latent load on the coil. The increase of the latent load compromised COP enhancement in comparison to the speed control only test.

8.2 Recommendations for Future Research on This Topic Area

The use of economizers and an indoor fan that could reduce its speed were the technologies tested in this project. A series of tests were required to understand the thermal and flow interaction between the chamber and the RTU when these technologies were installed on it. Suggestions for future projects might be as follows:

- a) A project to study possible additional instrumentation enhancements to psychrometric chambers including for example watt meters to measure conditioning loop fans power, refrigerant/water mass flow meters in the conditioning loops coils and temperature measurements of the refrigerant/water entering and leaving the conditioning coils. This could allow estimating the load being set in the chamber in an alternative way from air side measurements. This could be valuable for: 1) validate air side measurements, 2) allow the

- chamber to automatically adjust load setting when changes in the RTU controls caused the load setting to vary and 3) study the thermal inertia of the chamber.
- b) A project that understands interaction between the psychrometric chamber and the RTU and feasibility of load-based tests when technologies such as variable refrigerant flow, evaporative cooling, enthalpy wheels and other technologies are used.
 - c) A project on which similar units would be tested in different psychrometric chambers (preferably of different size) to understand the effects of different thermal inertias in the final measured capacities and coefficients of performance. In this way, if the experimental results are used for building simulation, the influence of building inertia can be better accounted for in an experimental correlation.
 - d) A project on which temperature and load time daily series are applied on RTUs. In this case, loads and outdoor temperatures would not be constant and would allow to understand energy consumption at longer periods of time and compare the response of different technologies to varying loads and outdoor temperatures. Understanding the feasibility of setting different outdoor temperatures and loads applied to an RTU in a psychrometric chamber could be a first phase of such project.

NOMENCLATURE

A_{nozzle} : Area of each nozzle, ft² (m²)

C : Nozzle coefficient of discharge, dimensionless

COP : Unit total coefficient of performance, dimensionless

COP_{sens} : Unit sensible coefficient of performance, dimensionless

COP' : Load-based coefficient of performance without ventilation effects, dimensionless

$c_{p,return}$: Return air specific heat at constant pressure as a function of return air dry and wet bulb temperatures and atmospheric air pressure (calculated with EES), BTU/lbm (kJ/kg)

$c_{p,supply}$: Supply air specific heat at constant pressure as a function of supply air dry and wet bulb temperatures and supply air pressure (calculated with EES), BTU/lbm (kJ/kg)

D_{nozzle} : Nozzle diameter, ft (m)

h_{supply} : Supply air enthalpy as a function of supply air dry and wet bulb temperatures and supply air pressure (calculated with EES), BTU/lbm (kJ/kg)

h_{return} : Return air enthalpy as a function of return air dry and wet bulb temperatures and atmospheric air pressure (calculated with EES), BTU/lbm (kJ/kg)

$h_{fg,steam}$: Steam enthalpy of vaporization BTU/lbm (kJ/kg)

\dot{m}_{steam} : Mass flow rate of steam generated by the humidifier, lbm/h (kg/s)

\dot{m}_{air} : Supply air mass flow rate, lbm/h (kg/s)

\dot{m}_{ref} : Refrigerant mass flow rate, lbm/h (kg/s)

$P_{barometer}$: Atmospheric air pressure, inH₂O (Pa)

$P_{discharge}$: Refrigerant pressure at compressor outlet, psi (Pa)

$P_{nozzle,absolute}$: Absolute air pressure at code tester nozzle inlet, inH2O (Pa)

$P_{nozzle,gage}$: Measured manometric air pressure at nozzle inlet, inH2O (Pa)

P_{supply} : Absolute supply air pressure, inH2O (Pa)

$P_{suction}$: Refrigerant pressure at compressor inlet, psi (Pa)

\dot{Q}_{sens} : Unit sensible capacity or indoor room sensible load, BTU/h (kW)

$\dot{Q}_{sens,average}$: Unit sensible capacity or indoor room sensible load averaged throughout the entire length of the test, BTU/h (kW)

\dot{Q}_{total} : Unit total capacity or indoor room total load, BTU/h (kW)

$\dot{Q}_{total,average}$: Unit total capacity or indoor room total load averaged throughout the entire length of the test, BTU/h (kW)

$\dot{Q}_{total,average}'$: Average indoor total load without ventilation effects, BTU/h (kW)

\dot{Q}_{lat} : Measured indoor room latent load, BTU/h (kW)

$\dot{Q}_{lat,humidifier}$: Latent load set by the steam wand in the indoor room, BTU/h (kW)

R: Ideal gas constant of air, ft-lbf/lbm-R (J/kg-K)

Re: Reynolds number at the nozzle

$T_{db,out}$: Outdoor air dry bulb temperature, °F (°C)

$T_{db,return}$: Return air dry bulb temperature, °F (°C)

$T_{db,return,target}$: Target set point dry bulb return temperature, °F (°C)

$T_{db,supply}$: Supply air dry bulb temperature, °F (°C)

$T_{discharge}$: Refrigerant temperature at compressor outlet, °F (°C)

T_{nozzle} : Dry bulb temperature at the nozzle, °F (°C)

$T_{suction}$: Refrigerant temperature at compressor inlet, °F (°C)

$T_{wb,out}$: Outdoor air wet bulb temperature, °F (°C)

$T_{wb,return}$: Return air wet bulb temperature, °F (°C)

$T_{wb,supply}$: Supply air wet bulb temperature, °F (°C)

$\dot{V}_{econ,moa,f}$: Economizer airflow rate for minimum outside air with full fan speed position, cfm (m³/s)

$\dot{V}_{econ,moa,l}$: Economizer airflow rate for minimum outside air with low fan speed position, cfm (m³/s)

$\dot{V}_{econ,fo}$: Economizer airflow rate for fully open position, cfm (m³/s)

\dot{V}_{supply} : Supply airflow rate, CFM (m³/s)

\dot{W}_{Fans} : Conditioning loop fan power consumption or sensible load set by the fans in the indoor room, BTU/h (kW)

$\dot{W}_{Heaters}$: Conditioning loop electric heaters power or sensible load set by the heaters in the indoor room, BTU/h (kW)

$\dot{W}_{unit,average}$: Unit power consumption averaged throughout the entire length of the test, BTU/h (kW)

Y: Expansion factor, dimensionless

α : Alpha ratio (ratio of absolute nozzle exit pressure to absolute pressure)

$\Delta_{p,unit}$: Static pressure difference across the unit (external resistance to airflow), inH₂O (Pa)

$\Delta_{p,nozzle}$: Static pressure difference across the nozzle bank, inH₂O (Pa)

$\Delta_{p,econ}$: Static pressure difference across economizer inlet, inH₂O (Pa)

ρ_{nozzle} : Air density at nozzle as a function of dry bulb temperature at the nozzle, pressure at nozzle inlet and supply air humidity ratio (calculated with EES), lbm/ft³ (kg/m³)

σ_{return} : Return temperature control figure of merit, °F (°C)

ω_{supply} : Supply air humidity ratio as a function of supply air dry and wet bulb temperatures and supply air pressure, lb_{H₂O}/lb_{dry air} (kg_{H₂O}/kg_{dry air})

ACRONYMS

Act: Economizer damper actuator

AHRI: Air Conditioning and Refrigeration Institute

ASHRAE: American Society for Heating Refrigerating and Air Conditioning Engineers

EER: Energy Efficiency Ratio

HVAC: Heat, Ventilating and Air Conditioning

HSPF: Heat Seasonal Performance Factor

IEER: Integrated Energy Efficiency Ratio

MA: Mixed Air (before coil)

MOA, Min OA: Minimum Outside Air

OA: Outside Air

RA: Return Air (indoor)

RTU: Roof Top Unit

SA: Supply Air

SEER: Seasonal Energy Efficiency Ratio

US DOE: United States Department of Energy

REFERENCES

- ANSI/AHRI (2007). AHRI Standard 340/360-2007. Commercial and Industrial Unitary Air-Conditioning and Heat Pump Equipment. Arlington, VA, USA, AHRI.
- ANSI/AHRI (2008). AHRI Standard 210/240-2008. Performance Rating of Unitary Air-Conditioning & Air-Source Heat Pump Equipment. Arlington, VA, USA, AHRI.
- ASHRAE (1992). ANSI/ASHRAE Standard 41.2-1987. Standard Methods for Laboratory Airflow Measurement. Atlanta, ASHRAE.
- ASHRAE (2009a). ANSI/ASHRAE Standard 37-2009. Methods of Testing for Rating Electrically Driven Unitary Air-Conditioning and Heat Pump Equipment. Atlanta, ASHRAE.
- ASHRAE (2009b). ASHRAE Handbook – Fundamentals. Atlanta, ASHRAE.
- ASHRAE (2010). ANSI/ASHRAE Standard 116-2010. Methods of Testing for Rating Seasonal Efficiency of Unitary Air Conditioners and Heat Pumps. Atlanta, ASHRAE.
- ASHRAE (2012). ASHRAE Handbook - Heating, Ventilating, and Air-Conditioning Systems and Equipment. Atlanta, ASHRAE.
- ASHRAE (2013). "1608-TRP Development of a Load-Based Method of Test for Light Commercial Unitary HVAC." Request-for-Proposal (RFP).
- Cengel, Y. A. and A. J. Ghajar (2014). Heat and Mass Transfer: Fundamentals & Applications. New York, NY, McGraw-Hill.
- Corti, G. and S. Marelli (2013). Experimental analysis of an air-to-air heat pump equipped with digital scroll compressor and evaluation of the pulsing flow influence on the refrigerant/air side and on the overall performances. M.S. Thesis.
- Cowan, A. (2004). Review of Recent Commercial Roof Top Unit Field Studies in The Pacific Northwest and California. White Salmon, Washington, New Buildings Institute.
- Cremaschi, L. (2013). "Development of a Load-Based Method of Test for Light Commercial Unitary HVAC." Research Proposal submitted to ASHRAE Research Administration Committee.
- Cremaschi, L. and E. Lee (2008). "Design and heat transfer analysis of a new psychrometric environmental chamber for heat pump and refrigeration systems testing." ASHRAE Transactions **114(2)**: 619-631.
- EIA (2015a). "Annual Energy Outlook 2015 with projections to 2040." US Energy Information Administration DOE/EIA-0383(2015).
- EIA (2015b). "International Energy Statistics available online at <http://www.eia.gov/cfapps/ipdbproject/IEDIndex3.cfm?tid=44&pid=44&aid=2>."

- Fairey, P., B. Wilcox, D. S. Parker and M. Lombardi (2004). "Climatic Impacts on Heating Seasonal Performance Factor (HSPF) and Seasonal Energy Efficiency Ratio (SEER) for Air-Source Heat Pumps." ASHRAE Transactions **110**(2).
- Gatley, D. P. (2004). "Psychrometric Chart Celebrates 100th Anniversary." ASHRAE Journal **46**(11): 16-21.
- Hart, R., D. Morehouse and W. Price (2006). The Premium Economizer: An Idea Whose Time Has Come. Proceedings of the 2006 ACEEE Summer Study on Energy Efficiency in Buildings, Washington, D.C.
- Hart, R., D. Morehouse, W. Price, J. Taylor, H. Reichmuth and M. Cherniack (2008). Up on the Roof: From the Past to the Future. Proceedings of the 2008 ACEEE Summer Study on Energy Efficiency in Buildings, Washington, D.C.
- Hyland, R. and A. Wexler (1983a). "Formulations for the thermodynamic properties of the saturated phases of H₂O from 173.15 K to 473.15 K." ASHRAE Transactions **89**: 500-519.
- Hyland, R. and A. Wexler (1983b). "Formulations for the thermodynamic properties of dry air from 173.15 K to 473.15 K, and of saturated moist air from 173.15 K to 372.15 K, at pressures to 5 MPa." ASHRAE transactions **89**: 520-535.
- Jacobs, P., V. Smith and C. Higgins (2003). Small Commercial Rooftops: Field Problems, Solutions and the Role of Manufacturers. Proceedings of the National Conference on Building Commissioning.
- Kavanaugh, S. (2002). "Limitations of SEER for Measuring Efficiency." ASHRAE Journal **44**(7).
- Klein, S. A. and F. L. Alvarado (2015). EES: Engineering Equation Solver for the Microsoft Windows Operating System, F-Chart software.
- Knebel, D. E. (1983). Simplified energy analysis using the modified bin method. Atlanta, GA, ASHRAE.
- McQuiston, F., J. Parker and J. D. Spitler (2005). Heating, Ventilating, & Air Conditioning: Analysis and Design. New York, John Wiley & Sons.
- Nagengast, B. (1999). "Early twentieth century air-conditioning engineering." ASHRAE Journal **41**: 55-62.
- NPCC (2010). The Sixth Northwest Electric, Power and Conservation Plan. Portland, OR, Northwest Power and Conservation Council.
- Proctor, J. and D. Parker (2000). Hidden power drains: Trends in residential heating and cooling fan watt power demand. Proceedings of the ACEEE Summer Study on Energy Efficiency in Buildings, Washington, D.C.
- Wang, W., S. Katipamula, H. Ngo and R. M. Underhill (2015). Field Evaluation of the Performance of the RTU Challenge Unit: Daikin Rebel. Richland, WA, Pacific Northwest National Laboratory (PNNL).
- Wilcox, S. and W. Marion (2008). Users manual for TMY3 data sets. Golden, CO, National Renewable Energy Laboratory
- Worthington, K. (2011). Calibration of the OSU psychrometric chamber and first experiments. M.S. Thesis.

VITA

Pedro Pablo Perez Paez

Candidate for the Degree of

Master of Science

Thesis: DEVELOPMENT OF A LOAD-BASED METHOD OF TEST FOR LIGHT COMMERCIAL UNITARY HVAC

Major Field: Mechanical and Aerospace Engineering

Biographical: Born in Maracaibo, Venezuela. Son of Janny Paez and Orlando Perez and grandson of Pedro Paez Bermudez and Aira Paez de Wilhelm.

Education:

Completed the requirements for the Master of Science in Mechanical Engineering at Oklahoma State University, Stillwater, Oklahoma in December, 2015.

Completed the requirements for the Bachelor of Science in Mechanical Engineering at La Universidad del Zulia, Maracaibo, Venezuela in 2009.

Experience:

- Graduate Research Assistant at Oklahoma State University Psychrometric Chamber laboratory.
- Piping and Mechanical Field Engineer at the construction of the ancillary facilities for the Urea and Ammonia Plant in Moron, Venezuela.

Professional Memberships:

- American Society of Heating, Refrigeration and Air-conditioning Engineers (ASHRAE).
- American Society of Mechanical Engineers (ASME).